cGMP regulates hemin-induced ferroptosis of platelets

Dissertation

der Mathematisch-Naturwissenschaftlichen Fakultät

der Eberhard Karls Universität Tübingen

zur Erlangung des Grades eines

Doktors der Naturwissenschaften

(Dr. rer. nat.)

vorgelegt von

Marcel Kremser

aus Wuppertal

Tübingen

2023

Gedruckt mit Genehmigung der Mathematisch-Naturwissenschaftlichen Fakultät der Eberhard Karls Universität Tübingen.

Tag der mündlichen Qualifikation:	27.11.2023
Dekan:	Prof. Dr. Thilo Stehle
1. Berichterstatter:	Prof. Dr. Meinrad Paul Gawaz
2. Berichterstatter:	Prof. Dr. Robert Feil
3. Berichterstatter:	M.D. Ph.D. Dmitriy Atochin

Table of contents

Acknowledgement

I stand at the culmination of a remarkable journey, and it is with deep appreciation and heartfelt gratitude that I acknowledge the individuals and institutions who have been instrumental in shaping my PhD thesis.

First and foremost, I express my sincere gratitude to Prof. Dr. Meinrad Gawaz for his unwavering guidance, support, and mentorship. His vast knowledge, profound insights, and relentless dedication to excellence have been a constant source of inspiration throughout my research. I am truly grateful for his invaluable contributions to my academic growth. I extend my deepest appreciation to Prof. Dr. Robert Feil and M.D. Ph.D. Dmitriy Atochin for their inestimably valuable guidance and collaboration. Their expertise and scholarly engagement have significantly enriched my thesis, pushing the boundaries of my research and opening new avenues of exploration. Their unwavering commitment to excellence has been truly inspiring.

I am immensely grateful to Patrick Münzer for his contributions to my research. Our joint efforts in conducting calcium measurements, his thoughtful review of my work, and the invaluable feedback he provided have been instrumental in shaping the outcome of my thesis. I would also like to express my gratitude to Madhumita Chatterjee, whose valuable insights and discussions have broadened my perspectives and enriched my understanding of the subject. Her intellectual contributions were truly invaluable.

To Annalena Fink, David Schaale, and Jeremy Nestele, I owe a debt of gratitude. Teaching and mentoring them in the laboratory not only enhanced their skills but also deepened my own understanding and reinforced my commitment to research and education. Furthermore, I would like to express my sincere gratitude to the members of the Gawaz laboratory, both past and present, for their valuable contributions in creating a welcoming and professional working environment. Namely I want to thank: Tatsiana Castor, Valerie Dicenta, Kyra Kolb, Zoi Laspa, Manuel Sigle, Sarah Gekeler, Lydia Laptev, Claudia Posavec, Melina Fischer and Ferdinand Kollotzek. Each day, I found immense joy in coming to work, and I am grateful for the teamwork and support that I was fortunate to experience.

A special acknowledgment goes to Álvaro Petersen-Uribe, with whom I embarked on a journey of first publication, manuscript writing, and the first revision. Our collaboration not only contributed to the advancement of my research but also forged a lasting friendship. The memories we created together will forever be cherished. May the 4th be with you!

I extend my gratitude to Xiaoqing Fu and AG Lämmerhofer for their collaboration on the Lipidomics research. Their expertise, assistance, and commitment have significantly contributed to the success of this aspect of my thesis. My sincere appreciation goes to Manuel Sigle and AG Schenke-Layland for their collaboration on the raman spectroscopy research. Their support, technical expertise, and dedication to advancing scientific knowledge have been invaluable.

I would also like to acknowledge the support provided by the German Research Foundation (DFG)—project number 335549539-GRK2381. This financial assistance has been crucial in enabling the completion of my research, and I am deeply grateful for their belief in my work. To all the members of the GRK2381 program, I extend my gratitude for the engaging discussions, intellectual stimulation, and the opportunity to grow academically through their valuable insights and feedback. Their diverse perspectives and unwavering support have played a significant role in shaping my research and personal development.

Lastly, I want to express my heartfelt appreciation to my family, friends, and my loving wife. Their unwavering support, understanding, and encouragement have sustained me throughout this academic journey. Their love, belief in my abilities, and patience during the countless hours dedicated to my research have been my greatest strength.

In conclusion, I am deeply grateful to all these individuals and institutions for their unwavering support, guidance, and contributions. Without their involvement, this thesis would not have been possible.

Zusammenfassung

Autoimmunhämolyse ist eine Erkrankung, die durch erhöhte Aktivierung von Thrombozyten und durch ihr Potenzial für thrombotische Komplikationen gekennzeichnet ist. Trotz ihrer klinischen Bedeutung sind die Behandlungsmöglichkeiten für Autoimmunhämolyse begrenzt, was den Bedarf an verbesserten therapeutischen Strategien unterstreicht.

In den letzten Jahren hat sich ein neues Forschungsfeld entwickelt, das sich auf die Rolle der Ferroptose in der Funktion von Thrombozyten konzentriert. Ferroptose ist eine Form des regulierten Zelltods, die durch die Anhäufung von Lipidperoxiden und reaktiven Sauerstoffspezies gekennzeichnet ist, was zu oxidativem Schaden und Zelltod führt. Interessanterweise zeigen erste Publikationen, dass Hemin, ein Nebenprodukt der Hämolyse, in Thrombozyten Ferroptose auslösen kann.

Die Erforschung der Mechanismen, die zur Entstehung von Ferroptose in Thrombozyten führen und ihrer Verbindung zur Autoimmunhämolyse, bietet vielversprechende Möglichkeiten für die Entwicklung gezielter Therapien zur Reduzierung des thrombotischen Risikos bei Patienten mit Autoimmunhämolyse. Diese Arbeit zielt darauf ab, den Effekt von durch Hemin-induzierter Ferroptose auf die Aktivierung von Thrombozyten zu untersuchen und das Potenzial der Modulation des zyklischen Guanosinmonophosphat (cGMP)-Signalwegs als therapeutischen Ansatz zu erforschen.

Daher führten wir *in vitro* Experimente mit Thrombozyten von Patienten und gesunden Kontrollen durch, um die Plättchenaggregation als Indikator für die Aktivierung zu bewerten. Plasmaproben von Patienten zeigten eine signifikante Zunahme der Plättchenaggregation im Vergleich zu Kontrollplasma, insbesondere unter ADP-Stimulation. Es wurden keine signifikanten Unterschiede bei der CRP-induzierten Aggregation beobachtet. Die Behandlung mit cGMP-Modulatoren reduzierte die Aggregation in den Plättchen der Patienten, was auf die Rolle der cGMP-Modulation bei der Verringerung der Plättchenaktivierung in hämolytischem Plasma hinweist.

Wir untersuchten den direkten Effekt von Hemin auf die Plättchenaktivierung und dessen Interaktion mit der cGMP-Modulation. Die Behandlung mit Hemin führte zu einer Stimulation der Plättchenaktivierung, wie sie durch eine erhöhte Oberflächenexpression von P-Selektin und PAC-1, Fibrinogenbindung, ATP-Freisetzung und morphologische Veränderungen nachgewiesen wurde. Die cGMP-Modulation konnte diese durch Hemin induzierten Effekte signifikant abschwächen.

Darüber hinaus konnte festgestellt werden, dass cGMP die durch Hemin induzierte Ferroptose in den Thrombozyten reguliert, was wir durch erhöhte Phosphatidylserin-Exposition und ROS-Aktivität, sowie ein vermindertes mitochondriales Membranpotential belegen konnten. Unsere umfassende Analyse des Thrombozyten-Lipidoms zeigte neben signifikanten konzentrations-abhängigen Veränderungen, die durch Hemin induziert wurden, auch die modulierenden Effekte von DEA/NO und Riociguat auf das Lipidom der Thrombozyten. Zudem enthüllte unsere Untersuchung der ferroptosebezogenen Lipide deutliche Veränderungen in Reaktion auf Hemin und cGMP-Modulation, was ihre entscheidende Rolle im Ferroptose-Signalweg betont.

Unsere Studie liefert Erkenntnisse über die prothrombotischen Eigenschaften von hämolytischem Plasma und das Zusammenspiel von Hemin, Plättchenaktivierung und cGMP-Modulation. Die Modulation der cGMP-Spiegel durch DEA/NO, Riociguat oder Cinaciguat zeigte vielversprechende hemmende Effekte auf die durch Hemin und ADP induzierte Plättchenaktivierung. Diese Erkenntnisse verdeutlichen das therapeutische Potenzial der gezielten Modulation des cGMP-Signalwegs zur Verringerung der Plättchenhyperaktivität und Ferroptose bei Autoimmunhämolyse. Weitere Forschung ist erforderlich, um die zugrunde liegenden Mechanismen aufzuklären und die klinischen Anwendungen der cGMP-Modulation in diesem Zusammenhang zu erforschen.

Summary

Autoimmune hemolysis is a condition characterized by increased platelet activation and the potential for thrombotic complications. Despite its clinical significance, the treatment options for autoimmune hemolysis remain limited, underscoring the need for improved therapeutic strategies.

In recent years, a novel field of research has emerged, focusing on the role of ferroptosis in platelet function. Ferroptosis is a form of regulated cell death characterized by the accumulation of lipid peroxides and reactive oxygen species, leading to oxidative damage and cell demise. Interestingly, some publications already showed that hemin, a byproduct of hemolysis, can induce ferroptosis in platelets.

Understanding the mechanisms underlying ferroptosis induction in platelets and its relationship to autoimmune hemolysis holds great promise for the development of targeted therapies. By elucidating the signaling pathways involved in platelet activation and ferroptosis, we can identify potential therapeutic targets and interventions to mitigate thrombotic risk in patients with autoimmune hemolysis. This thesis aims to investigate the effect of hemin-induced ferroptosis on platelet activation and explore the potential of modulating cyclic guanosine monophosphate (cGMP) signaling as a therapeutic approach.

Therefore, we conducted *in vitro* experiments using platelets from patients and healthy controls to assess platelet aggregation as an indicator of activation. Patient-derived plasma showed a significant increase in platelet aggregation compared to control plasma, particularly with ADP stimulation. No significant differences were observed with CRP-induced aggregation. Treatment with cGMP modulators reduced aggregation in patient platelets, suggesting the role of cGMP modulation in attenuating platelet activation in hemolytic plasma.

We investigated the direct effect of hemin on platelet activation and its interaction with cGMP modulation. Hemin treatment stimulated platelet activation, as evidenced by increased P-selectin and PAC-1 expression, fibrinogen binding, ATP release, and morphological changes. Notably, cGMP modulation effectively attenuated these hemin-induced effects.

Furthermore, cGMP was found to regulate platelet ferroptosis induced by hemin, as indicated by increased phosphatidyl serine exposure, ROS activity, and decreased mitochondrial membrane potential. Our comprehensive analysis of the platelet lipidome demonstrated significant concentration-dependent alterations induced by hemin. We also observed the modulating effects of DEA/NO and riociguat on the platelet lipidome. Additionally, our investigation of ferroptosis-related lipids revealed distinct changes in response to hemin and cGMP modulation, highlighting their crucial role in the ferroptosis pathway.

Our study provides insights into the pro-thrombotic properties of hemolytic plasma and the interplay between hemin, platelet activation, and cGMP modulation. Modulating cGMP levels through DEA/NO, riociguat, or cinaciguat demonstrated promising inhibitory effects on platelet activation induced by hemin and ADP. These findings highlight the potential therapeutic implications of targeting the cGMP pathway to mitigate platelet hyperreactivity and ferroptosis associated with autoimmune hemolysis. Further research is warranted to elucidate the underlying mechanisms and explore the clinical applications of cGMP modulation in this context.

List of figures

List of tables

List of abbreviations

AA ..... *Arachidonic acid*
ACD ..... *Acid-citrate-dextrose*
ADP ..... *Adenosine diphosphate*
AIHA ..... *Autoimmune hemolytic anemia*
ANP ..... *Atrial natriuretic peptide*
ATP ..... *Adenosine triphosphate*
BH_4 ..... *Tetrahydrobiopterin*
BNP ..... *Brain natriuretic peptide*
CAD ..... *Cold agglutinin disease*
cAIHA ..... *Cold autoimmune hemolytic anemia*
cAMP ..... *Cyclic adenosine monophosphate*
CDPA ..... *Citrate-phosphate-dextrose adenine*
cGK ..... *cGMP-dependent protein kinase*
cGMP ..... *Cyclic guanosine monophosphate*
CLEC-2 ..... *C-type-lectin-like receptor-2*
CNG ..... *Cyclic nucleotide-gated cation channel*
CNP ..... *C-type natriuretic peptide*
CoQ10 ..... *Coenzyme Q10*
COX ..... *Cyclooxygenase*
DCFDH-DA ..... *2',7'-Dichlor-fluorescein-diacetat*
DHA ..... *docosahexaenoic acid*
DIC ..... *Disseminated intravascular coagulation*
ELISA ..... *Enzyme-linked Immunosorbent Assay*
eNOS ..... *Endothelial NOS*
ESI ..... *electrospray ionization*
Fer-1 ..... *Ferrostatin-1*
GP ..... *Glycoprotein*
GPCR ..... *G-Protein-coupled receptor*
GSH ..... *Glutathione*
Hb ..... H*emoglobin*
HETE ..... *Hydroxyeicosatetraenoic acid*

Hp ..... *Haptoglobin*
HPETE ..... *Hydroperoxyeicosatetraenoic acid*
HPLC ..... *High-Performance Liquid Chromatography*
Hpx ..... *Hemopexin*
HUS ..... *Hemolytic uremic syndrome*
IE ..... *Infective endocarditis*
iNOS ..... *Inducible NOS*
IP_3 ..... *Inositol-1,4,5-trisphosphate*
IRAG ... *Inositol-1,4,5-trisphosphate receptor-associated cGMP kinase substrate*
Lip-1 ..... *Liproxstatin-1*
LOOH ..... *Lipid hydroperoxide*
LOX ..... *Lipoxygenase*
LPS ..... *Lipopolysaccharide*
MRP ..... *Multidrug resistance protein*
MUFA ..... *Monounsaturated fatty acid*
nNOS ..... *Neuronal NOS*
NO ..... *Nitric oxide*
NO-GC ..... *NO-sensitive guanylyl cyclase*
NOS ..... *Nitric oxide synthase*
PBS ..... *Phosphate-buffered saline*
PDE ..... *Phosphodiesterase*
PDGF ..... *Platelet-derived growth factor*
pGC ..... *Particulate guanylyl cyclase*
PGE_2 ..... *prostaglandin E_2*
PGI_2 ..... *Prostacyclin*
PLCγ2 ..... *Phospholipase C gamma 2*
PMP ..... *Platelet-derived microparticle*
PRP ..... *Platelet-rich plasma*
PS ..... *Phosphatidylserine*
PUFA ..... *Polyunsaturated fatty acid*
PVDF ..... *Polyvinylidene fluoride*
RBC ..... *Red blood cell*

ROS ..... *Reactive oxygen species*
RT ..... *Room temperature*
RTA ..... *Radical-trapping antioxidant*
SCD ..... *Sickle cell disease*
SDS-PAGE ..... *Sodium dodecyl sulfate-polyacrylamide gel electrophoresis*
sGC ..... *Soluble guanylyl cyclase*
Syk ..... *Spleen tyrosine kinase*
TLR ..... *Toll-like receptor*
TMRE ..... *Tetramethylrhodamine ethyl ester*
TXA_2 ..... *Thromboxane* A_2
TXB_2 ..... *thromboxane* B_2
VASP ..... *Vasodilator-stimulated phosphoprotein*
vWF ..... *Von Willebrand factor*
wAIHA ..... *Warm autoimmune hemolytic anemia*
$\Delta\Psi m$ ..... *Mitochondrial transmembrane potential*

1 Introduction

1.1 Hemolysis

Hemolysis can be divided into two mechanisms: Intravascular hemolysis is the destruction of red blood cells (RBCs) in the circulation releasing cell contents into the plasma, while mechanical hemolysis for instance results from a damaged endothelium, or infectious agents causing direct membrane degradation and cell destruction[1]. The causes of hemolytic anemias vary from genetic mutations (e.g., for sickle cell disease (SCD)[2] and thalassemia[3]), infections (e.g., malaria[4] and bacteria involved in sepsis, such as Shiga toxin-producing Escherichia coli in hemolytic uremic syndrome (HUS)[5]), certain drugs[6], and transfusion reactions[7] to autoimmune hemolytic anemia (AIHA)[8,9].

AIHA is a rare condition with an estimated incidence of 0.8–3 per 10^5/year in adults and a prevalence of 17 per 100,000. It is caused by autoimmune antibodies and can be further classified as warm (wAIHA), cold (cAIHA), or mixed, depending on the pathogenic antibodies causing the disease[9]. To date, the treatment has been based on expert opinions or retrospective studies, and while most patients respond to first-line therapy, many have a chronic relapsing cause that requires subsequent therapies. Furthermore, there is a risk of infection and immunosuppression associated with second- and third-line therapies for AIHA[10]. Additionally, hemolytic diseases are generally associated with an increased risk of thromboembolic complications, illustrated by a strong thrombophilic nature[11]. Moreover, since hemolysis can be rapid, severe, and life-threatening, there is a high medical need for novel, effective, and safe therapies for AIHA.

The most important protein in RBCs is the oxygen-carrying protein hemoglobin (Hb), which consists of four globin chains, two α chains, and two β chains. Oxygen is transported in the blood by reversible binding to the ferrous ion (Fe^{2+}) in each heme group[12].

During hemolysis, Hb and its metabolite, free heme, are released from RBCs directly into circulation, promoting oxidative stress, inflammation and thrombosis. Thus, heme and its iron must be degraded to counter heme toxicity. Haptoglobin

(Hp) and hemopexin (Hpx) are heme binding plasma proteins with the highest binding affinities for Hb and heme[13] delivering Hb and heme to CD91 receptors on hepatocytes and CD163 receptors on macrophages[14,15]. However, when these clearance and detoxifying systems are overwhelmed by intravascular hemolysis, Hb and heme trigger vascular and organ dysfunction, leading to adverse clinical effects **(Figure 1)**[16–18].

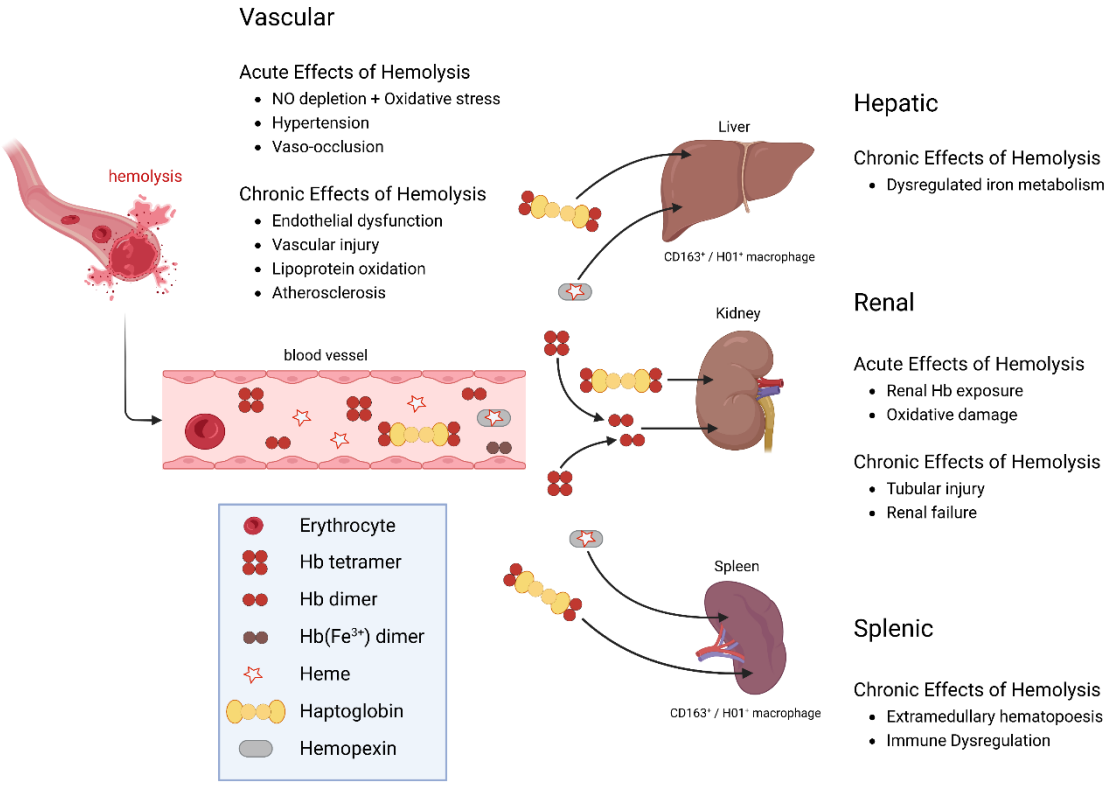

Figure 1: Schematic representation of the various compartments involved in the clearance of Hb and pathologies linked to Intravascular Hemolysis. The presence of hemoglobin and hemin scavenger proteins, specifically Hp and Hpx, plays a critical role in rebalancing the physiological equilibrium, shifting it away from tissue damage and towards protective mechanisms. Nevertheless, under conditions where intravascular hemolysis surpasses the capacity of these clearance and detoxifying systems, such as in sickle cell disease, blood transfusion, malaria, or sepsis, Hb and hemin induce vascular and organ dysfunction, leading to detrimental clinical consequences. Created with BioRender.com. Modified from Schaer et al., 2013[16].

Upon release, heme is rapidly and spontaneously oxidized in the blood into its ferric form, hemin, with levels between 2 µM and 50 µM observed within the plasma in hemolytic diseases[18,19]. The most common complication of hemolytic anemia is thromboembolic events due to the lack of platelet inhibition, as Hb limits the bioavailability of nitric oxide (NO), a potent vasodilator and anti-thrombotic

agent that stimulates the production of cyclic guanosine monophosphate (cGMP)[20–22]. Furthermore, it has recently been shown that heme mediates the activation and death of human platelets through ferroptosis[23].

1.1.1 Cold autoimmune hemolytic anemia (cAIHA)

The phenomenon of blood agglutination at cold temperatures was first observed by Landsteiner in the early 1900s and later designated as the term cold agglutinin disease (CAD) by Schubothe[24,25]. CAD, also known as cAIHA, is in 90% of patients an immunoglobulin M (IgM) mediated process, with rare findings of monoclonal IgG and IgA[26].

IgM is typically not bound to RBCs in the core of the body. However, as blood flows to the peripheral circulation and cools down, IgM temporarily binds to the RBC membrane, and thus activates the complement cascade subsequently, leading to the attachment of the complement factor C3b to the cell surface. As the C3b-coated cells return to the core of the body, IgM dissociates and the C3b-coated cells are then removed by macrophages, primarily in the liver, leading to extravascular and potentially intravascular hemolysis[25,27].

Treatment of CAD typically involves the use of immunosuppressive drugs and/or plasmapheresis to remove the antibodies from the circulation. Rituximab, a B-cell depleting monoclonal antibody, has been used in the treatment of CAD. Recent studies have shown that the use of Rituximab in CAD patients had a response rate of 45% to 58% with only rare complete responses and furthermore relapse is common, with 57-89% of patients who initially respond experiencing a return of their symptoms[25,28,29].

As current therapies have limitations and relapse rates are high, there is a urgent need for new and improved treatment options for CAD.

1.2 Platelets

Platelets, also known as thrombocytes, are 2- to 4- µm anucleate cells, but containing mitochondria, mRNA, and all the translational machinery needed for protein synthesis[30]. They are produced at a daily rate of around 10^{11} from bone marrow megakaryocytes and circulate in the plasma for approximately seven to ten days at a concentration of 150–400 10^3/µl before being cleared by the macrophagic system, especially in the spleen and liver[31].

Human platelets are crucially involved in hemostasis and wound healing. Furthermore, platelets have been described to participate in inflammatory pathologies, such as the promotion of atherosclerosis, tumor growth, and metastasis[32]. To prevent bleeding at the site of endothelial injury, platelets form a hemostatic plug (thrombus).

Studies so far have distinguished three phases in thrombus formation under flow: The first being the initiation by adhesion of platelets to extracellular matrix components like collagen via the collagen receptor glycoprotein (GP) Ia-IIa (integrin α2β1) and GPVI **(Figure 2)**. Following the activation process of the platelets is the phase of extension, where several intracellular signaling pathways can lead to a shape change and granule secretion of e.g., adenosine diphosphate (ADP), and thromboxane A_2 (TXA_2), which act through G-Protein-coupled receptors (GPCRs) **(Figure 2)**. Moreover, intracellular calcium is released, and platelet co-aggregation further stabilizes the thrombus via the fibrinogen receptor, integrin $\alpha_{IIb}\beta_3$, also called GPIIb/IIIa. In the final third phase, which is called perpetuation, the formed thrombus is further stabilized by thrombus contraction via thrombin and formation of a fibrin network by converting fibrinogen to fibrin[33,34].

Platelets also play a role in inflammation and immune response. They release a variety of pro-inflammatory and pro-coagulant molecules, such as platelet-derived growth factor (PDGF), platelet-derived microparticles (PMPs), and microvesicles, which can promote the recruitment and activation of immune cells. Additionally, platelets can also bind to and engulf pathogens, such as bacteria and viruses, via their wide range of bacterial receptors, including complement

receptors, FcγRIIa, Toll-like receptors (TLRs), GPIIb/IIIa, and GPIb receptor and act as a bridge between innate and adaptive immunity[35].

TLRs are a family of receptors found in the innate immune system that play a vital role in recognizing and responding to pathogens. To date, at least eleven TLRs have been identified in various immune and non-immune cells, including platelets. Studies have shown that platelets express TLR2, TLR4, and TLR9 and have very weak expression of TLR1, TLR6, and TLR8, highlighting the role of platelets as primitive immune cells in host defense[36]. Recent research has focused on the role of TLRs in platelet function, specifically TLR2 and TLR4. The ligand for TLR4 is the lipopolysaccharide (LPS) from Gram-negative bacteria[37].

Platelet disorders include thrombocythemia and thrombocytosis, thrombocytopenia, and platelet dysfunction. An increased risk of bleeding could be present when the platelet count is reduced (thrombocytopenia) and/or one of their functions is defective. Conversely, thrombocythemia and thrombocytosis are associated with increased platelet count and reactivity leading to improper thrombus formation[38]. Activated platelets exhibit adhesion and aggregation within atherosclerotic lesions, contributing to the formation of occlusive arterial thrombi. These thrombi are responsible for the development of atherothrombotic manifestations, including stroke and myocardial infarction. These events are among the primary causes of morbidity and mortality in Western populations.[39,40]. Furthermore, non-wound-related activation of platelets by pathogens can have profound implications, manifesting as serious conditions such as infective endocarditis (IE) and disseminated intravascular coagulation (DIC)[37].

In response to activation stimuli, platelets undergo aggregation, but they are also subject to inhibitory stimuli to prevent abnormal vessel occlusion. The two major endogenous platelet inhibitors, NO and prostacyclin (PGI_2), are constantly secreted by endothelial cells into the vessel lumen, triggering the cGMP and cyclic adenosine monophosphate (cAMP) signaling pathway in platelets (Figure 2), respectively[41].

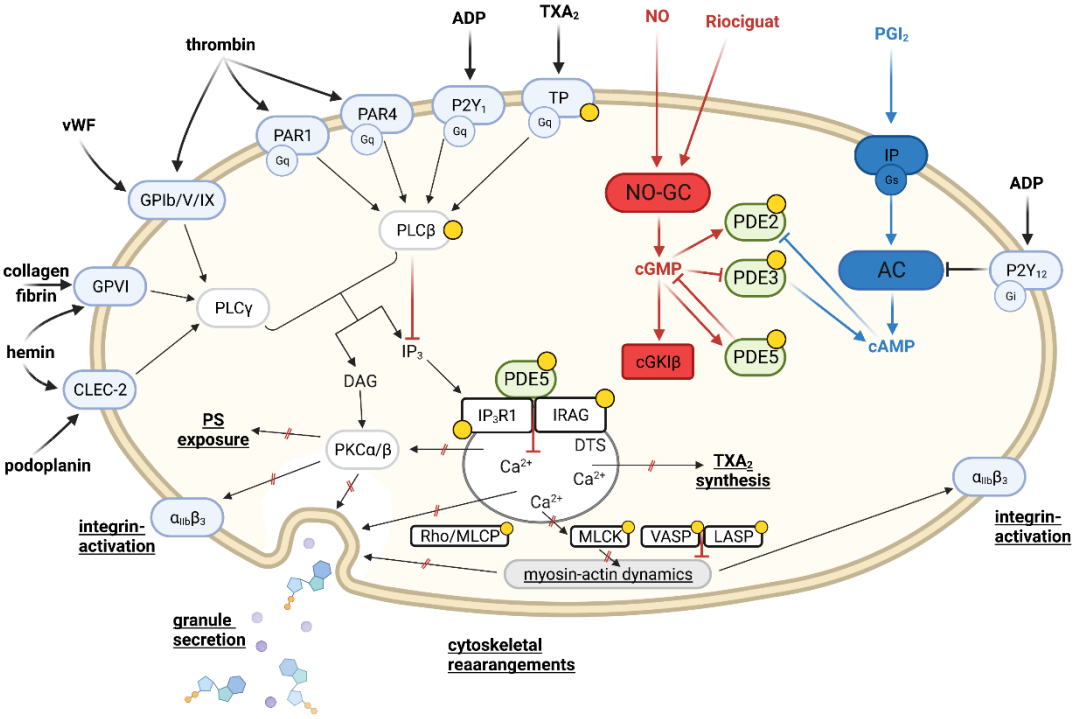

Figure 2: Modulation of protein phosphorylation and platelet function by the cGMP signaling pathway. Platelet activation is triggered by soluble agonists (thrombin, ADP, TXA2 and hemin) and adhesion molecules (vWF, collagen, fibrin, podoplanin) through specific membrane receptors and signaling pathways. These activations induce various platelet responses including cytoskeletal rearrangements, integrin $\alpha_{IIb}\beta_3$ activation, granule secretion, and phosphatidylserine (PS) exposure, crucial for adhesion, aggregation, and thrombin generation. The cGMP pathway, facilitated by NO and sGC stimulators like riociguat, inhibits several platelet activation responses at multiple points in the activation pathways (indicated by red blocked arrows). This includes inhibiting Ca2+ release from intracellular stores, PKCα and PKCβ activation. PDE regulation by cGMP and phosphorylation modulates this pathway. Known phosphorylation targets of cGKI are marked by an orange dot. Phosphorylation of these proteins, such as RGS18, PLCβ, IP3R1, IRAG, Rho, MLCK, VASP, LASP, predominantly hinders specific platelet activation steps (indicated by red blockades). Interactions occur between the cGMP (red) and cAMP (blue) signaling pathways, facilitated by the regulation of PDE2 and PDE3. Created with BioRender.com. Modified from Makhoul et al., 2018[42].

In the clinics, numerous drugs have been developed to inhibit platelet aggregation by targeting various signaling pathways involved in platelet activation. However, these drugs often carry the side effect of increased bleeding[43]. Therefore, investigating and comprehending the underlying mechanisms governing platelet activation and inhibition is of significant scientific and clinical research importance.

1.3 Ferroptosis

There are three major types in which cell death was typically divided: apoptosis, autophagic cell death and necrosis[44]. However, further research has shown that there are more distinct forms of cell death. Therefore, the Nomenclature Committee on Cell Death updated the list in 2018 and added new types of regulated cell death, each showing different characteristics in terms of the molecular machinery involved and the signals that are modulated. One of the newer forms of cell death is the so called ferroptosis[45].

Ferroptosis was first described in 2012 by Dixon as an iron-dependent non-apoptotic cell death[46]. Since then, many researchers have studied ferroptosis in different diseases and cell types showing that ferroptosis plays an important regulatory role in the occurrence and development of many diseases **(Figure 3)**[47].

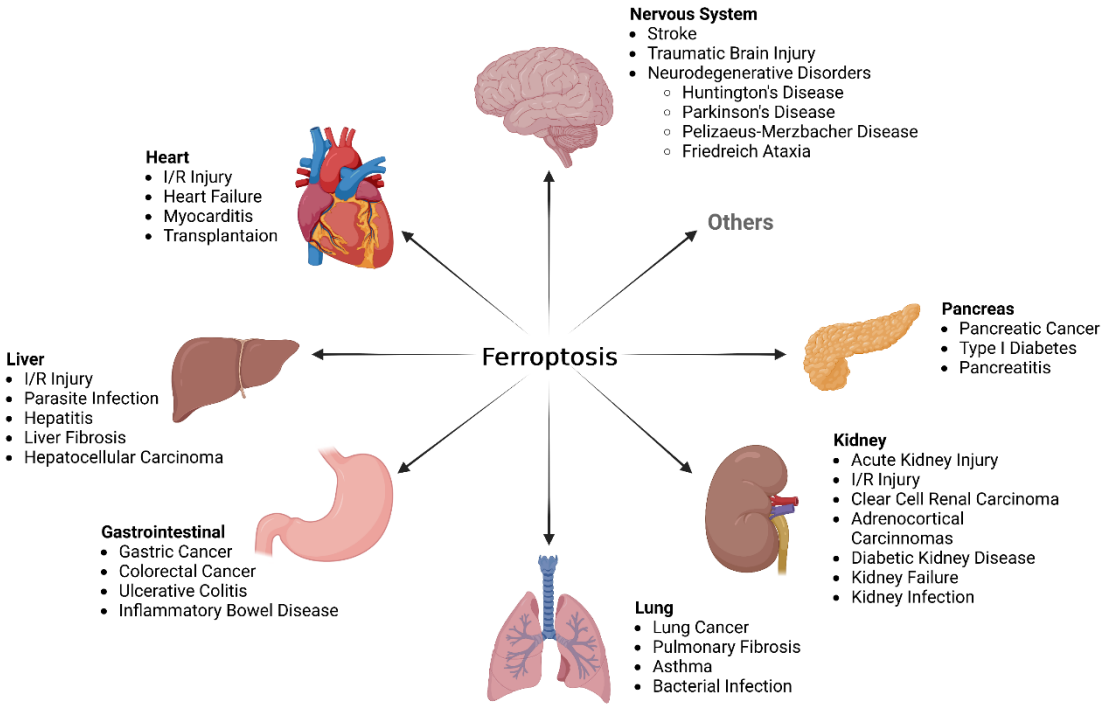

Figure 3: Roles of Ferroptosis in Pathological Processes. Ferroptosis plays a crucial role in a wide range of systemic diseases, including those affecting the nervous system, heart, liver, gastrointestinal tract, lungs, kidneys, pancreas. It is also associated with cancers and other pathological processes such as the suppression of immune function of T cells and more. Created with BioRender.com. Modified from Li et al., 2020[47].

Beside its iron-dependence the hallmark for ferroptosis is lipid peroxidation, which is the process of oxidative degradation of lipids containing carbon-carbon double bond(s), especially polyunsaturated fatty acids (PUFAs). Induced by an increased amount of reactive oxygen species (ROS) for example, free radical species such as oxyl radicals and hydroxyl radicals remove electrons from lipids and subsequently produce reactive intermediates that can undergo further reactions[48]. Interestingly, it has been found that PUFAs (especially arachidonic acid and adrenic acid) promote ferroptosis, whereas monounsaturated fatty acids (MUFAs) (especially oleic acid and palmitoleic acid) limit ferroptosis because the structure of PUFA and MUFA differ in their susceptibility to lipid peroxidation[49].

Additionally, lipid peroxidation can not only be caused by non-enzymatic mechanisms, since iron can cause ferroptosis also by increasing the activity of lipoxygenases (LOXs). The LOX family is a group of non heme-iron containing dioxygenases that are responsible for the metabolism of PUFAs to generate different hydroperoxy PUFA derivatives, such as the initial lipid hydroperoxides (LOOHs) including hydroxyeicosatetraenoic acids (HETEs)[49,50]. The three main LOXs are 5-LOX, 12-LOX, and 15-LOX which are named according to their positional specificity on arachidonic acid (AA), producing their respective hydroperoxyeicosatetraenoic acid (HPETE) products. The HPETE products are subsequently reduced by cellular peroxidases to the bioactive lipid, HETE[51]. Platelets express two types of LOX enzymes, 12-LOX and 15-LOX[52]. The 12/15-LOX enzymes have been shown to play a role in the regulation of inflammation and have been linked to several diseases, including cancer, atherosclerosis, and inflammation. Moreover, studies have shown that 12/15-LOX plays a role in platelet activation and aggregation, as well as in the regulation of platelet function in cardiovascular disease[53]. Additionally, platelet-derived 12-HETE exerts pronounced autocrine and paracrine effects on platelets, specifically playing a pivotal role in mediating coronary thrombosis through the activation of platelet integrin $\alpha_{IIb}\beta_3$[54].

To prevent ferroptosis, cells have an integrated antioxidant defense system that includes the synthesis of antioxidants such as glutathione (GSH), coenzyme Q10 (CoQ10), and tetrahydrobiopterin (BH_4).

The GSH system is one of the main defense mechanisms in ferroptosis. GSH is formed by the condensation of glutamic acid, cysteine, and glycine. The inhibition of GSH synthesis and utilization is a classic method of inducing ferroptosis. The inhibition of system Xc- (using e.g. erastin), which is an amino acid transporter that plays a role in the antioxidant system of cells triggers a decrease in the antioxidant capacity of various cells and accumulation of lipid ROS, ultimately resulting in oxidative damage and ferroptosis[55]. The main anti-ferroptotic activity of GSH is related to GPX4, which reduces phospholipid hydroperoxide production to prevent the accumulation of lipid peroxides. Ferroptosis can also be induced by activating the P53 gene or through the use of ferroptosis-inducing agents, such as RSL3, which directly acts on GPX4 and inhibits its activity, leading to a reduction in cell antioxidant capacity and accumulation of ROS[47,56].

CoQ10 is a vitamin-like molecule that acts as an electron carrier in the mitochondrial respiratory chain, providing energy for the cell. It also has a role in the scavenging of free radicals and the protection of mitochondrial membrane integrity[57]. CoQ10 deficiency has been linked to the development of ferroptosis in various cells[55].

BH_4 is a cofactor of various enzymes, including nitric oxide synthases (NOSs), that are responsible for the production of NO, which is a major antioxidant and anti-inflammatory molecule[58]. BH_4 deficiency has also been linked to the development of ferroptosis in various cells[55].

Research has found that using certain types of antioxidants, known as radical-trapping antioxidants (RTAs), can prevent ferroptosis in different types of cells. One example of this is vitamin E, which has been shown to regulate ferroptosis by inhibiting the activity of LOX. While vitamin E is an effective antioxidant, it is not as potent as other aromatic amines such as ferrostatin-1 (Fer-1) and liproxstatin-1 (Lip-1), which were discovered through high-throughput screening. Additionally, melatonin, a naturally occurring antioxidant, has been shown to protect against ferroptosis-related cell death in platelets by neutralizing reactive oxygen species[59,60].

1.3.1 Ferroptosis in platelets

In 2018 researchers could show for the first time that hemin induces human platelet activation and platelet death through ferroptosis (**Figure 4**)[23]. Although hemin is known to bind to TLR4 on endothelial cells resulting in endothelial cell activation, it has been found that hemin activates platelets in a manner that does not involve TLR4 signaling. This was demonstrated by the observation that blocking TLR4 using TAK-242 did not prevent hemin-induced activation of platelets, indicating that hemin activates platelets through an alternative pathway[19]. Instead, hemin is an endogenous agonist for C-type-lectin-like receptor-2 (CLEC-2) and GPVI leading to phosphorylation of spleen tyrosine kinase (Syk) and subsequently phospholipase C gamma 2 (PLCγ2) and activation of integrin GPIIb/IIIa at low concentrations and platelet agglutination at high concentrations **(Figure 4)**.

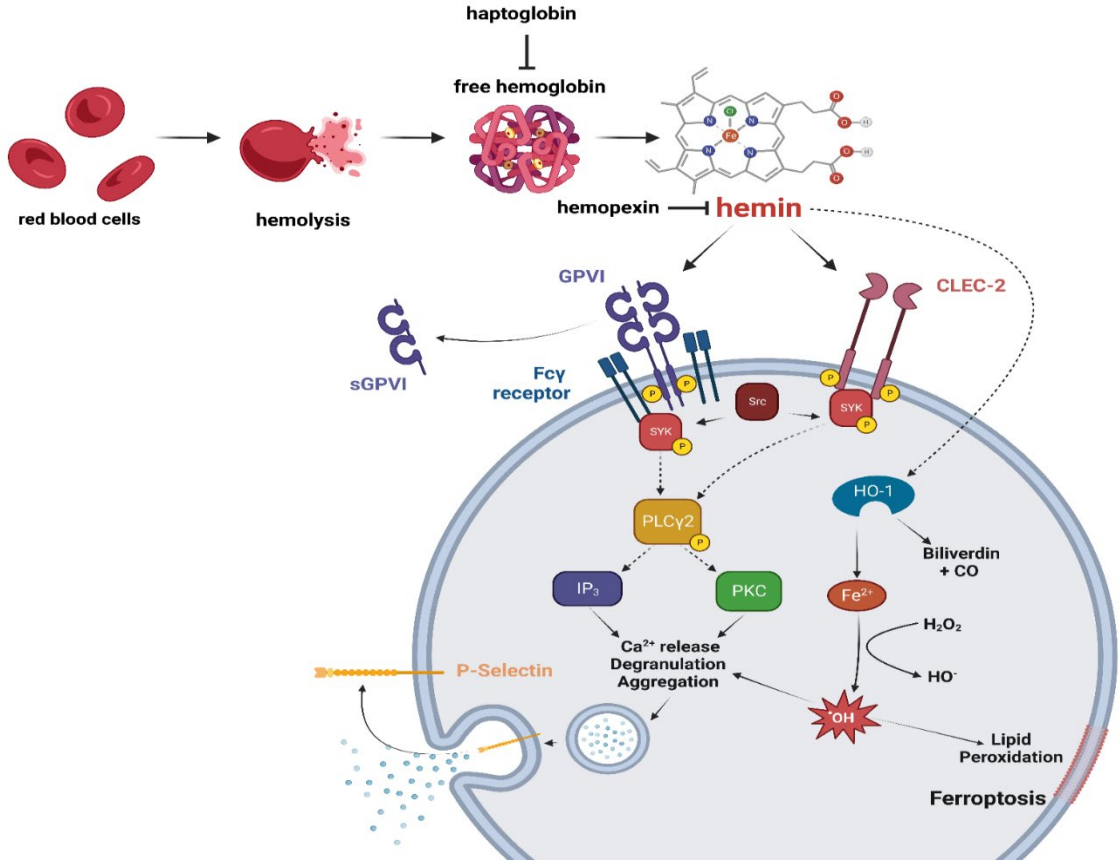

Figure 4: Hemin induced platelet activation and ferroptosis. Excessive hemolysis overwhelms clearance and detoxifying systems (haptoglobin and hemopexin), resulting in the release of free hemin. Hemin can directly bind to CLEC-2 and GPVI, initiating human platelet activation through the Syk-PLCγ2 pathway. This activation cascade involves increased calcium release, degranulation, and platelet aggregation. Moreover, hemin triggers lipid peroxidation in platelets leading ultimately to ferroptosis. Created with BioRender.com. Modified from NaveenKumar et al., 2019[59].

Moreover, hemin induced platelet activation is not affected by inhibitors of cyclooxygenase (COX), such as indomethacin, or $P2Y_{12}$, such as cangrelor, indicating that, unlike the CLEC-2 agonist podoplanin, additional mediators are not needed for hemin-induced platelet activation.

These novel findings highlight the increased platelet hyperreactivity associated with elevated free heme levels during hemolysis. Given the limited treatment options available for these diseases, there is an undoubtful need for new forms of therapeutic intervention to inhibit platelet activation in hemolytic diseases.

1.4 The cGMP signaling

A vital second messenger molecule that controls a wide range of physiological processes in mammals is cGMP. Following the discovery and identification of cAMP as the first hormone acting as second messenger by Sutherland and colleagues in 1957, cGMP was discovered in rat urine in 1963 and has since been found to be important in regulating cardiovascular homeostasis[61,62]. It is known for playing a role in regulating various cellular processes including platelet activation, cellular growth and contraction, inflammation, learning, axon branching, and more[63,64].

Within the cell cGMP can be generated by two types of guanylyl cyclases: membrane-bound particulate guanylyl cyclases (pGCs) and NO-sensitive guanylyl cyclases (NO-GCs), also called soluble guanylyl cyclases (sGCs). Both enzymes exist in different isoforms[65]. The pGCs are activated by natriuretic peptides including atrial natriuretic peptide (ANP), brain natriuretic peptide (BNP), and C-type natriuretic peptide (CNP). The key molecule driving cGMP generation via the NO-GC is nitric oxide, which is synthesized from L-arginine by enzymes known as NOSs, including the endothelial NOS (eNOS), neuronal NOS (nNOS), and inducible NOS (iNOS)[65,66]. eNOS and nNOS are constitutively expressed, while the expression of iNOS is triggered by external stimuli, such as LPS or cytokines, in specific cell types such as macrophages, VSMCs, and endothelial cells[67,68].

Once generated, cGMP can bind and activate three main types of downstream effectors: cyclic nucleotide-gated cation channels (CNGs), cGMP-dependent protein kinases (cGKs), and phosphodiesterases (PDEs)[64,65]. These effectors are responsible for the wide range of physiological processes that are regulated by the cGMP signaling pathway. CNGs are ion channels that open or close in response to changes in cGMP concentrations, allowing for the flow of ions such as calcium and potassium into or out of the cell. This can lead to changes in cell physiology such as muscle relaxation or contraction[63]. cGKs are enzymes that phosphorylate other proteins in response to changes in cGMP concentrations, leading to changes in protein activity and function[63,65]. PDEs are enzymes that break down cGMP, returning the cell to a baseline state[69]. The balance of cGMP-generating and -degrading enzymes, as well as the activity of the downstream effectors, ultimately determines the overall level of cGMP in the cell and the resulting physiological response **(Figure 5)**.

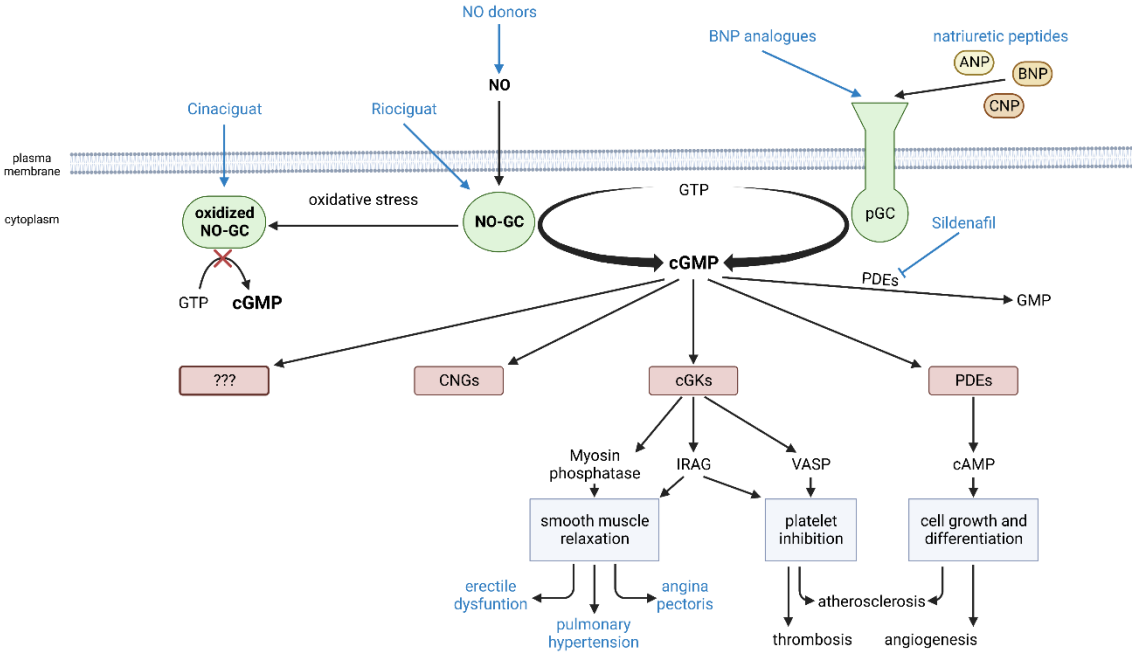

Figure 5: Overview of the cGMP Signaling Pathway. The cGMP signaling pathway involves two distinct guanylyl cyclases (green): the NO-GC (previously sGC) and transmembrane particulate guanylyl cyclases (pGCs). Nitric oxide (NO), produced by NO synthases (NOSs), activates the NO-GC, while pGCs are activated by natriuretic peptides like ANP, BNP or CNP. Effectors of cGMP signaling (red squares) include cyclic nucleotide-gated channels (CNGs), cGMP-dependent protein kinases (cGKs), phosphodiesterases (PDEs), and other unidentified proteins. PDEs hydrolyze cGMP to GMP. Cellular functions (grey boxes) involving cGMP include smooth muscle cell relaxation, platelet inhibition and regulation of cell growth and differentiation Modulation of the cGMP pathway is achieved through specific drugs (blue), such as sGC activators like cinaciguat targeting oxidized NO-GC, sGC stimulators like riociguat stimulating non-oxidized NO-GC, BNP analogues binding to the pGC GC-A, and Sildenafil inhibiting PDE5-mediated cGMP degradation. Created with BioRender.com. Modified from Feil & Kemp-Harper, 2006[70].

In the medical field, a variety of drugs targeting the cGMP signaling pathway have been approved for therapeutic use, particularly those that increase cGMP levels for the treatment of cardiovascular diseases **(Figure 5)**. Some notable examples include sildenafil for erectile dysfunction, organic nitrates for angina, and riociguat for specific types of severe pulmonary hypertension[71]. These drugs work by increasing cGMP concentrations in different ways. For instance, riociguat activates the NO-sensitive ferrous form (Fe^{2+}) of the NO-GC while cinaciguat targets the NO-insensitive oxidized ferric form (Fe^{3+}) or heme-free state of the NO-GC[71,72]. Due to the markedly increased plasma BNP and serum N-terminal proBNP levels in patients with heart failure, their potential as biomarkers in heart failure was investigated and has led to their establishment as a diagnostic tool and for predicting prognosis of these diseases[73,74]. Moreover, BNP analogues also induce cGMP generation through the pGCs and recombinant human BNP (nesiritide) is used as treatment for acute heart failure[74]. PDE5 inhibitors such as sildenafil and tadalafil, on the other hand, decrease the breakdown of cGMP, mainly resulting in smooth muscle relaxation and are used to treat erectile dysfunction and pulmonary hypertension[71,75]. Despite the potential of the cGMP signaling pathway for drug development, many of the effects of the already approved drugs remain unclear.

1.4.1 cGMP signaling in platelets

Platelets play a crucial role in maintaining the integrity of the vascular system. In this regard, the regulation of platelet activity through cGMP signaling is a crucial mechanism that allows the body to respond to possible vessel occlusion, preventing harmful consequences such as thrombosis.

cGMP synthesis in platelets is exclusively triggered by the activation of sGC by NO, produced by eNOS in the endothelium[76]. Interestingly, platelet-activating agonists, such as von Willebrand factor (vWF), collagen, and thrombin, also trigger the elevation of cGMP in platelets[77–79].

The NO-induced elevation of cGMP in platelets affects several processes in platelets, including inhibition of cytoskeletal remodeling, intracellular calcium release, agonist-induced integrin activation, granule secretion, and TXA_2 synthesis and release[69,80,81].

There are three types of PDEs expressed in platelets that can break down cGMP, including PDE2, PDE3, and PDE5[79,80,82]. When cGMP binds to an allosteric site of PDE2, it promotes the allosteric stimulation of cGMP and cAMP hydrolysis. PDE3, on the other hand, is known as the "cGMP-inhibited" PDE, as cGMP can competitively inhibit cAMP breakdown. Thus, cGMP can modulate platelet activity also by regulating cAMP signaling through the stimulatory or inhibitory effect of cGMP on cAMP hydrolysis by PDE2 or PDE3[83]. Additionally, cGMP can enhance the catalytic activity of PDE5 by binding to its allosteric site, ultimately leading to its own degradation[84].

In addition to PDEs, cGMP transporters also play a role in removing cGMP from platelets by facilitating its efflux[85]. While platelets lack multidrug resistance proteins (MRPs) 5 and 8, they are known to contain high levels of MRP4 within their dense granules, as well as lower levels in their plasma membrane, which mediates cGMP efflux[79,86,87].

Platelets also express substrates of the main cGMP effector cGKI, such as vasodilator-stimulated phosphoprotein (VASP) and inositol-1,4,5-trisphosphate (IP_3) receptor-associated cGMP kinase substrate (IRAG). Both substrates have

been demonstrated to inhibit platelet aggregation[88,89]. IRAG suppresses intracellular Ca^{2+} release by forming a complex with cGKI and the IP_3 receptor type 1[88,90], while VASP is phosphorylated at Ser157 and Ser239, playing an inhibitory role in actin fiber formation, a crucial process in cytoskeletal remodeling and platelet shape change, and integrin $\alpha_{IIb}\beta_3$ activation[89,91,92].

Most of our understanding of the cGMP signaling pathway in platelets is derived from *in vitro* studies. Consequently, extrapolating the findings from these experiments to the *in vivo* context poses challenges in terms of interpretation. A recent study utilized transgenic cGMP sensor mice to investigate cGMP signaling in real-time under flow conditions, aiming to overcome the limitations of *in vitro* analyses of platelets. The study revealed that cGMP generation in pre-activated platelets in the presence of NO was largely shear dependent. Additionally, cGMP levels were analyzed *in vivo* using an intravital imaging setup, and it was observed that platelet cGMP signals were more intense in the periphery of the forming thrombus after a mechanical or laser-induced injury of a vessel[93].

Importantly, it is now increasingly evident that the NO-cGMP signaling cascade in fact plays biphasic roles in platelet activation and besides being a major mechanism for platelet inhibition, cGMP is involved in the activation induced by different receptor signaling pathways[76,78].

Therefore, the dynamic flow-regulated NO-cGMP signaling might indeed act as both a self-regulating gas and brake for optimal platelet activation, making it a promising target for antithrombotic therapy with reduced bleeding risk.

1.4.2 cGMP signaling and hemolysis

cGMP is a critical signaling molecule in various physiological processes, including blood homeostasis. In hemolytic conditions, such as SCD, cGMP signaling plays a crucial role in disease pathogenesis as impaired NO metabolism is a significant aspect of its pathophysiology[94]. Chronic intravascular hemolysis leads to the release of free heme and hemoglobin, which binds to NO, causing its depletion[95]. Moreover, arginase, released by lysed erythrocytes, destroys L-arginine, leading to further depletion of endothelial NO, resulting in endothelial dysfunction and vasoconstriction[96]. Consequently, cGMP production is impaired, leading to increased platelet aggregation and vaso-occlusion.

Studies in mice have provided further insight into the role of cGMP signaling in hemolytic anemia. Mice deficient in the cGKI show anemia, splenomegaly, and increased susceptibility to hemolysis. These findings suggest that cGMP signaling through cGKI is essential for erythrocyte survival[97].

Given the critical role of cGMP in SCD pathogenesis, several studies have investigated the therapeutic potential of cGMP modulation in treating the disease. One study evaluated the use of the sGC stimulator olinciguat in mouse models of SCD. The results showed that olinciguat treatment reduced inflammation, vaso-occlusion, and nephropathy, indicating its potential use in treating SCD[98].

Other studies have focused on the role of cGMP signaling in regulating blood flow and preventing vaso-occlusion. One study investigated the use of nitrite, a source of NO, as a potential therapy for SCD. The study showed that nitrite administration reduced vaso-occlusion and improved blood flow in SCD patients[99].

In conclusion, cGMP signaling plays a crucial role in hemolysis and SCD pathophysiology and indeed cGMP modulation might be an option for pharmacotherapy for SCD and other hemolytic conditions[100].

1.5 Aim of the work

The main objective of this work is to gain further insight into the mechanism of hemin-induced platelet activation and identify the signaling pathways involved in this process. Although classic COX and $P2Y_{12}$ inhibitors, such as indomethacin or cangrelor, have no effect on hemin-induced platelet activation, there may be other inhibitory pathways involved during ferroptosis in platelets. Since the relationship between cGMP and hemin-induced ferroptosis of platelets is not well understood and the cGMP signaling has a significant role in hemolysis and SCD pathophysiology, this study aims to investigate the potential therapeutic effects of cGMP stimulators and activators against hemin-induced ferroptosis in platelets.

To accomplish these objectives, we utilized conventional techniques to assess platelet activation and thrombus formation such as light transmission aggregometry, ATP release, calcium release and perfusion experiments on immobilized collagen. Furthermore, we incorporated Raman microscopy to visualize hemin binding on platelets and assess morphological changes associated with hemin-induced activation. Additionally, we utilized flow cytometry to examine alterations in platelet surface receptors and evaluated the effect of hemin-induced platelet activation and the sGC stimulator riociguat on the platelet lipidome, as lipid peroxidation is a significant aspect of ferroptosis. Furthermore, we investigated the role of cGMP in hemin-induced platelet activation by using sGC knockout mice and blood samples from cAIHA patients, aiming to translate the research findings into clinical applications and contribute to our understanding of platelet dysfunction and therapeutic strategies for managing thrombotic complications.

2 Material and methods

2.1 Material

2.1.1 Equipment

Table 1: List of used equipment.

Description	Equipment	Company
Centrifuges	Centrifuge 5417R	Eppendorf SE, Hamburg, Germany
	Multifuge 1S	Thermo-Fisher Scientific, Waltham, MA, USA
	Rotina 420R	Andreas Hettich GmbH & Co. KG, Tuttlingen, Germany
	Multifuge 3S+	Thermo-Fisher Scientific, Waltham, MA, USA
Flow chamber	Flow chamber 5 µm	Maastricht Instruments BV, Maastricht, Netherlands
Flow cytometer	BD FACS CALIBUR	BD Biosciences, Franklin Lakes, NJ, USA
Fluorescence microscope	Nikon Eclipse Ti2	Nikon Instruments Europe BV, Amsterdam, Netherlands
Hematology analyzer	KX-21N	Sysmex Deutschland GmbH, Norderstedt, Germany
Incubator	Sanyo - CO_2 Incubator	Sanyo Chemical Laboratory, Kyoto, Japan
Light transmission aggregometer	Chrono-Log Modell 700	Chrono-Log Corporation, Haverton, PA, USA

Luminescence Spectrophotometer	Perkin Elmer LS-55	PerkinElmer, Inc., Waltham, Massachusetts, USA
Magnetic stirrer	IKAMAG®RH	IKA Werke GmbH, Staufen im Breisgau, Germany
	IKAMAG®RET-GS	IKA Werke GmbH, Staufen im Breisgau, Germany
Microplate Reader - ELISA	Bio-RAD Model 550 Microplate Reader	Bio-RAD Laboratories Inc., Hercules, CA, USA
Microplate Reader - Protein determination	Glomax Multi Detection System	Promega Corporation, Fitchburg, WI, USA
Microscope camera	Nikon DS-Qi2	Nikon Instruments Europe BV, Amsterdam, Netherlands
Odyssey® infrared scanner	Li-Cor® Biosciences	Li-Cor® Biosciences, Bad Homburg, Germany
PCR cycler	Flex Cycler Block T48	analytik Jena, Jena, Germany
Perfusor	KDS100 laboratory syringe pump	KD Scientific Inc., Holliston, Massachusetts, USA
pH Meter	HI 9025	Hanna Instruments, Woonsocket, Rhode Island, USA
Power supply – Western Blot	Bio-RAD PowerPac Basic	Bio-RAD Laboratories Inc., Hercules, CA, USA
Raman microspectroscope	Alpha300R	WITec, Ulm, Germany
Sterile bench	Herasafe^{TM}, Type HS18	Heraeus Holding GmbH, Hanau, Germany

Table centrifuge	Color Sprout Plus Mini-Zentrifuge	Biozym Scientific GmbH, Hessisch Oldendorf, Germany
Thermomixer	Thermomixer comfort	Eppendorf SE, Hamburg, Germany
Vortex mixer	IKA®MS3 digital	IKA Werke GmbH, Staufen im Breisgau, Germany
Western Blot system	Bio-RAD MiniPROTEAN® Tetra Cell	Bio-RAD Laboratories Inc., Hercules, CA, USA
White light excitation source	SOLA light engine	Lumencor, Inc., Beaverton, Oregon, USA

2.1.2 Reagents and buffers

Table 2: List of used reagents.

Reagents	Company
2-Mercaptoethanol	Sigma-Aldrich, St. Louis, MO, USA
ADP	Sigma-Aldrich, St. Louis, MO, USA
Agarose	Bioenzym, Hessisch Oldendorf, Germany
Albumin (BSA) Fraction V (pH 7,0)	AppliChem GmbH, Darmstadt, Germany
Ammonium persulfate (APS)	Carl Roth, Karlsruhe, Germany
Apyrase	Sigma-Aldrich, St. Louis, MO, USA
ATP- standard solution	Chrono-Log Corporation, Havertown, PA, USA
BD FACS Clean Solution	BD Biosciences, Franklin Lakes, NJ, USA
BD FACS Rinse Solution	BD Biosciences, Franklin Lakes, NJ, USA

BD FACSFlow Sheath Fluid	BD Biosciences, Franklin Lakes, NJ, USA
Bio-Rad Protein Assay Dye Reagent	Bio-RAD Laboratories Inc., Hercules, CA, USA
Bovine Serum Albumin (BSA)	AppliChem GmbH, Darmstadt, Germany
Calcium chloride ($CaCl_2$)	Merck Group, Darmstadt, Germany
Cinaciguat	MedChemExpress, Princeton, New Jersey, USA
Citric acid	SIGMA-ALDRICH, Co., St. Louis, Missouri, USA
Collagen-related Peptide (CRP-XL)	Richard Farndale, University of Cambridge, United Kingdom
D (+) Saccharose	Carl Roth, Karlsruhe, Germany
DEA/NO	Abcam, Cambridge, United Kingdom
Dulbeccos Phosphate Buffered Saline (Modified, without $CaCl_2$ and $MgCl_2$)	SIGMA-ALDRICH, Co., St. Louis, Missouri, USA
Dulbeccos Phosphate Buffered Saline (With $CaCl_2$ and $MgCl_2$)	SIGMA-ALDRICH, Co., St. Louis, Missouri, USA
Fibrinogen	Sigma-Aldrich, St. Louis, MO, USA
Formaldehyd 4%	Otto Fischar GmbH & Co KG, Saarbrücken, Germany
Fura-2 acetoxymethylester	Invitrogen, Carlsbad, California, USA
Glucose	Carl Roth GmbH + Co. KG, Karlsruhe, Germany
GoTaq® G2 Flexi DNA Polymerase	Promega, Madison, Wisconsin, USA
Hemin	SIGMA-ALDRICH, Co., St. Louis, Missouri, USA

Hepes	SIGMA-ALDRICH, Co., St. Louis, Missouri, USA
Hydrochloric acid (HCl)	Carl Roth, Karlsruhe, Germany
Isopropanol	Merck AG, Darmstadt, Germany
Kollagen HORM	Takeda Austria GmbH, Linz, Austria
Methanol	Merck AG, Darmstadt, Germany
My Taq HS Red Mix, 2x	BioCat GmbH, Heidelberg, Germany
ODQ	SIGMA-ALDRICH, Co., St. Louis, Missouri, USA
Pluronic F-127	Biotium, Hayward, California, USA
Potassium chloride (KCl)	Carl Roth GmbH + Co. KG, Karlsruhe, Germany
Prostaglandin I_2	Merck AG, Darmstadt, Germany
Protease/Phosphatase Inhibitor	Cell Signalling Technology, Danvers, MA, USA
Protein marker - Precision Plus Dual Color	Bio-RAD Laboratories Inc., Hercules, CA, USA
Riociguat	Ambeed, Inc., Arlington Heights, Illinois, USA
SKF-solution	Takeda Austria GmbH, Linz, Austria
Sodium chloride (NaCl)	Carl Roth GmbH + Co. KG, Karlsruhe, Germany
Sodium citrate ($Na_3C_6H_5O_7$)	AppliChem GmbH, Darmstadt, Germany
Sodium dodecyl sulfate (SDS)	Carl Roth, Karlsruhe, Germany
Sodium hydrogen carbonate ($NaHCO_3$)	Merck Group, Darmstadt, Germany
Sodium hydroxide (NaOH)	Carl Roth, Karlsruhe, Germany
TBS tablets	Carl Roth, Karlsruhe, Germany
TEMED	Carl Roth, Karlsruhe, Germany
Triton X-100	Sigma-Aldrich, St. Louis, MO, USA
Tween®20	Merck AG, Darmstadt, Germany

Table 3: List of used buffers.

Name	Composition
ACD buffer	116 mM sodium citrate 70 mM citric acid 110 mM glucose adjust pH to 4.6 with NaOH
Annexin V binding buffer	10 mM Hepes 140 mM sodium chloride 2.5 mM calcium chloride ad 1000 ml H_2O adjust pH to 7.4 with NaOH
10x blot buffer	25 mM Tris 150 mM Glycin ad 1000 ml H_2O
1x blot buffer	100 ml 10x blot buffer 200 ml Methanol ad 1000 ml H_2O
SDS loading buffer (5x Laemmli)	6,5 ml 1 M Tris-HCl pH 6,8 2 ml 10 %iges SDS 1 ml Glycerin 1 Spatula tip Bromophenol blue before use + 25 µl β-mercaptoethanol
10x SDS running buffer	25 mM Tris 193 mM Glycin 1 % SDS ad 1000 ml H_2O
1x SDS running buffer	100 ml 10x Laufpuffer ad 1000 ml H_2O
PBS-T	1000 ml PBS Gibco 0,5 ml Tween-20

TBS-T	2 TBS tablets 0,05 % Tween®20 (v/v) ad 1000 ml H_2O
10x Tyrode buffer	1,34 M sodium chloride 119 mM sodium bicarbonate 2,68 mM potassium chloride ad 1000 ml H_2O filter sterile, store at 4°C
1x Tyrode buffer	10 ml 10x Tyrode buffer ad 100 ml H_2O 0,1 g BSA 0,1 g D-(+)-Glucose adjust pH to 6.5 with Hepes adjust pH to 7.4 with HCl

2.1.3 Consumables

Table 4: List of used consumables.

Consumables	Company
1 ml syringes	B. Braun Melsungen AG, Melsungen, Germany
5 ml syringes	B. Braun Melsungen AG, Melsungen, Germany
10 ml syringes	B. Braun Melsungen AG, Melsungen, Germany
12-well chamber	ibidi GmbH, Gräfelfing, Germany
15 ml Polypropylen Tubes	Greiner Bio-One GmbH, Frickenhausen, Germany
20 ml syringes	B. Braun Melsungen AG, Melsungen, Germany
50 ml Polypropylen Tubes	Greiner Bio-One GmbH, Frickenhausen, Germany
Aggregometry cuvettes	Chrono-log Havertown, PA, US
Citrat Monovettes	Sarstedt AG & Co., Nümbrecht, Germany
CPDA Monovettes 8.5 ml	Sarstedt AG & Co., Nümbrecht, Germany

Eppendorf Tubes	Eppendorf AG, Hamburg, Germany
FACS tube	BD Biosciences, Franklin Lakes, NJ, USA
Injectomat Line, 200 cm	Fresenius Kabi Deutschland GmbH, Bad Homburg, Germany
Membrane adapter	Sarstedt AG & Co., Nümbrecht, Germany
Microscope Cover Glasses (24 x 60 mm)	Paul Marienfeld GmbH, Lauda-Königshofen, Germany
Pipette tips	Greiner Bio One, Frickenhausen, Germany
Pur-Zellin®	PAUL HARTMANN AG, Heidenheim, Germany
PVDF-Membrane	Merck AG, Darmstadt, Germany
Reaction vials 1.5 ml black	Carl Roth GmbH + Co. KG, Karlsruhe, Germany
Reaction vials 2 ml	Sarstedt AG & Co., Nümbrecht, Germany
Safety-Multifly	Sarstedt AG & Co., Nümbrecht, Germany
Serological pipettes	Corning Incoporated, Corning, USA
Single-use capillaries	Hirschmann Laborgeräte GmbH, Eberstadt, Germany
Stir bars	Chrono-log Havertown, PA, US
Whatman™ *Blotting Paper*	GE Healthcare, Chicago, IL, USA

2.1.4 Antibody

Table 5: List of used antibodies.

Antibody	**Company**
Flow Cytometry	
anti-CD62P PE	Beckman Coulter, Brea, California, USA
anti-PAC-1 FITC	BD Bioscience, San Jose, California, USA
anti-CD41 FITC	Miltenyi Biotec, Bergisch Gladbach, Germany
anti-CD61 FITC	Miltenyi Biotec, Bergisch Gladbach, Germany

Fibrinogen FITC	Sigma-Aldrich, St. Louis, Missouri, USA
Annexin V FITC	ImmunoTools GmbH, Friesoythe, Germany
Tetramethylrhodamin, Ethylester, Perchlorat (TMRE)	Invitrogen, Waltham, Massachusetts, USA
BODIPY 581/591 C11	Invitrogen, Waltham, Massachusetts, USA
2′,7′-Dichlorfluorescein-Diacetat (DCF DA)	Sigma-Aldrich, St. Louis, Missouri, USA
Immunoblot	
anti-pVASP	Cell Signaling Technology, Danvers, Massachusetts, USA
IRDye 800CW goat anti-rat	Li-Cor Bioscience GmbH, Nebraska, USA
IRDye 680RD donkey anti-rabbit	Li-Cor Bioscience GmbH, Nebraska, USA
GAPDH	Cell Signaling Technology, Danvers, Massachusetts, USA
AKT	Cell Signaling Technology, Danvers, Massachusetts, USA
pAKT	Cell Signaling Technology, Danvers, Massachusetts, USA

2.1.5 Software

Table 6: List of used software.

Software	Company
Aggro/Link 5.1.2	Chrono-log Corporation, Havertown, Pennsylvania, USA
BioRender	Science Suite Inc., Toronto, Ontario, Canada
CellQuest Pro, Version 5.3.3f4b	BD Biosciences, San Jose, California, USA
Citavi	Swiss Academic Software, Wädenswil, Switzerland
FlowJo Version 10.5.3	BD Biosciences, San Jose, California, USA
FL Winlab 4.0.12	PerkinElmer, Inc., Waltham, Massachusetts, USA
GraphPad Prism (Version 9.1.2)	GraphPad Software, San Diego, California, USA
ImageJ (Version 1.53a)	National Institutes of Health, Bethesda, Maryland, USA
NIS-Elements AR (Version 5.21.00)	Nikon Instruments Europe BV, Amsterdam, Netherlands
NIS-Elements BR (Version 5.21.00)	Nikon Instruments Europe BV, Amsterdam, Netherlands
QuantumCapt 16.07	Quantum Cooperation, San Jose, California, USA

2.2 Methods

2.2.1 Isolation of human platelets

To isolate human platelets, 16 ml of venous blood was collected from voluntary donors free of platelet-affecting drugs for at least 10 days using a Safety-Multifly 21G needle into syringes containing 4 ml of acid-citrate-dextrose (ACD) buffer. The ACD-anticoagulated blood was then centrifuged at 209 x g for 20 min at room temperature (RT) without brakes. The resulting platelet-rich plasma (PRP) was transferred to a Falcon™ tube containing 35 ml modified Tyrode-HEPES buffer (137 mM NaCl, 2.8 mM KCl, 12 mM $NaHCO_3$, 5 mM glucose, 10 mM HEPES, 0.1 % BSA, pH 6.5) followed by a second centrifugation at 430 x g for 10 min at RT to obtain the platelet pellet. The supernatant was discarded, the platelet pellet was resuspended in Tyrode's buffer pH 7.4 and the platelet count was determined using a Sysmex hematology analyzer. Subsequently, the platelet count was adjusted to the desired level for various experimental purposes.

2.2.2 Preparation of human platelet rich plasma

To obtain human PRP for experiments, venous blood was collected from volunteer donors who had not taken any platelet-affecting drugs for at least 10 days. Citrate-phosphate-dextrose adenine (CDPA) monovettes were used for flow cytometry experiments, while citrate monovettes were used for aggregation experiments. The collected blood samples were centrifuged at 204 x g for 20 minutes at room temperature, and the upper phase containing PRP was carefully collected.

2.2.3 Study patients

Patients with autoimmuno hemolysis were admitted to the Department of Cardiology of the University of Tübingen, Germany. All subjects gave written informed consent. Collected blood samples were immediately processed and analyzed for aggregation levels by light transmission aggregometry (see 2.2.12).

2.2.4 Isolation of murine platelets

For the isolation of murine platelets, blood was collected from 8 – 12 week old mice. Mice were anesthetized with isoflurane and at least 1 ml blood was drawn from the retro-orbital plexus into a tube containing 300 µl of ACD buffer using a heparin-coated capillary. After bleeding, a cervical dislocation was subsequently performed on the mouse. Subsequently, blood samples were then centrifuged at 260 x g for 5 minutes at room temperature without braking. PRP settled as the upper phase, which was carefully transferred to a new reaction tube along with a small portion of the lower phase. To ease platelets, apyrase (0.02 U/ml and prostaglandin I_2 (0.5 µM) were added to the PRP. After further adding 200 µl of Tyrode's buffer pH 7.4, the PRP was centrifuged again at 52 x g without braking for 6 minutes at room temperature. The upper phase was collected and transferred to a new reaction tube. The remaining lower phase was mixed with 200 µl of Tyrode's buffer pH 7.4 and centrifuged again at 52 x g without braking for 6 minutes at room temperature. The clear supernatants were combined and centrifuged at 640 x g for 5 minutes at room temperature. The supernatant was discarded and the remaining platelet pellet was resuspended and washed in Tyrode-HEPES buffer pH 7.4. The platelet count in the platelet suspension was determined using the Sysmex hematology analyzer and adjusted to the desired number with Tyrode's buffer pH 7.4.

2.2.5 Determination of protein concentration (Bradford assay)

The protein concentration of lysates was quantified using Bradford assays. To perform the assay, a 1:30 dilution of the lysates was prepared, and then 10 µl of the diluted lysates were mixed with the Bradford reagent. The shift in the absorption spectrum from 470 nm to 595 nm, resulting from the reaction of the proteins in the lysate with the Bradford reagent, was quantitatively evaluated by photometric analysis using a BSA standard curve.

2.2.6 Enzyme-Linked Immunosorbent Assay (ELISA)

The cGMP concentration of differently treated isolated platelets was quantified using the cGMP Enzyme-linked Immunosorbent Assay (ELISA) kit from Enzo Life Sciences. For the determination of cGMP content in platelets, a pellet of 2 x 10^8 isolated platelets (see 2.2.1) was lysed in 20 µl 3.3 M HCl. The lysate was then centrifuged without braking at 600 x g for 10 minutes at RT. The supernatant was collected and 200 µl of cGMP assay buffer was added. The sample was shock-frozen in liquid nitrogen and stored at -80°C until the assay was performed as stated in the manufactures protocol.

2.2.7 Protein separation by SDS-PAGE

Proteins were separated based on their size using the sodium dodecyl sulfate-polyacrylamide gel electrophoresis (SDS-PAGE). To initiate the separation process, the proteins of interest were mixed with a reducing buffer containing SDS (Laemmli buffer with β-mercaptoethanol) and denatured by incubating them at 95°C for 10 minutes, allowing their protein structure to unfold. This denaturation process was crucial for achieving a uniform charge on the linear protein chains. To facilitate the separation, negatively charged sodium dodecyl sulfate was introduced, effectively overlaying the inherent charge of the proteins. The resulting mixture was loaded into a polyacrylamide gel, which was then subjected to an electric field. In this study, polyacrylamide gels with different acrylamide concentrations were employed: 1%, 12.5% and 15% in the separating gel, and 5% in the stacking gel. The protein samples, after being incubated with the reducing buffer, were carefully pipetted into the wells of the stacking gel. An electric field was applied, and as the proteins migrated through the stacking gel, they initially reached a common position at the gel interface before further separation occurred in the separating gel.

The stacking gel was prepared as follows:

Table 7: Ingredients for the stacking gel - final volume 5 ml.

Substances	**Volumes for a stacking gel**
Destilled H_2O	3, 4 ml
Acylamide/Bis solution (30 %)	830 µl
1.5 M TRIS pH 8.8	-
1 M TRIS pH 6.8	630 µl
10 % (w/v) SDS	50 µl
10 % (w/v) Ammonium persulfate	50 µl
TEMED	5 µl

The stacking gel, located beneath the separating gel, allowed for the precise determination of protein size. A protein size marker was applied to serve as a reference for the size of the proteins of interest.

Table 8: Ingredients for the separating gel - final volume 5 ml.

Substances	**Volumes for a 10% separating gel**
Destilled H_2O	4 ml
Acylamide/Bis solution (30 %)	3,3 ml
1.5 M TRIS pH 8.8	2,5 ml
1 M TRIS pH 6.8	-
10 % (w/v) SDS	100 µl
10 % (w/v) Ammonium persulfate	100 µl
TEMED	4 µl

Once the samples were loaded into the stacking gel, an initial voltage of 80 V was applied for 30 minutes. Subsequently, the voltage was increased to 120 V, and the protein bands continued to migrate until they reached the lower edge of the gel.

2.2.8 Protein detection by immunoblotting (Western blot)

The proteins separated in the gel were transferred onto a polyvinylidene fluoride (PVDF) membrane for further detection using the Western blot method. There are two different transfer methods, Semi-Dry and Wet Blot. In this study the Wet-Blot method was used.

Therefore, the hydrophobic PVDF membrane was activated in methanol for 5 minutes. Subsequently, the gel, activated membrane, and Whatman paper were assembled in the Wet-Blot or chamber, allowing the proteins to migrate from the gel onto the membrane in the direction of the anode under an applied voltage. A voltage of 115 V was applied for 75 minutes.

Following the transfer, the membrane was incubated for 1 hour at room temperature in a blocking solution (Roti®-Block) on a shaker. Then, the primary antibody, diluted in the blocking solution, was incubated with the membrane overnight at 4°C for immune detection. Afterward, the membrane was washed three times for 10 minutes each with 20 ml of TBS + 0.1% Tween-20 (TBS-T). Subsequently, the membrane was incubated with the corresponding fluorophore-conjugated secondary antibody (1:15,000) for two hours at room temperature. To minimize nonspecific background signals, the membrane was washed again three times for 10 minutes each with 20 ml of TBS-T. Finally, the membrane was air-dried between dry Whatman paper for at least 2 hours. The fluorescence signal of the bound secondary antibody was detected using the LI-COR infrared imaging system.

2.2.9 Light transmission aggregometry

The aggregation of human platelets (see 2.2.1) were evaluated using the lumi-aggregometer Model 700 (Chrono-Log Corporation). A platelet suspension (8 x 10^7 platelets/sample) in Tyrode's buffer at pH 7.4 was incubated with 100 µg/ml fibrinogen and 2 mM $CaCl_2$ in a total volume of 500 µl in a glass cuvette with a stirring bar at 1000 RPM and 37°C. Following calibration, aggregation was recorded upon the addition of various agonists at different concentrations. This involved pre-incubation with 10 µM cangrelor, indomethacin, or eptifibatide at

37°C for 2 minutes. Alternatively, pre-incubation with riociguat was carried out at concentrations ranging from 220 nM to 25 µM for 5 min prior to further pre-incubate with 0.5 - 1 µM DEA/NO for 2 min at 37°C. As another option, a 10-minute pre-incubation with 10 µM ODQ was performed followed by 25 µM cinaciguat pre-incubation for 5 min at 37°C prior to the activation with hemin, ADP, or CRP-XL. The measurement was conducted for a duration of 5 minutes. The degree of aggregation was calculated as the percentage of light transmission through the platelet suspension at the beginning compared to the transmission after 5 minutes. Tyrode's buffer at pH 7.4 served as a reference. The analysis was performed using the AggroLink software and GraphPad Prism.

2.2.10 Light transmission aggregometry of patient samples

Measurement of platelet aggregation in patient samples was conducted using light transmission aggregometry. Platelet-rich plasma (PRP) obtained from autoimmune hemolytic patients or healthy individuals (see 2.2.2) was centrifuged to isolate plasma at 2561 x g for 10 min at RT. Platelets isolated from healthy individuals (see 2.2.1) were then resuspended in either healthy or patient plasma to obtain a concentration of 8 x 10^7 washed platelets per sample. In cases where specified, platelets were pre-treated with 220 nM riociguat for 5 min at 37°C, followed by further pre-incubation with 0.5 µM DEA/NO for 2 min at 37°C. Aggregation was induced by adding 2.5 - 5 µM ADP or 0.125 - 0.25 µg/ml CRP-XL, and the measurements were carried out for 5 min at 1,000 rpm and 37°C using the Model 700 lumi-aggregometer (Chrono-Log Corporation). The degree of aggregation was determined by calculating the percentage of light transmission through the platelet suspension at the beginning compared to the transmission after 5 minutes. Platelet-poor plasma (PPP) was used as a reference. Data analysis was performed using the AggroLink software and GraphPad Prism.

2.2.11 ATP release

The quantification of adenosine triphosphate (ATP) released by activated platelets was also performed using the lumi-aggregometer Modell 700 from Chrono-Log Corporation. Human isolated platelets (see 2.2.1) at a concentration of 50 x 10^6 platelets/sample in Tyrode's buffer (pH 7.4) were incubated with 100 µg/ml fibrinogen and 2 mM $CaCl_2$ and supplemented with 10 µl of luciferase solution. After calibration of one sample with 2.5 µl of an ATP standard solution, the ATP concentration of the remaining samples was determined. The system was calibrated to detect ATP concentrations as low as 0.2 nM by adjusting its sensitivity and subsequently, the ATP secretion from activated platelets in samples treated with either 6 µM hemin or 1 µg/ml CRP-XL was measured. In cases where specified, platelets were pre-incubated with 220 nM riociguat for 5 min at 37°C, followed by further pre-incubation with 0.5 µM DEA/NO for 2 min at 37°C. The measurements were carried out for a duration of 10 minutes, and data analysis was performed using the AggroLink software and GraphPad Prism.

2.2.12 Calcium measurement

The cytosolic calcium levels of isolated human platelets (see 2.2.1) were determined using a fluorescence-based method. Platelets were loaded with 5 µmol/ml Fura-2 acetoxymethylester and 0.2 µg/ml Pluronic F-127 for 30 min at 37°C to allow intracellular uptake of the calcium indicator. Where indicated, platelets were pre-incubated with 25 µM riociguat for 5 minutes. Subsequently, the loaded platelets were stimulated with 25 µM hemin and the resulting calcium responses were measured under stirring conditions using a spectrofluorometer (LS 55, PerkinElmer) in the presence (intracellular Ca^{2+} mobilization) or absence (extracellular Ca^{2+} influx) of 0.5 mM extracellular EGTA. The fluorescence emission was measured at alternate excitation wavelengths of 340 and 380 nm at 37 °C. The 340/380-nm ratio values were converted into nanomolar concentrations of Ca^{2+} by lysis with Triton X-100 and subsequently a surplus of EGTA. This allowed for accurate quantification of cytosolic calcium levels in the platelets according to the Grynkiewicz equation[101].

2.2.13 Flow chamber perfusion assay

Thrombus formation was visualized by fluorescent microscopy using a Nikon Eclipse Ti2-A and a flow chamber from Maastricht Instruments B.V. at low shear rates (500 s^{-1}). Cover slips were coated with 100 µg/ml collagen suspension for 2 h at RT or at 4°C over night. To prevent unspecific molecular binding to collagen, cover slips were blocked for 1 h at RT with 1 % BSA in PBS. Samples of 800 µl washed human platelets (see 2.2.1) were diluted with 200 µl PBS. Afterwards samples ($400x10^6$ platelets in total) were incubated with the fluorochrome 3,3´-dihexyloxacarbocyanine iodine (DiOC6) for 10 min at RT in the dark. 1 mM $CaCl_2$ were added and where indicated samples were pre-incubated with 220 nM riociguat for 5 min at RT before adding 0.5µM DEA/NO for 2 min at RT. Again, where indicated varying concentrations of hemin (ranging from 1.6 µM to 50 µM) were added immediately before perfusion at a flow rate of 4.25 ml/h, corresponding to a shear rate of 500 s^{-1}. After perfusion PBS was used to wash off non-adhesive residue. Images of four to five independently selected areas were taken after the perfusion. Quantitative analysis and data transformation were performed using NIS-Elements AR and GraphPad Prism.

2.2.14 Generation of erythrocyte lysates

For the generation of erythrocyte lysates 16 ml of blood was collected from volunteer donors using a syringe containing 4 ml of ACD to prevent coagulation. The blood was then centrifuged at 209 x g for 20 minutes. After the hematocrit level, indicated by the red lower layer, and the plasma level, indicated by the yellowish upper layer, were marked on the tube, the plasma was discarded and the tube was filled up to the marked line, representing the original level of plasma, with a 150 mM NaCl solution. The tube was capped and inverted a few times to mix the contents before centrifugation at 500 x g for 5 minutes. This process of washing the blood cells was repeated once more before the lysis was initiated by incubating the washed erythrocytes at RT for 5 minutes with distilled water. After incubation, the lysed erythrocytes were centrifuged once more at 500 x g for 5 minutes and the supernatant was transferred to a new tube for future use.

2.2.15 Flow cytometry

Isolated platelets (see 2.2.1) were obtained for performing flow cytometry of human platelets. After determining the cell count using the KX21N hematology analyzer, for each sample $1x10^6$ isolated platelets were incubated with fluorescently labeled primary antibodies, anti-CD62P-PE and PAC-1-FITC, Fibrinogen-FITC, anti-CD41-FITC or anti-CD61-FITC, in Dulbecco's phosphate-buffered saline (PBS) containing 0.5 mM $MgCl_2$ and 0.9 mM $CaCl_2$ at RT for 30 min in the dark to determine platelet activation and fibrinogen binding. Where indicated samples were subjected to pre-incubation with specific agents. This involved pre-incubation with 10 µM cangrelor, indomethacin, or eptifibatide at room temperature for 2 minutes. Alternatively, pre-incubation with riociguat was carried out at concentrations ranging from 220 nM to 25 µM for 5 min prior to further pre-incubate with 0.5 - 1 µM DEA/NO for 2 min at RT. As another option, a 10-minute pre-incubation with 10 µM ODQ was performed followed by 25 µM cinaciguat pre-incubation for 5 min prior to the activation with hemin. Where specified, platelets were exposed to hemin at concentrations ranging from 1.6 µM to 50 µM for 30 minutes. After the incubation period, platelets were fixed using 300 µl 0.5 % formaldehyde. Flow cytometry measurements were performed using a FACS Calibur instrument and the accompanying software. Data analysis was carried out using FlowJo software and GraphPad Prism.

To measure platelet apoptosis the annexin-V binding and mitochondrial transmembrane potential loss ($\Delta\Psi m$) were determined using flow cytometry. Isolated platelets (see 2.2.1) were adjusted to $1x10^6$ platelets per sample. Platelets were subjected to either resting conditions or treated with varying concentrations of hemin (ranging from 1.6 µM to 50 µM) for 30 minutes at RT to induce activation. Where indicated samples were subjected to pre-incubation with 220 nM riociguat for 5 min prior to further pre-incubate with 0.5 µM DEA/NO for 2 min at RT. Annexin V-FITC was used to assess the surface externalization of phosphatidylserine (PS), while tetramethylrhodamine ethyl ester (TMRE) was used to stain platelets for 30 minutes at room temperature in the dark to evaluate mitochondrial transmembrane potential loss.

After the incubation period, 300 µl annexin buffer was added to the Annexin V-FITC stained samples and 300 µl PBS to the TMRE stained samples. Flow cytometry measurements of the unfixed platelets were performed immediately using a FACS Calibur instrument and the accompanying software. Data analysis was carried out using FlowJo software and GraphPad Prism.

ROS generation in washed platelets from human platelets (see 2.2.1) was determined using flow cytometry. Platelets ($1x10^6$/sample) were preloaded with 10 µM 2′,7′-Dichlor-fluorescein-diacetat (DCFDH-DA) for general detection of all reactive oxygen and nitrogen species. The preloading step was carried out for a duration of 30 minutes in the dark at room temperature while maintaining the platelets under resting conditions or treating them with hemin (ranging from 1.6 µM to 50 µM). Where indicated samples were subjected to pre-incubation with 220 nM riociguat for 5 min prior to further pre-incubate with 0.5 µM DEA/NO for 2 min at RT. Following the incubation period, 300 µl PBS were added and the samples were promptly analyzed using a FACS Calibur instrument and the accompanying software. Data analysis was carried out using FlowJo software and GraphPad Prism.

To detect lipid peroxidation, $1x10^6$ platelets/sample (see 2.2.1) were preloaded with the C-11-BODIPY 581/591 sensor at a concentration of 5µM for a duration of 30 minutes at room temperature in the dark. The platelets loaded with the lipid peroxidation sensor were either maintained under resting conditions or treated with hemin (ranging from 1.6 µM to 50 µM) for 30 min at room temperature. In cases where specified, the platelets were pre-treated with 220 nM riociguat for 5 min prior to further pre-incubate with 0.5 µM DEA/NO for 2 min at RT. After the incubation period, 300 µl PBS were added and the samples were immediately analyzed using a FACS Calibur instrument and the accompanying software. Data analysis was carried out using FlowJo software and GraphPad Prism.

2.2.16 Lipidomics

For lipid extraction, washed platelets were isolated (see 2.2.1) and 2 x 10^8 platelets/sample was resuspended in cold (4°C) isopropanol and water mixture (IPA/H_2O, v/v, 90/10) with spiked internal standard mixtures (EquiSPLASH™ LIPIDOMIX® Quantitative Mass Spec Internal Standard from Avanti Polar Lipids (Alabaster, AL, USA)) and subjected to gentle sonication for lysis while maintaining a low temperature (5 cycles for 2 min sonication). All sample preparation steps were performed under light protection. After centrifugation to remove cellular debris, the extracted supernatants were then dried with an EZ2 evaporator from GeneVac (Ipswich, UK) under nitrogen protection and reconstituted in 100 µl of cold (4°C) methanol. Following centrifugation, the supernatant was transferred into High-Performance Liquid Chromatography (HPLC) vials for UHPLC-ESI-QTOF-MS/MS analysis. A pooled quality control sample was prepared by mixing 15 µl aliquots of each re-constituted samples.

The lipid extract was analyzed using an Agilent 1290 UHPLC instrument hyphenated to a Sciex TripleTOF 5600+ hybrid mass spectrometer. Chromatographic separation was performed on ACQUITY UPLC CSH C18 column (100 mm × 2.1 mm; particles: 1.7 µm; Waters Corporation, Millford, MA, USA) with precolumn (5 mm x 2.1 mm; 1.7 µm particles). The column temperature was 65°C and the flow rate 0.6 ml/min. Mobile phase A was composed of H_2O/ACN 2:3 (v/v) containing 10 mM ammonium formate and 0.1% formic acid (v/v) while mobile phase B was IPA/ACN/H_2O 90:9:1 (v/v/v) containing 10 mM ammonium formate and 0.1% FA (v/v). The gradient elution started from 15% B to 30% B in 2 min, followed by increase of B to 48% in 0.5 min. Then mobile phase B was further increased to 82% at 11 min and quickly reached 99% in the next 0.5 min followed by holding this percentage for another 0.5 min. Afterwards, the percentage of B was back to starting conditions (15% B) in 0.1 min to re-equilibrate the column for the next injection (2.9 min).

The mass spectrometer operated in electrospray ionization (ESI) positive mode with specific parameters. An MS full scan experiment with mass range m/z 50-1250 was selected while different SWATH windows were acquired for MS/MS experiments (**Table 9**). The ion source temperature was set to 350°C with curtain

gas (CUR, nitrogen), nebulizer gas (GS1, zero grade air) and heater gas (GS2, zero grade air) pressures 35 psi, 60 psi and 60 psi, respectively, for both modes. The ion spray voltage was set to 5500 V in the positive mode and -4500 V in negative mode. The declustering potential was adjusted to 80 V and -80 V for positive and negative polarity mode, respectively. The cycle time was always 720 ms.

Commercial software, including PeakView, MasterView, and MarkerView, along with freely available MS-DIAL, were used for data processing. Data processing involved the use of MS-DIAL for peak finding, Lipid Blast database search, normalization to internal standards and LOWESS, and identification through spectral matching. MarkerView software was utilized for logarithmic transformation (base 10) and autoscaling.

Table 9: MS parameters.

			ESI (+)			ESI (-)		
Experiment	Scan typ	Acc. Time (ms)	Start (m/z)	Stop (m/z)	CE (V)	Start (m/z)	Stop (m/z)	CE (V)
1	MS Full Scan	50	50	1250	10	50	1250	-10
2	SWATH	31	50	217.6	45±15	50	213.5	-45±15
3	SWATH	31	216.6	340.3	45±15	212.5	271.4	-45±15
4	SWATH	31	339.3	441.4	45±15	270.4	314.6	-45±15
5	SWATH	31	440.4	524.9	45±15	313.6	382.6	-45±15
6	SWATH	31	523.9	571.6	45±15	381.6	427.5	-45±15
7	SWATH	31	570.6	643.4	45±15	426.5	464.3	-45±15
8	SWATH	31	642.4	687.3	45±15	463.3	501	-45±15
9	SWATH	31	686.3	720.1	45±15	500	540.8	-45±15
10	SWATH	31	719.1	740.1	45±15	539.8	617.5	-45±15
11	SWATH	31	739.1	755	45±15	616.5	680.3	-45±15
12	SWATH	31	754	764.1	45±15	679.3	697.1	-45±15
13	SWATH	31	763.1	775.1	45±15	696.1	724	-45±15
14	SWATH	31	774.1	786.1	45±15	723	749	-45±15
15	SWATH	31	785.1	793.1	45±15	748	775.6	-45±15
16	SWATH	31	792.1	806.1	45±15	774.6	793.1	-45±15
17	SWATH	31	805.1	814.2	45±15	792.1	811	-45±15
18	SWATH	31	813.2	829.6	45±15	810	832.6	-45±15
19	SWATH	31	828.6	842.7	45±15	831.6	854.1	-45±15
20	SWATH	31	841.7	903.3	45±15	853.1	861.2	-45±15
21	SWATH	31	902.3	1250	45±15	860.2	1050	-45±15

2.2.17 Raman

Raman measurements were conducted using a commercial Raman microspectroscope system (Alpha300R, WITec). The system included a 532-nm laser, a filter to separate scattered light from the excitation light, and a CCD camera (1,024 × 127 pixels) for spectrum detection. Samples were hydrated with DPBS and observed through a 63× dipping objective with a numerical aperture of 1. The laser light scattered from the samples was collected by the objective and detected by the CCD camera. To minimize potential artifacts, the entire system was operated in a dark room, and the CCD cameras were cooled to -60°C. Prior to measurements, the performance of the Raman microspectroscope was validated using a silicon wafer. The samples were excited with a laser power of 60 mW, and the scattered signal was analyzed using a grating of 1,800 g/mm centered at 1,300 rel. 1/cm. The microscope was equipped with a fluorescence filter set for visualizing stained tissues. All samples were maintained in DPBS before and during the Raman measurements.

For the experimental setup, 100 µl of washed platelets with 1 mM $CaCl_2$ were placed in each well of a 12-well chamber (ibidi GmbH). The samples were pre-incubated with 220 nM riociguat for 5 min at room temperature (RT), followed by the addition of 0.5 µM DEA for 2 min at RT. Additionally, 25 µM hemin was added for 30 min at RT in cases where indicated. After the incubation, the platelets were fixed using 0.5% formaldehyde, and the 12-well chamber was subjected to centrifugation at 500 x g for 10 min at RT. The supernatant was removed, and the samples were washed with PBS. For better identification the scan and a bright field image of the same area were overlapped.

2.2.18 PCR

To amplify desired DNA segments for subsequent experiments or analyses, the polymerase chain reaction (PCR) technique was employed using specific primers **(Table 10)**. DNA extraction from murine tissue samples was performed using the MyTaq™ Extract-PCR Kit (BioCat GmbH). For the PCR reaction, 2 µl of the isolated DNA were combined with 23 µl of a PCR buffer mixture **(Table 11)**.

Different PCR programs were used due to variations in optimal annealing temperature determined based on the melting points of the primers and variations in optimal polymerization time depending on the size of the DNA section to be polymerized **(Table 12)**.

Table 10: List of primers with their sequences.

Primer	Gene	Sequence (5' to 3')
Cre1	Pf4-Cre	CCCATACAGCACACCTTTTG
Cre2	Pf4-Cre	TGCACAGTCAGCAGGTT
Cre3	Pf4-Cre	CAAATGTTGCTTGTCTGGTG
Cre4	Pf4-Cre	GTCAGTCGAGTGCACAGTTT

Table 11: Composition of the PCR buffer mixture.

Substances	Volumes for 23µl PCR buffer mixture
My Taq HS Red Mix, 2x	12.5
Primer 1	1
Primer 2	1
Primer 3	1
(Primer 4)	1
Nuclease free water	add 23 µL

Table 12: Used PCR program.

Allele	Primers	Product size	PCR Program		
iCre	Cre1	cre+: 450 bp	95°C	3 min	
cre+	Cre2	and 200 bp	95°C	15 sec	35x
cre-	Cre3	cre-: 200 bp	55°C	15 sec	
	Cre4		72°C	15 sec	
			72°C	10 min	
			4°C	∞	

2.2.19 Gel electrophoresis

Gel electrophoresis was employed to separate and detect DNA fragments based on their size following PCR or restriction digestion in an agarose gel. Specifically, agarose gels with a concentration of 1.5% (w/v) in TAE buffer were utilized in this study. The DNA samples were separated by applying a voltage of 135 V for 35 minutes. Subsequently, the DNA within the gel was stained through incubation with an ethidium bromide solution. The resulting band pattern was detected under UV light and could be accurately classified based on size using a pre-pipetted DNA size marker.

2.2.20 Nanodrop

DNA concentration was determined using the NanoDrop ND-1000 device. In this method, 2 µl of the DNA solution being analyzed were pipetted onto the measurement unit, and the absorbance was measured at a wavelength of 260 nm. The DNA concentration of the sample was obtained by calculating the difference between the measured absorbance value and the blank value (absorbance of the solvent without DNA), applying the Lambert-Beer law.

2.2.21 Statistics

Graphs have been created with the GraphPad Prism software (version 9.1.2) and represent biological replicates as indicated in the figure legends. The data in this study underwent statistical analysis using GraphPad Prism software. Initially, the normality of the data was assessed.

For comparing two groups, either a two-tailed paired or unpaired t-test was used, depending on the experimental design. Differences within a single group were assessed using the one-way ANOVA with Dunnett’s test or Šídák's test as post-test respectively, depending on the experimental design. In cases where the data did not follow a normal distribution, a Mann-Whitney U test at 95% CI was applied. Statistical significance was assigned to results with *($p<0.05$), **($p<0.01$), ***($p<0.001$) and ****($p<0.0001$).

3 Results

3.1 Aggregation of platelets resuspended in plasma derived from patients with autoimmunohemolysis is enhanced

In vitro and *in vivo* studies have demonstrated that hemolysis exerts a potent activating effect on platelets, and various mechanisms have been proposed to explain this phenomenon including direct activation by hemoglobin, scavenging of nitric oxide by released hemoglobin, and release of intraerythrocytic ADP[102].

To evaluate the impact of plasma derived from patients with autoimmune hemolysis on platelet function, an experimental setup was designed involving the resuspension of platelets in plasma obtained from both patients and healthy controls and to measure platelet aggregation as an indicator of activation. To provoke platelet activation, two different concentrations of ADP, namely 2.5 µM and 5 µM, were employed as stimulating agents. The results revealed a noteworthy and statistically significant increase in light transmittance platelet aggregation when patient plasma was compared to control plasma ($p<0.01$) **(Figure 6)**. It is worth mentioning that even at the lower concentration of 2.5 µM ADP, samples treated with patient-derived plasma exhibited higher levels of aggregation than those treated with patient-derived plasma stimulated with 5 µM ADP. This compelling evidence highlights the presence of a pro-thrombotic effect associated with hemolytic plasma.

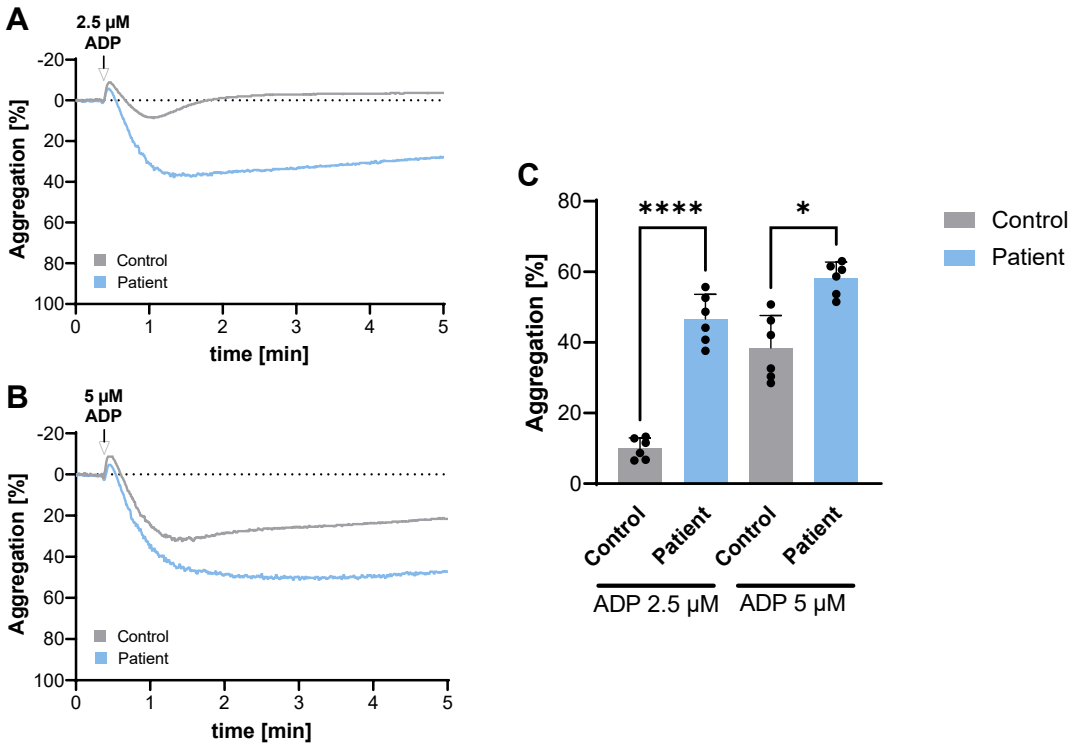

Figure 6: ADP induced platelet aggregation of patients with CAD. (A) Representative graph illustrating the 5-minute platelet aggregation curve induced by 2.5 µM ADP in platelets resuspended in patient (with autoimmune hemolysis) plasma (blue) and control plasma (gray). (B) Graph displaying the platelet aggregation response using 5 µM ADP as the stimulus, comparing patient plasma (blue) and control plasma (gray). (C) Bar chart summarizing the results from all n=6 experiments, demonstrating a significant increase in light transmittance platelet aggregation in patient plasma compared to control plasma. All data are presented as mean + SD. Statistical significance was determined using a one-way ANOVA with Šídák's multiple comparisons test. Asterisks denote the level of statistical significance compared to the control condition, with * indicating p≤0.05 and **** indicating p≤0.0001.

To further investigate the impact of plasma on platelet aggregation, additional experiments were conducted. Specifically, platelet aggregation was induced by CRP at concentrations of 0.125 µg/ml and 0.25 µg/ml **(Figure 7)**. Interestingly, in these experiments, no significant differences were observed between patient and control plasma. These results indicate that the effect of plasma from patients with autoimmune hemolysis on platelet aggregation appears to be specific to ADP stimulation, whereas CRP-induced aggregation did not demonstrate any substantial distinctions between patient and control plasma conditions.

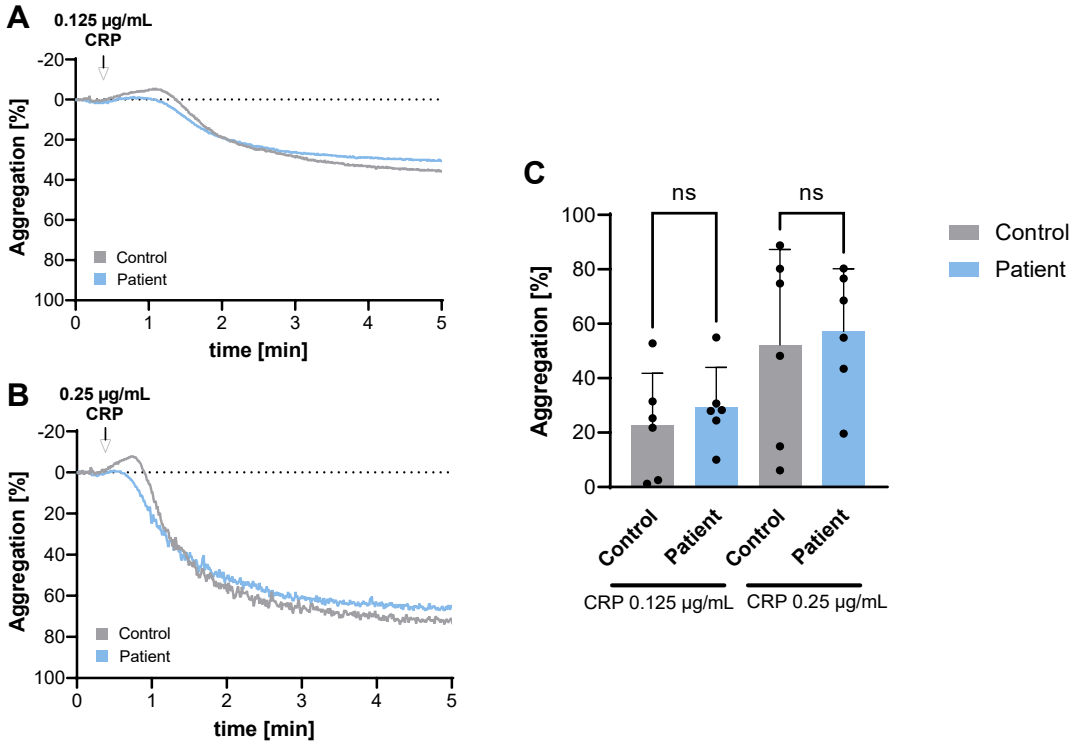

Figure 7: CRP induced platelet aggregation of patients with CAD. (A) Representative graph illustrating the 5-minute platelet aggregation curve induced by 0.125 µg/ml CRP in platelets resuspended in patient (with autoimmune hemolysis) plasma (blue) and control plasma (gray). (B) Graph displaying the platelet aggregation response using 0.25 µg/ml CRP as the stimulus, comparing patient plasma (blue) and control plasma (gray). (C) Bar chart summarizing the results from all n=6 experiments, demonstrating a significant increase in light transmittance platelet aggregation in patient plasma compared to control plasma. All data are presented as mean + SD. Statistical significance was determined using a one-way ANOVA with Šídák's multiple comparisons test with n.s. = non-significant (p>0.05).

Overall, the findings from this study shed light on the potential pro-thrombotic properties of hemolytic plasma and emphasize the importance of further investigation into the underlying mechanisms driving platelet activation in the context of autoimmune hemolysis.

After the pre-treatment of platelets with DEA/NO and riociguat, a remarkable reduction in platelet aggregation was observed in samples obtained from patients, whereas no significant changes were observed in control samples **(Figure 8)**.

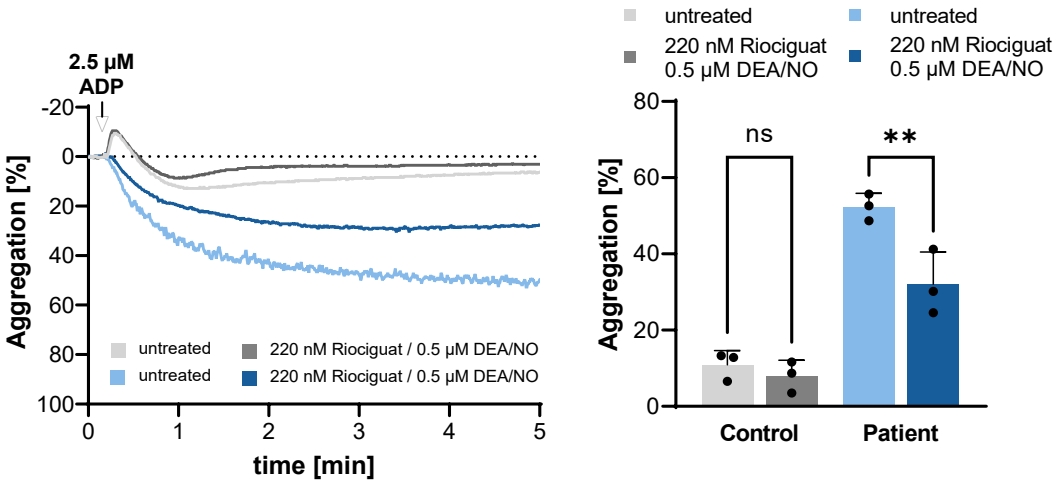

Figure 8: Effects of cGMP modulation on ADP-induced platelet aggregation in patients with CAD. Graph representing the aggregation curves induced by 2.5 µM ADP in platelets resuspended in patient plasma (blue) and control plasma (gray), either untreated or treated with 220 nM riociguat and 0.5 µM DEA/NO. Bar chart summarizing the results from all three experiments, showing the percentage of platelet aggregation. All data are presented as mean + SD. Statistical significance was determined using a one-way ANOVA with Šídák's multiple comparisons test; n.s. = non-significant ($p>0.05$) and ** indicating $p\leq0.01$.

This intriguing finding suggests that the modulation of cGMP levels within platelets could potentially play a critical role in mitigating the augmented platelet activation observed in the presence of hemolytic plasma.

3.2 Hemin induces platelet activation which is dependent on cGMP

To evaluate the effect of cGMP modulating compounds on platelet cGMP levels, isolated platelets were treated with DEA/NO or riociguat, either alone or in combination with the sGC inhibitor ODQ. Interestingly, our findings showed that both DEA/NO and riociguat treatment led to a significant elevation in platelet cGMP levels. However, this increase in cGMP levels was attenuated when ODQ, the sGC inhibitor, was present **(Figure 9A)**. These results demonstrate that we have the ability to modulate platelet cGMP levels using the given compounds.

Given that during hemolysis the release of hemoglobin leads to the rapid generation of hemin, a known stimulator of platelet activation[19], we further explored the impact of free hemoglobin on platelet function. Specifically, we assessed platelet degranulation, as indicated by P-selectin surface expression, in the presence of erythrocyte lysates and hemin. Our findings revealed that erythrocyte lysates and hemin alone were capable of stimulating P-selectin surface expression without the need for additional platelet agonists **(Figure 9B)**.

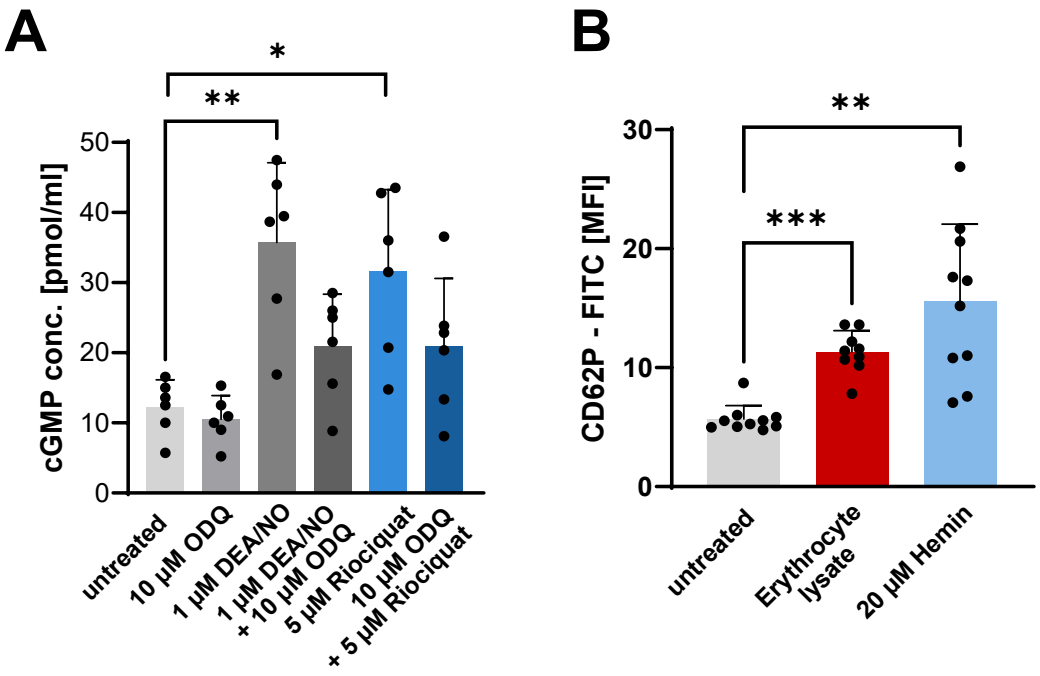

Figure 9: Effects of cGMP modulation on platelet cGMP levels and impact of free hemoglobin on platelet function. (A) Bar chart representing the results of a cGMP ELISA in isolated platelets treated with DEA/NO or riociguat, either alone or in combination with the sGC inhibitor ODQ (n=6). (B) Bar chart illustrating platelet degranulation, as indicated by P-selectin surface expression, in the presence of erythrocyte lysates and 20 µM hemin (n=10). All data are presented as mean + SD. Statistical significance was determined using a one-way ANOVA with Dunnett's multiple comparisons test. Asterisks denote the level of statistical significance compared to the control condition, with * indicating p≤0.05, ** indicating p≤0.01 and *** indicating p≤0.001.

We observed a concentration-dependent increase in P-selectin expression in response to hemin, consistent with previous reports[19]. Interestingly, in the presence of DEA/NO and riociguat, the expression of P-selectin was significantly reduced at lower concentrations of hemin. However, at higher concentrations of hemin, the decrease in P-selectin expression was independent of the presence of DEA/NO and riociguat treatment **(Figure 10A)**.

Additionally, we investigated the effect of hemin and cGMP modulation on another important aspect of platelet activation, namely the activation-dependent conformational change in the platelet integrin $\alpha_{IIb}\beta_3$, which can be measured by the surface expression of the PAC-1 antibody-binding epitope. Using flow cytometry, we analyzed PAC-1 surface expression on platelets treated with hemin in the presence or absence of DEA/NO and riociguat.

Consistent with our previous findings on P-selectin expression, we observed a concentration-dependent increase in PAC-1 surface expression in response to hemin stimulation. However, in the presence of DEA/NO and riociguat, we noticed a significant reduction in the hemin-induced increase in PAC-1 surface expression at every concentration of hemin used **(Figure 10B)**.

These results provide further evidence for the intricate interplay between hemin, cGMP modulation, and platelet activation pathways. The observed reduction in PAC-1 surface expression suggests that DEA/NO and riociguat treatment can attenuate the activation-dependent conformational change of $\alpha_{IIb}\beta_3$ integrin induced by hemin, highlighting the potential role of cGMP modulation in modulating platelet activation in the presence of hemin hemolytic plasma respectively.

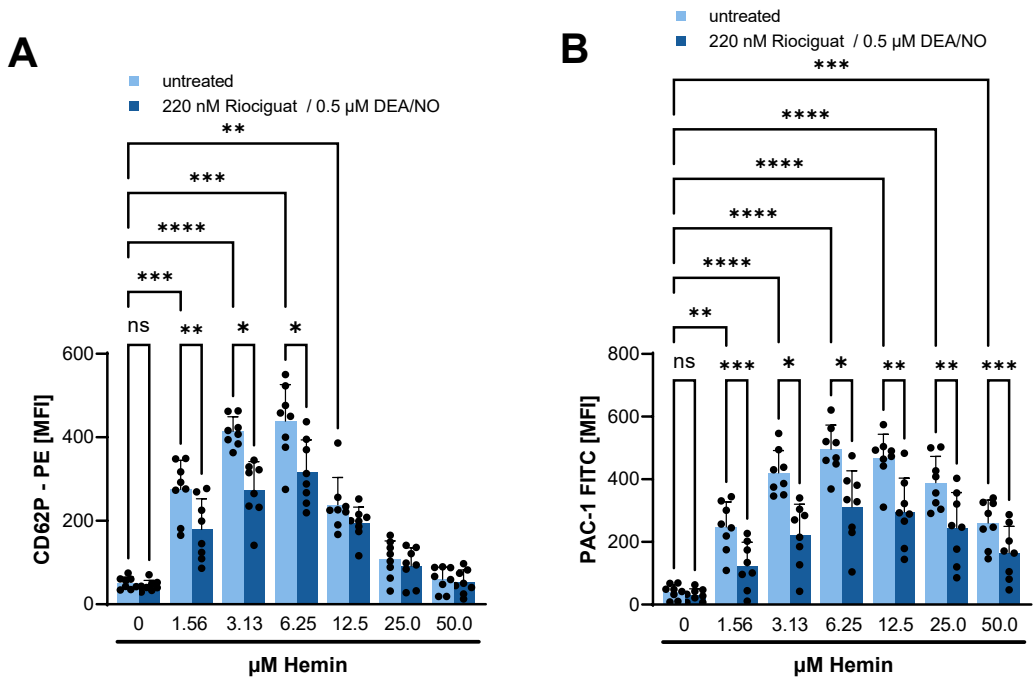

Figure 10: Modulation of P-selectin and PAC-1 surface expression in response to hemin and cGMP modulation. (A) Bar chart showing concentration-dependent increase in P-selectin expression with hemin stimulation (n=8). DEA/NO and riociguat reduce P-selectin expression at lower hemin concentrations but not at higher concentrations. (B) Bar chart revealing hemin-induced increase in PAC-1 surface expression (n=8). DEA/NO and riociguat significantly attenuate PAC-1 expression at all hemin concentrations. All data are presented as mean + SD. Statistical significance was determined using a one-way ANOVA with Šídák's multiple comparisons test. Asterisks denote the level of statistical significance compared to the control condition, with ** indicating p≤0.01, *** indicating p≤0.001 and **** indicating p≤0.0001.

Likewise, our investigation extended to the evaluation of the impact of the sGC activator cinaciguat on hemin-induced platelet activation markers. Specifically, we examined the effects of cinaciguat in combination with ODQ on P-selectin expression **(Figure 11A)** and the activation of the fibrinogen receptor GPIIb/IIIa **(Figure 11B)**. Remarkably, our results demonstrated that cinaciguat and ODQ combination exerted a significant inhibitory effect on both hemin-dependent P-selectin expression and GPIIb/IIIa activation. Furthermore, when using indomethacin and cangrelor alone, we also observed significant reductions in P-selectin expression and GPIIb/IIIa activation, underscoring the involvement of other pathways, such as COX inhibition and $P2Y_{12}$ receptor blockade, in mitigating hemin-induced platelet activation **(Figure 11)**.

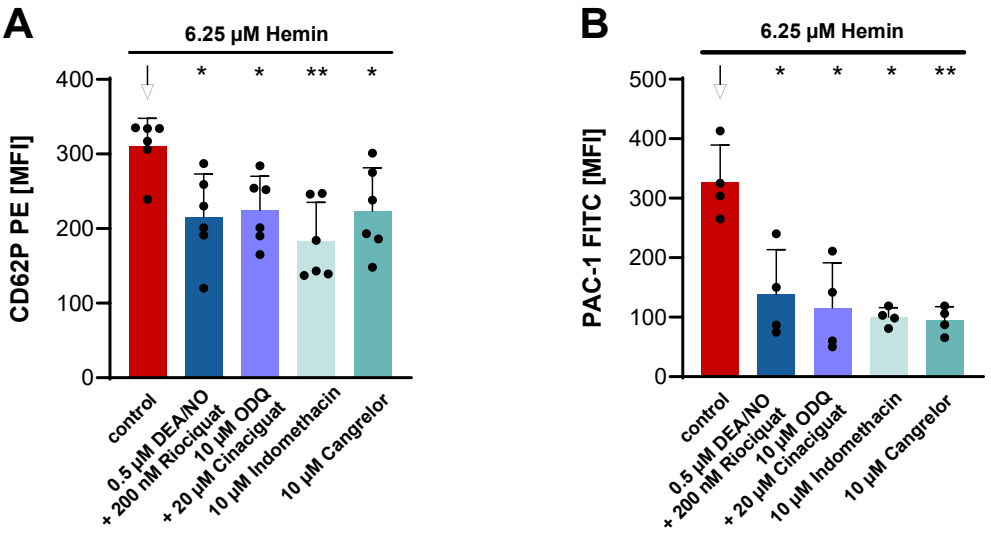

Figure 11: Modulation of P-selectin and GPIIb/IIIa surface expression by various compounds in response to hemin. (A) Bar chart illustrating the impact of DEA/NO in combination with riociguat, cinaciguat in combination with ODQ, cangrelor, and indomethacin on hemin-induced P-selectin expression. The combination treatments of DEA/NO with riociguat and cinaciguat with ODQ exhibit significant inhibition, while indomethacin and cangrelor alone also show significant reductions in CD62P surface expression. (B) Bar chart depicting the effect of DEA/NO in combination with riociguat, cinaciguat in combination with ODQ, cangrelor, and indomethacin on hemin-induced GPIIb/IIIa activation (n=6). The combination treatments of DEA/NO with riociguat and cinaciguat with ODQ demonstrate significant inhibition, while indomethacin and cangrelor alone also exhibit significant reductions in GPIIb/IIIa activation. All data are presented as mean + SD. Statistical significance was determined using a one-way ANOVA with Dunnett's multiple comparisons test. Asterisks denote the level of statistical significance compared to the control condition, with * indicating $p \leq 0.05$ and ** indicating $p \leq 0.01$.

To gain further insights into the impact of hemin on platelet activation, we conducted flow cytometry analysis to examine fibrinogen binding and the expression of CD41 and CD61 on the platelet surface **(Figure 12)**. CD41, also known as platelet GPIIb, is always non-covalently associated with CD61, or platelet GPIIIa, forming the GPIIb/IIIa (CD41/CD61) complex, which is also referred to as the fibrinogen receptor[103]. Our findings revealed a concentration-dependent increase in fibrinogen binding, indicating heightened platelet activation in response to hemin **(Figure 12A)**. Notably, CD41 expression on platelets exhibited a significant increase at a hemin concentration of 12.5 µM, followed by a decrease at 50 µM **(Figure 12B)**. Similarly, CD61 expression also showed a significant increase at both 12.5 µM and 50 µM hemin concentrations **(Figure 12C)**.

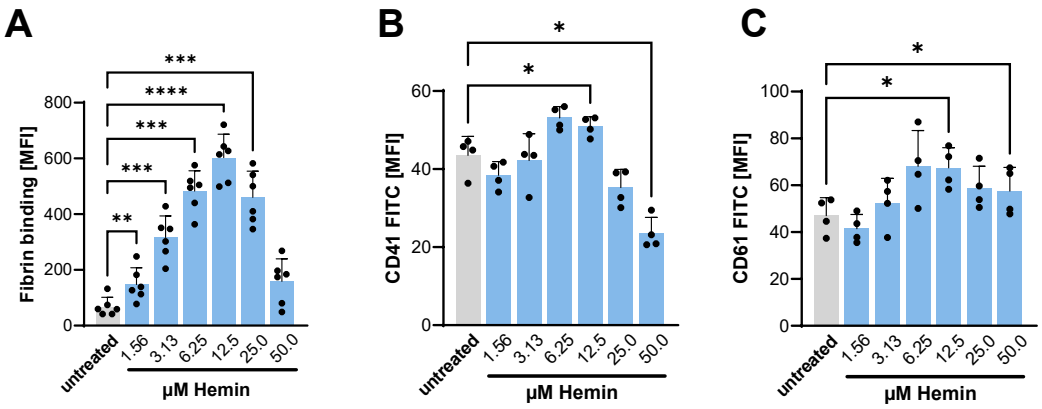

Figure 12: Flow cytometry analysis of the fibrinogen binding receptor in response to hemin stimulation. (A) Fibrinogen binding of isolated platelets showed a concentration-dependent increase in response to hemin stimulation, indicating heightened platelet activation. (B) CD41 expression on platelets exhibited a significant increase at a hemin concentration of 12.5 µM, followed by a subsequent decrease at 50 µM. (C) Similarly, CD61 expression also displayed a significant increase at both 12.5 µM and 50 µM hemin concentrations. All data (n=4) are presented as mean + SD. Statistical significance was determined using a one-way ANOVA with Šídák's multiple comparisons test. Asterisks denote the level of statistical significance compared to the control condition, with * indicating p≤0.05, ** indicating p≤0.01, *** indicating p≤0.001 and **** indicating p≤0.0001.

These observations emphasize the role of hemin in modulating fibrinogen binding and altering the expression levels of CD41 and CD61 on the platelet surface in a concentration-dependent manner.

Considering the significant impact of hemin on platelet activation, as evidenced by the modulation of fibrinogen binding and P-selectin expression, we sought to explore the role of calcium signaling in this process. Calcium is a crucial regulator of platelet activation, and alterations in intracellular and extracellular calcium levels have been associated with platelet function[104].

Therefore, we conducted additional experiments to measure the hemin-induced changes in intra and extracellular calcium expression. Notably, we observed that the enhanced hemin-induced increase in both intracellular **(Figure 13A)** and extracellular calcium **(Figure 13B)** was significantly attenuated in the presence of riociguat, providing further evidence for the involvement of cGMP modulation in mitigating hemin-induced platelet activation **(Figure 13)**.

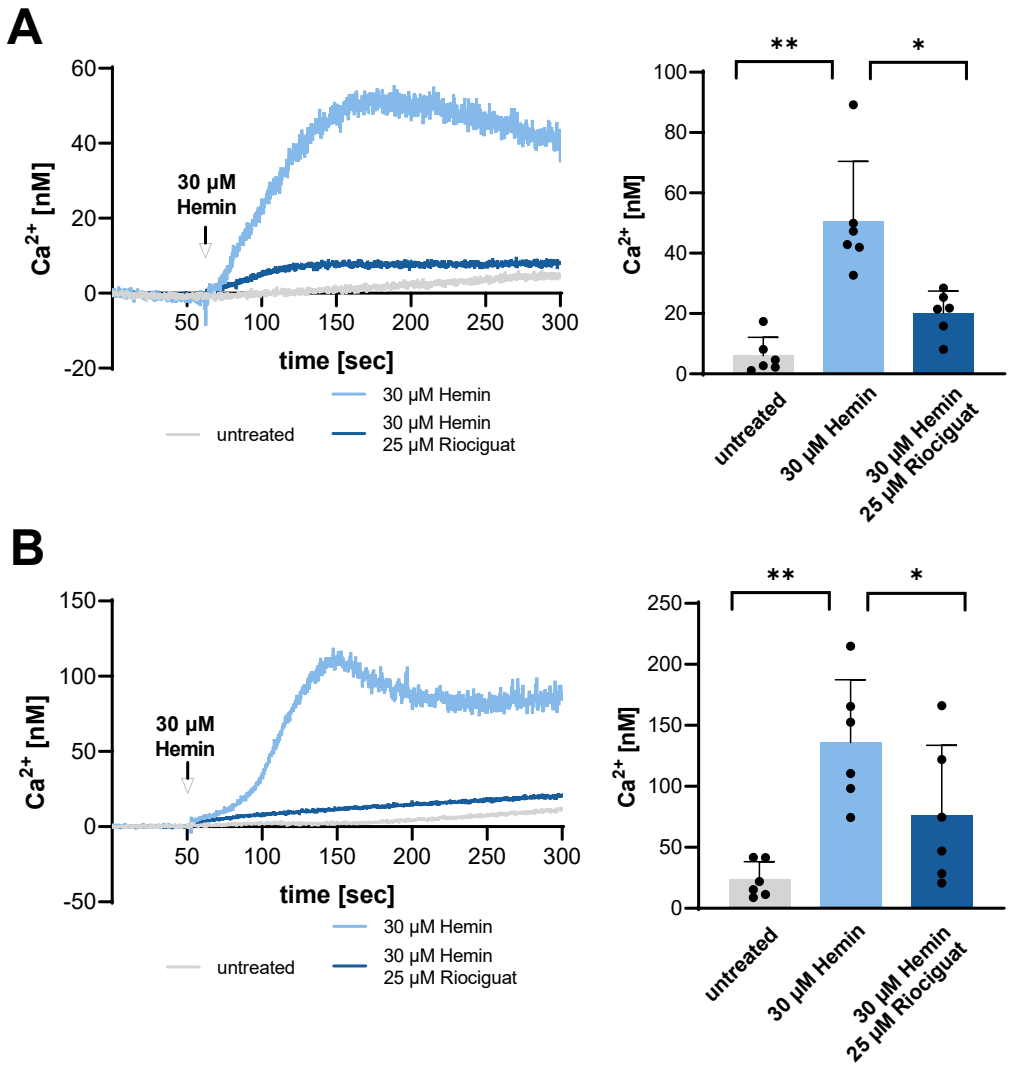

Figure 13: Modulation of hemin-induced calcium changes by riociguat. (A) Representative graph depicting the curves of intracellular calcium levels after stimulation with hemin, with and without riociguat (left). Bar chart illustrating the effect of riociguat on intracellular calcium levels in response to hemin stimulation (right). The presence of riociguat significantly attenuates the enhanced hemin-induced increase in intracellular calcium compared to hemin alone. (B) Representative graph depicting the curves of extracellular calcium levels after stimulation with hemin, with and without riociguat (left). Bar chart depicting the impact of riociguat on extracellular calcium levels in response to hemin stimulation (right). The presence of riociguat significantly reduces the enhanced hemin-induced increase in extracellular calcium compared to hemin alone. All data are presented as mean + SD. Statistical significance was determined using a one-way ANOVA with Dunnett's multiple comparisons test (n=6). Asterisks denote the level of statistical significance compared to the control condition, with * indicating p≤0.05 and ** indicating p≤0.01. Experiments performed in cooperation with Münzer P., analysis made by Kremser M.

To elucidate the molecular mechanisms underlying hemin-induced platelet activation and further assess the potential protective effects of cGMP modulation, we performed western blot analysis on isolated platelets. The platelets were treated with different concentrations of hemin (3.1 and 25 µM) in the presence or absence of DEA/NO and riociguat. We specifically analyzed the phosphorylation levels of VASP at Ser239, as phosphorylation at this site is regulated by cGMP-dependent kinases and serves as a marker for platelet activation. Additionally, we examined the phosphorylation levels of AKT, a key signaling molecule involved in platelet activation, along with the respective total protein levels.

The western blot results revealed that hemin treatment led to a concentration-dependent reduction in VASP phosphorylation and concurrently, hemin induced an increase in AKT phosphorylation **(Figure 14)**. Importantly, the cGMP modulation through DEA/NO and riociguat counteracted both effects of hemin. Specifically, cGMP modulation significantly increased VASP phosphorylation and attenuated hemin induced AKT phosphorylation. Notably, the decreased AKT phosphorylation was more pronounced with the lower concentration of hemin.

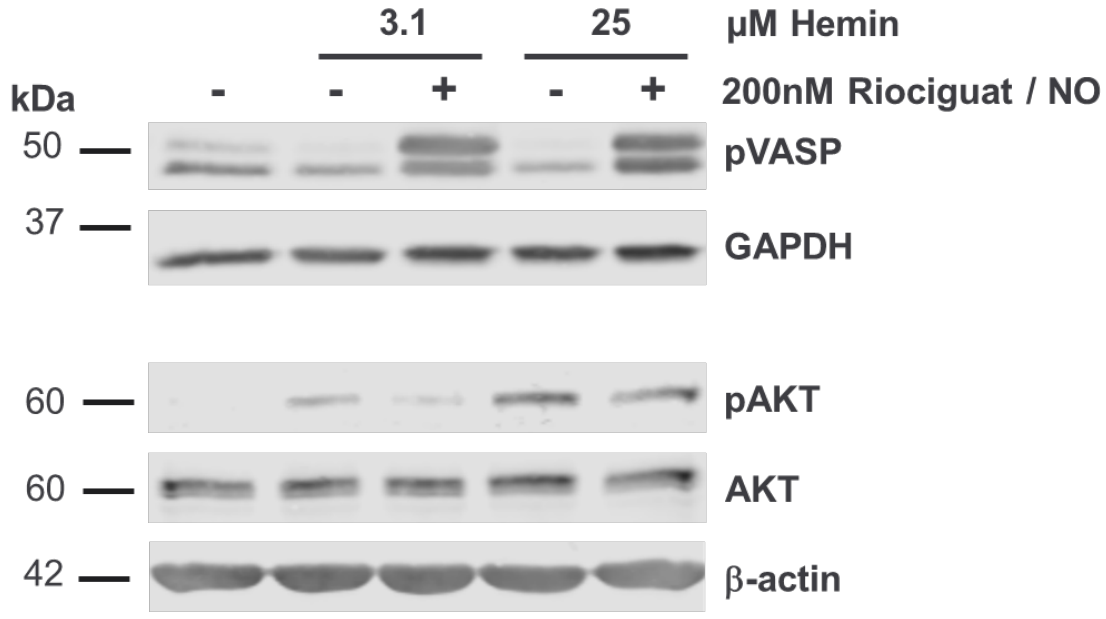

Figure 14: Western blot analysis of platelet activation and cGMP modulation in response to hemin treatment. Isolated platelets were treated with different concentrations of hemin (3.1 and 25 µM) in the presence or absence of 0.5 µM DEA/NO and 220 nM riociguat. The levels of phosphorylated VASP at Ser239 (pVASP) was assessed to indirectly measure cGK activity. Additionally, the phosphorylation levels of AKT (pAKT) and total AKT were analyzed as markers of platelet activation. GAPDH and beta-actin were used as loading controls. Experiments performed in cooperation with Rohlfing A.-K.

These findings demonstrate that the AKT pathway is at least partially involved during hemin induced platelet activation, as evidenced by increased AKT phosphorylation. Moreover, the modulation of cGMP by DEA/NO and riociguat effectively mitigates these effects, leading to enhanced VASP phosphorylation and decreased AKT phosphorylation.

In the next experiment, we utilized Raman spectroscopy to investigate the morphological changes and hemin binding in isolated platelets. The platelets were either left untreated or treated with hemin (30 µM) in the presence or absence of DEA/NO and riociguat. A specific Raman peak at 2940 cm^{-1}, associated with vibrations in lipids and proteins, was used to visualize the platelets. The untreated platelets appeared as round shapes, indicating their resting state. In contrast, the platelets treated with hemin exhibited a spreaded and activated morphology **(Figure 15A)**. Interestingly, when hemin was combined with DEA/NO and riociguat, the platelets displayed a reduced activated state.

To visualize the binding of hemin on platelets, we examined the Raman peak at 1372 cm^{-1}, which corresponds to the hemin vibrational mode. Platelets were washed to remove background noise before analysis. As expected, the untreated platelets showed no significant hemin intensity. However, the platelets treated solely with hemin displayed the most pronounced hemin binding intensity. Remarkably, when cGMP modulation was applied, the visible hemin binding was reduced almost back to the control level **(Figure 15B)**.

These results suggest that hemin treatment induces morphological changes and promotes hemin binding on platelets, which can be attenuated by cGMP modulation.

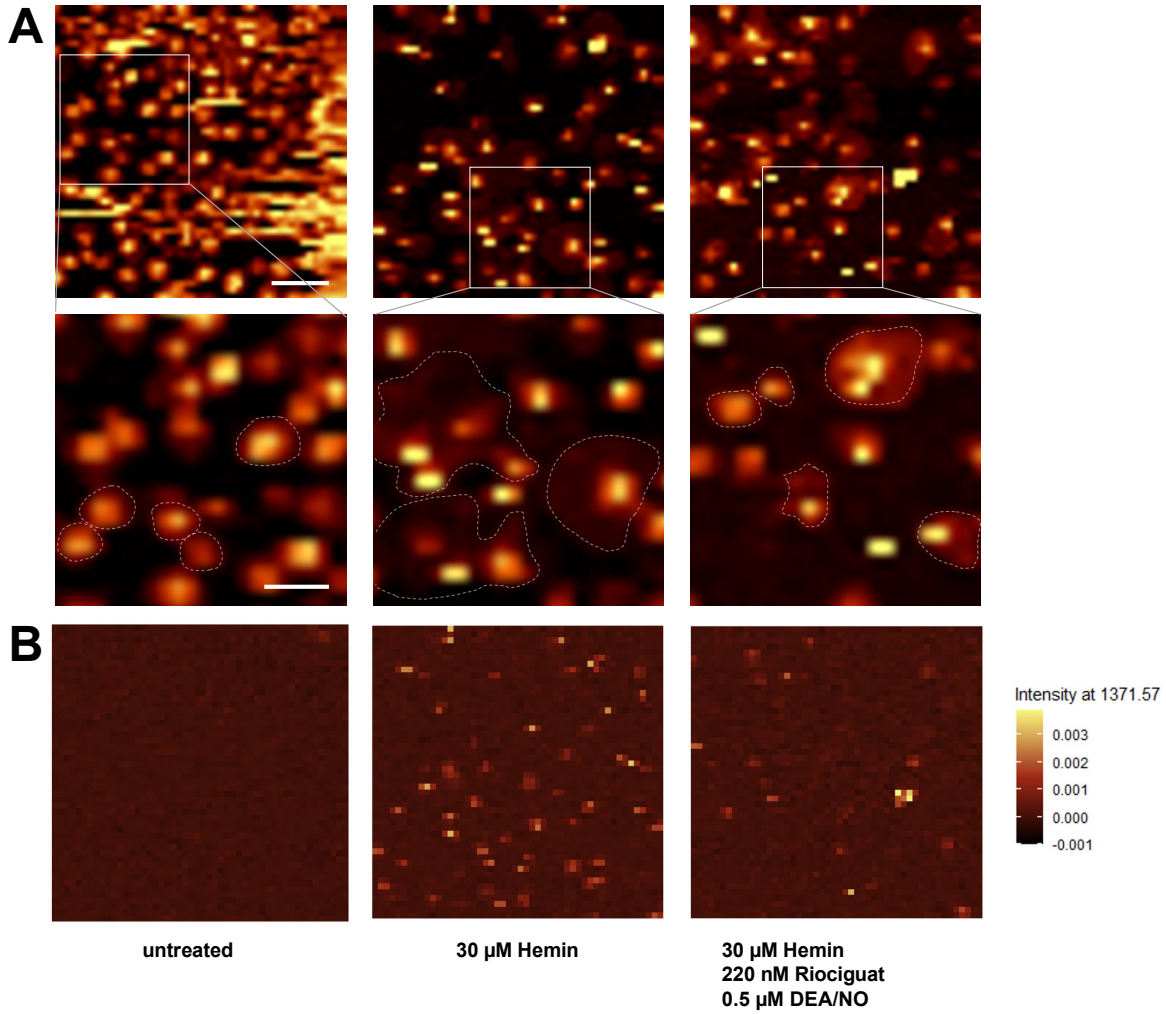

Figure 15: Raman spectroscopy analysis of isolated platelets in response to hemin treatment and cGMP modulation. Platelets were either left untreated or treated with hemin (30 µM) in the presence or absence of DEA/NO and riociguat. Raman spectroscopy was performed by M. Sigle. (A) Platelet morphology was visualized using a specific Raman peak at 2940 cm^{-1}, associated with vibrations in lipids and proteins. The upper row shows the original images with a scale bar of 10 µm, while the lower row zooms in on the white squares indicated in the upper row, with a scale bar of 5 µm. Some platelet shapes in the bottom row are marked with a white dotted line border. Untreated platelets exhibit a round shape, indicative of their resting state, whereas hemin-treated platelets display a spreaded and activated morphology. (B) Analysis of hemin binding using Raman peaks at 1372 cm^{-1} reveals no significant intensity in untreated platelets, prominent binding in hemin-treated platelets, and reduced binding intensity with cGMP modulation.

To investigate the effect of hemin concentration on platelet aggregation, we performed a dose-response experiment using varying concentrations of hemin. Consistent with previous findings[19], we observed a concentration-dependent increase in hemin-induced platelet aggregation **(Figure 16)**, highlighting the stimulatory effect of hemin on platelet activation.

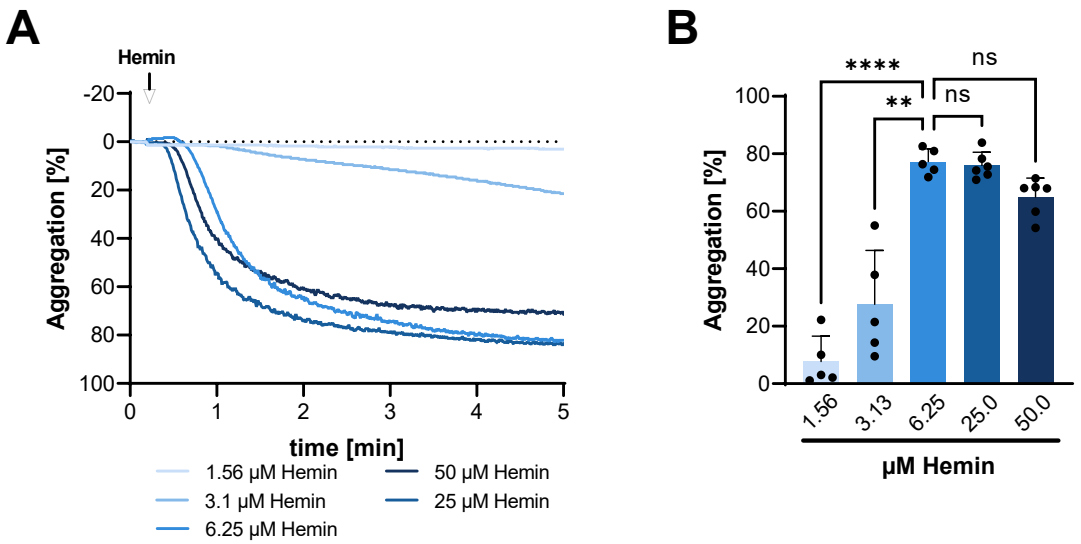

Figure 16: Dose-response effect of hemin on platelet aggregation. (A) Representative graph showing the aggregation curves of isolated platelets stimulated with varying concentrations of hemin. The concentrations of hemin ranged from 1.56 to 50 µM and light transmission aggregometry measurement was conducted for a duration of 5 minutes. (B) Bar chart summarizing the results of all n=5 experiments, showing the percentage of platelet aggregation. All data are presented as mean + SD. Statistical significance was determined using a one-way ANOVA with Šídák's multiple comparisons test; n.s. = non-significant ($p>0.05$), ** indicating $p\leq0.01$ and **** indicating $p\leq0.0001$.

In addition to assessing platelet hyperreactivity, we investigated the effects of hemin and CRP on ATP release from isolated platelets. Stimulation of platelets with 6.25 µM hemin **(Figure 17A)** and 1 µg/ml CRP **(Figure 17B)** resulted in a significant increase in ATP release. However, pretreatment of platelets with DEA/NO and riociguat significantly attenuated the hemin- and CRP-induced ATP release **(Figure 17)**. These findings suggest that modulation of cGMP levels through DEA/NO and riociguat can effectively mitigate platelet activation and ATP release in response to hemin and CRP stimulation.

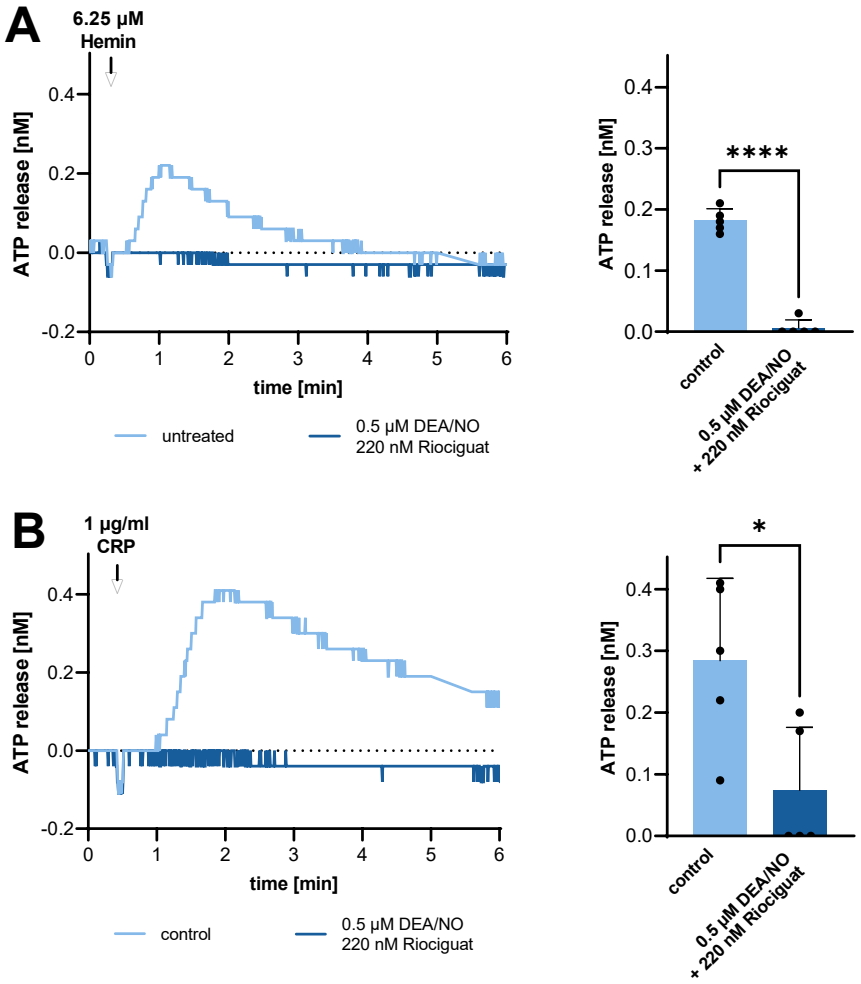

Figure 17: Effects of hemin and CRP on platelets ATP release and the impact of cGMP modulation. (A) Representative graph showing ATP release from isolated platelets stimulated with 6.25 µM hemin with and without DEA/NO and riociguat (left). Bar chart illustrating the ATP release from all n=5 experiments (right). The hemin-induced ATP release was significantly attenuated by pretreatment with DEA/NO and riociguat. (B) Representative graph showing ATP release from isolated platelets stimulated with 1 µg/ml CRP with and without DEA/NO and riociguat (left). Bar chart illustrating the ATP release from all n=5 experiments (right). The CRP-induced ATP release was significantly attenuated by pretreatment with DEA/NO and riociguat. All data are presented as mean + SD. Statistical significance was determined using a paired student's t-test. Asterisks denote the level of statistical significance compared to the control condition, with * indicating p≤0.05 and **** indicating p≤0.0001. Experiments performed in cooperation with Fischer M., analysis made by Kremser M.

To explore the impact of cGMP modulation on platelet aggregation, we further investigated the effects of DEA/NO and riociguat on both hemin-induced and ADP-induced platelet aggregation. Upon treatment with DEA/NO and riociguat, we noted a notable reduction in platelet aggregation induced by ADP, indicating the inhibitory role of cGMP in ADP-mediated platelet activation. Additionally, we

observed that hemin-induced platelet aggregation was also effectively inhibited by DEA/NO and riociguat **(Figure 18A)**, albeit to a lesser extent compared to ADP-induced aggregation **(Figure 18B)**. Notably, the inhibitory effects were most pronounced when both DEA/NO and riociguat were present simultaneously.

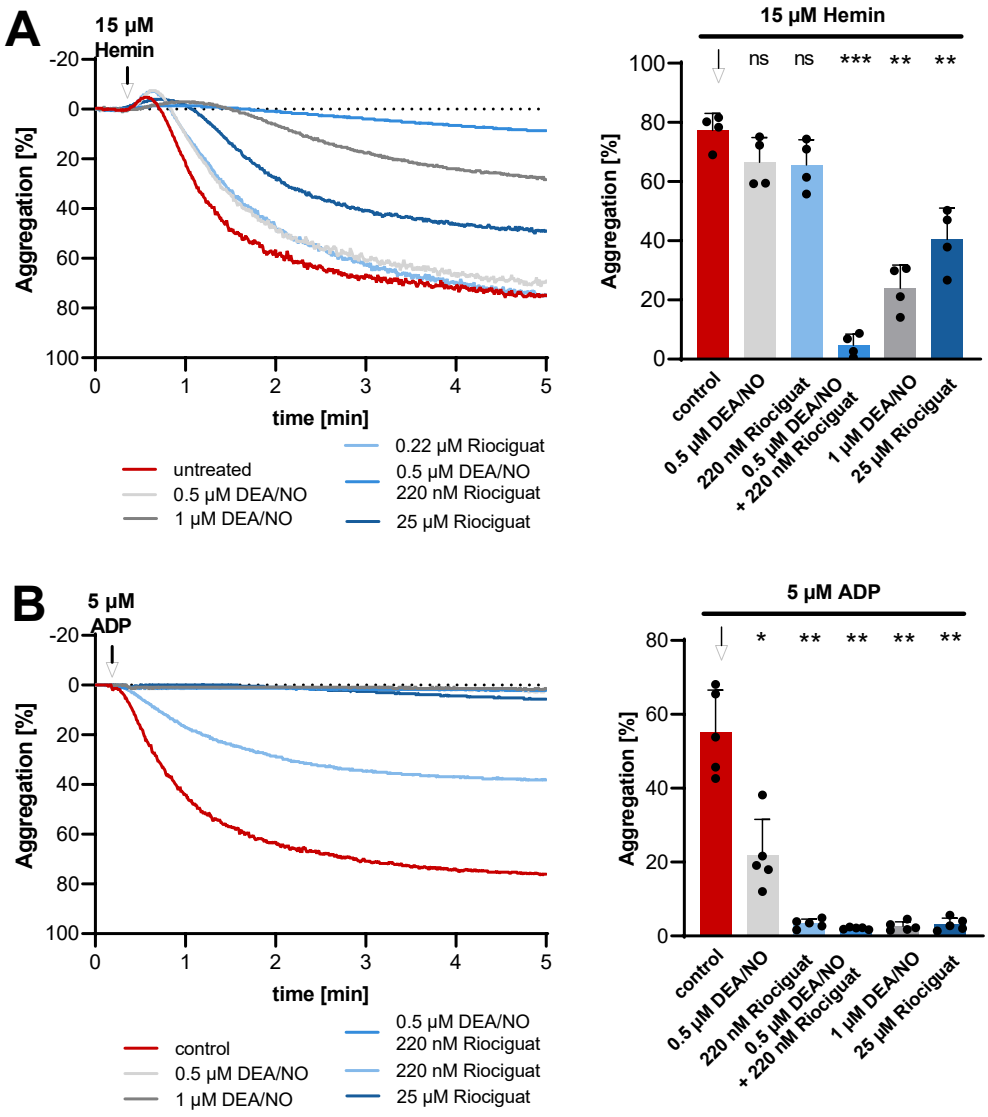

Figure 18: Modulation of hemin and ADP-induced platelet aggregation by DEA/NO and riociguat. (A) Representative graph showing platelet aggregation stimulated with 15 µM hemin with and without DEA/NO and riociguat (left). Bar chart showing the percentage of platelet aggregation from all n=4 experiments (right). The presence of DEA/NO, riociguat, or their combination significantly attenuates hemin-induced aggregation. (A) Representative graph showing platelet aggregation stimulated with 5 µM ADP with and without DEA/NO and riociguat (left). Bar chart showing the percentage of platelet aggregation from all n=5 experiments (right). The presence of DEA/NO, riociguat, or their combination significantly attenuates ADP-induced aggregation. All data are presented as mean + SD. Statistical significance was determined using a one-way ANOVA with Dunnett's multiple comparisons test and is always refered to the control (arrow); n.s. = non-significant ($p>0.05$), * indicating $p\leq0.05$, ** indicating $p\leq0.01$ and *** indicating $p\leq0.001$.

Furthermore, we investigated the effects of cinaciguat, alone and in combination with ODQ, on platelet aggregation induced by both hemin and ADP **(Figure 19)**. Interestingly, in the case of ADP-induced aggregation, cinaciguat alone exhibited a significant inhibitory effect, reducing platelet aggregation. Similarly, when cinaciguat was combined with ODQ, we observed a synergistic effect leading to a pronounced reduction in ADP-induced platelet aggregation **(Figure 19B)**.

In contrast, when examining hemin-induced platelet aggregation, cinaciguat alone did not show a substantial inhibitory effect. However, when combined with ODQ, cinaciguat exhibited a noticeable inhibitory effect **(Figure 19A)**.

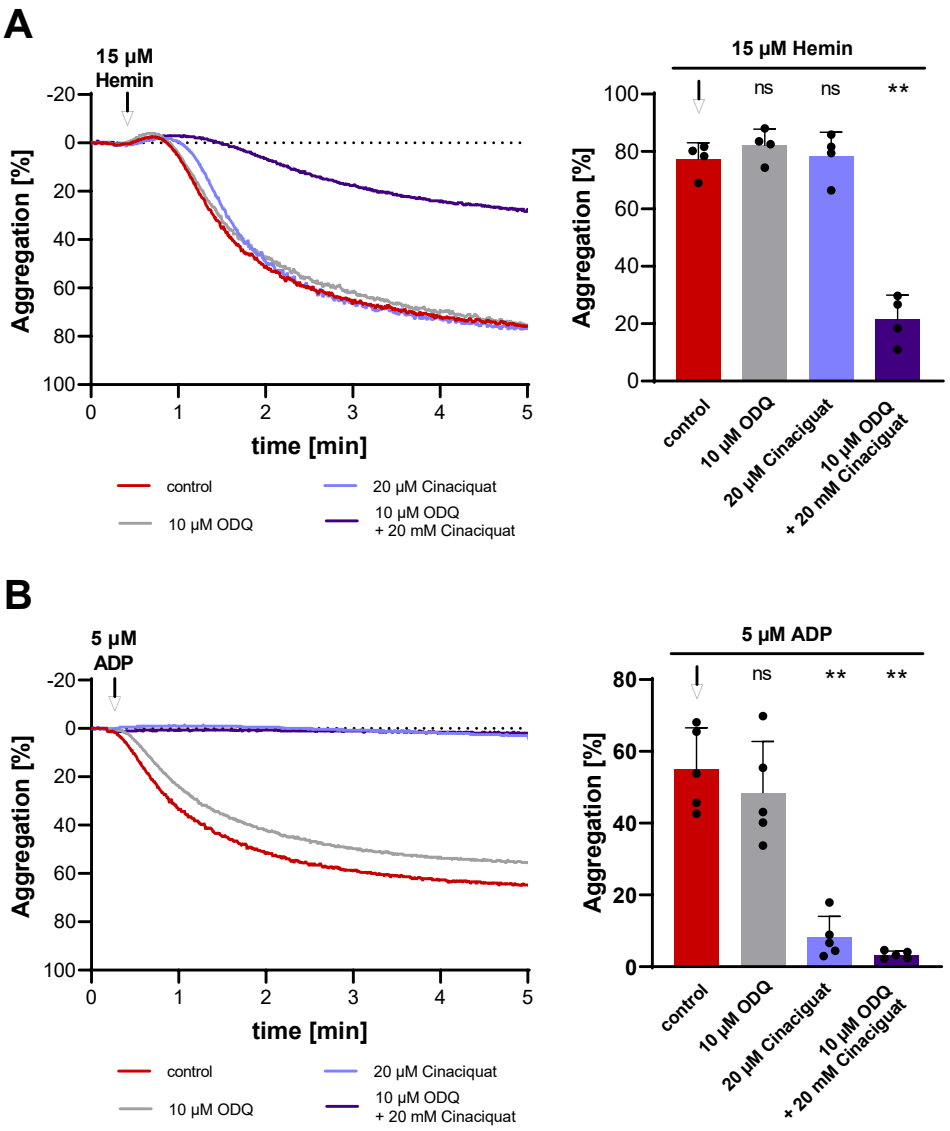

Figure 19: Modulation of hemin and ADP-induced platelet aggregation by ODQ and cinaguat. (A) Representative graph showing platelet aggregation stimulated with 15 µM hemin with and without ODQ and cinaciguat (left). Bar chart showing the percentage of platelet aggregation from all n=4 experiments (right). The presence of ODQ and cinaciguat in combination significantly attenuates hemin-induced aggregation. (A) Representative graph showing platelet aggregation stimulated with 5 µM ADP with and without ODQ and cinaciguat (left). Bar chart showing the percentage of platelet aggregation from all n=5 experiments (right). The presence of cinaciguat, or the combination of ODQ and cinaciguat significantly attenuates ADP-induced aggregation. All data are presented as mean + SD. Statistical significance was determined using a one-way ANOVA with Dunnett's multiple comparisons test and is always refered to the control (arrow); n.s. = non-significant ($p>0.05$) and ** indicating $p\leq0.01$.

These findings suggest that cGMP modulation exerts inhibitory effects on platelet aggregation, both in response to ADP and hemin stimulation.

In addition to the cGMP modulating drugs, we investigated the impact of other inhibitors, specifically indomethacin (COX-1 inhibitor), cangrelor ($P2Y_{12}$ receptor blocker) and eptifibatide (GPIIb/IIIa inhibitor), on hemin-induced platelet aggregation. Surprisingly, neither indomethacin nor cangrelor demonstrated the ability to prevent hemin-induced platelet aggregation **(Figure 20A)**. These results indicate that the mechanisms underlying hemin-induced platelet aggregation may not solely rely on COX-1 activity or $P2Y_{12}$ receptor signaling.

However, it is worth noting that eptifibatide, an inhibitor of the fibrinogen receptor GPIIb/IIIa, exhibited significant inhibitory effects on hemin-induced platelet aggregation. This finding suggests that the interaction between fibrinogen and its receptor plays a crucial role in the hemin-induced platelet aggregation pathway.

In contrast, all three inhibitors (indomethacin, cangrelor, and eptifibatide) demonstrated significant inhibitory effects on ADP-induced platelet aggregation, confirming their effectiveness in blocking this particular pathway **(Figure 20B)**.

These findings indicate that hemin-induced platelet aggregation may involve distinct mechanisms that are not solely dependent on COX-1 activity or $P2Y_{12}$ receptor signaling. Instead, the interaction between fibrinogen and GPIIb/IIIa appears to be critical in mediating hemin-induced platelet aggregation.

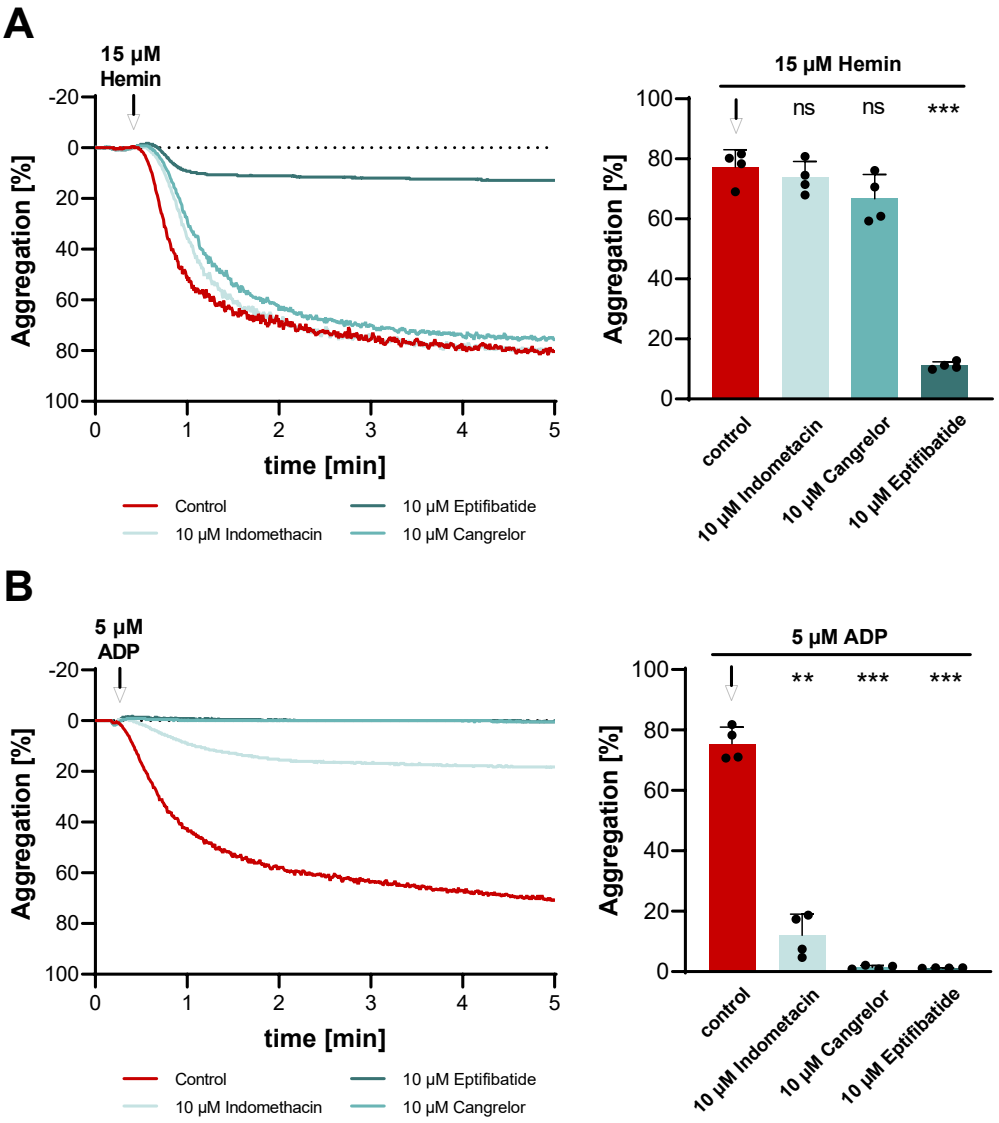

Figure 20: Modulation of hemin and ADP-induced platelet aggregation by indomethacin, cangrelor and eptifibatide. (A) Representative graph showing platelet aggregation stimulated with 15 µM hemin with and without indomethacin, cangrelor or eptifibatide (left). Bar chart showing the percentage of platelet aggregation from all n=4 experiments (right). The presence of eptifibatide significantly attenuates hemin-induced aggregation. (A) Representative graph showing platelet aggregation stimulated with 5 µM ADP with and without indomethacin, cangrelor or eptifibatide (left). Bar chart showing the percentage of platelet aggregation from all n=4 experiments (right). The presence of indomethacin, cangrelor or eptifibatide significantly attenuates ADP-induced aggregation. All data are presented as mean + SD. Statistical significance was determined using a one-way ANOVA with Dunnett's multiple comparisons test and is always refered to the control (arrow); n.s. = non-significant ($p>0.05$), ** indicating $p\leq0.01$ and *** indicating $p\leq0.001$.

Furthermore, we examined the impact of hemin on platelet aggregate formation on immobilized collagen. We observed that hemin significantly enhanced platelet aggregate formation of isolated platelets compared to the control condition. However, in the presence of DEA/NO and riociguat in combination, the formation of platelet aggregates was remarkably reduced **(Figure 21)**.

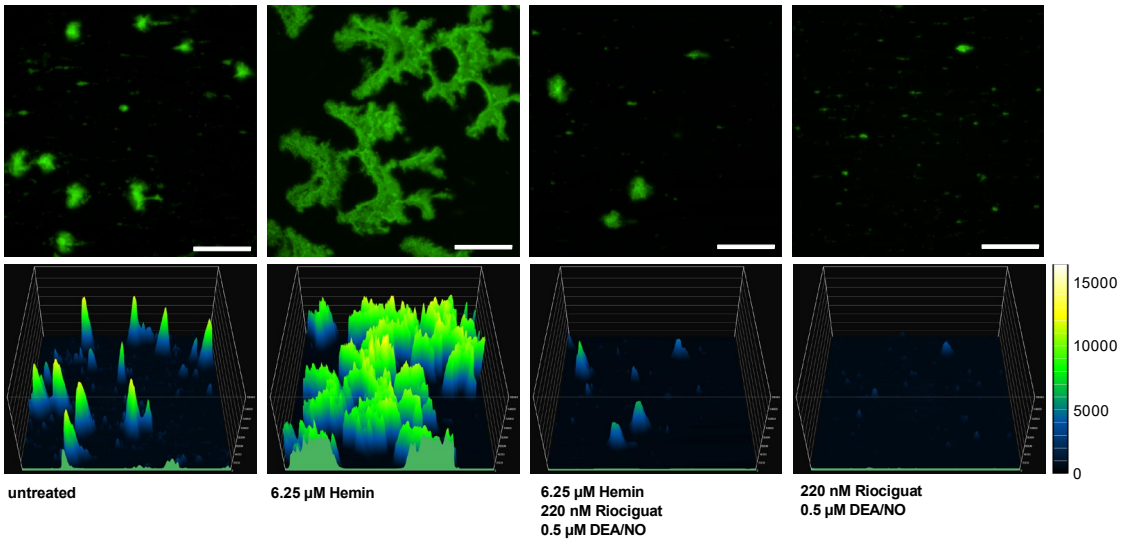

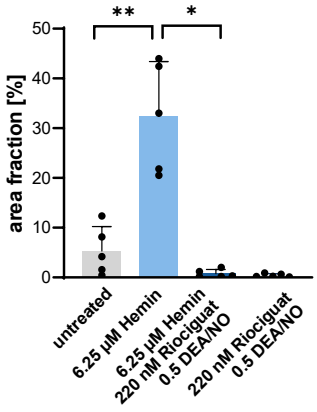

Figure 21: Effects of hemin and cGMP modulation on platelet aggregate formation on immobilized collagen. Representative fluorescence microscopic images of thrombus formation of isolated platelets after perfusion are shown (top) with a scale bar of 200 µm. Platelets were either pre-treated with riociguat and DEA/NO, hemin or the combination of both. The bottom panel presents the 3D intensity surface plots depicting the acquired flow chamber data. The bar chart illustrates the statistical analysis of the area fraction of thrombus formation after perfusion, with mean + SD values and n=5 experiments. Statistical significance was determined using a one-way ANOVA with Dunnett's multiple comparisons test. Asterisks denote the level of statistical significance compared to the control condition, with * indicating p≤0.05 and ** indicating p≤0.01.

These results indicate that hemin promotes platelet aggregate formation on immobilized collagen, suggesting a pro-thrombotic effect. However, the inhibitory effects of DEA/NO and riociguat on aggregate formation suggest that cGMP modulation can effectively counteract the pro-thrombotic activity of hemin.

Overall, these results provide further evidence supporting the crucial role of cGMP modulation in regulating hemin-induced platelet activation and aggregation. The data obtained from human platelets reinforce the potential therapeutic value of targeting the sGC-cGMP pathway in the context of hemin-mediated platelet dysfunction and thrombotic disorders.

3.3 Hemin induces ferroptosis which is dependent on cGMP modulation

Next, we aimed to determine the role of cGMP in regulating platelet ferroptosis. Therefore, isolated platelets were subjected to incubation with increasing concentrations of hemin, and several ferroptosis-related parameters were assessed using flow cytometry. These included phosphatidyl serine exposure measured by Annexin V binding **(Figure 22A)**, mitochondrial membrane potential evaluated using TMRE fluorescence **(Figure 22B)**, ROS generation detected by H2DCFDA fluorescence **(Figure 23A)**, and lipid peroxidation quantified using C11-BODIPY (581/591) **(Figure 23B)**.

Our results revealed that hemin treatment led to a significant increase in phosphatidyl serine exposure **(Figure 22A)** and ROS activity **(Figure 23A)**, indicating enhanced ferroptosis in a concentration-dependent manner. Conversely, the mitochondrial membrane potential showed a concentration-dependent decrease **(Figure 22B)**. Notably, the alterations in these ferroptosis-associated platelet parameters were notably attenuated in the presence of DEA/NO and riociguat.

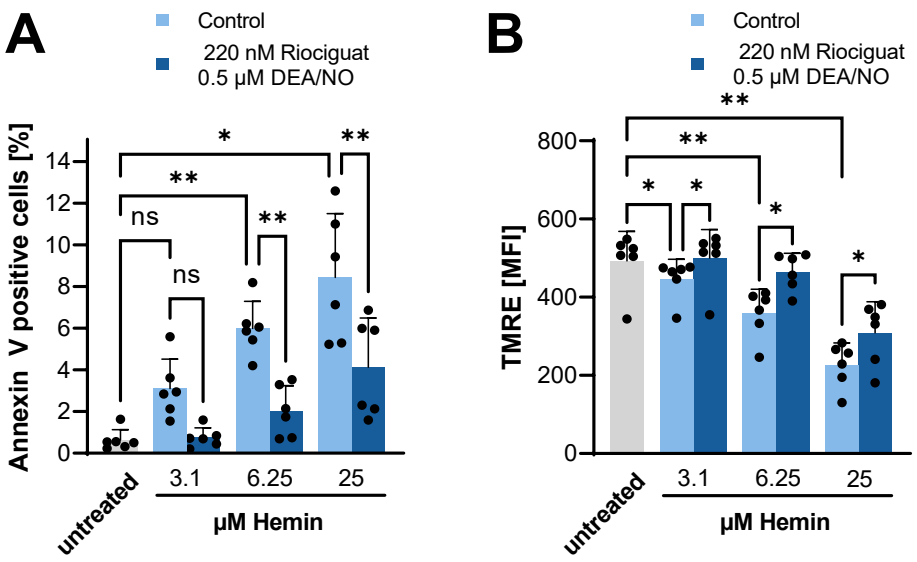

Figure 22: Regulation of PS exposure and mitochondrial membrane potential by hemin and the cGMP Signaling. (A) Flow cytometry analysis of isolated platelets showing hemin-induced phosphatidyl serine exposure measured by Annexin V binding. The presence of DEA/NO and riociguat attenuates hemin induced increae in Annexin V postive cells. (B) Evaluation of hemin-induced mitochondrial membrane potential changes in isolated platetes using TMRE fluorescence. The presence of DEA/NO and riociguat attenuates the loss of mitochondrial membrane potential induced by hemin. All data are presented as mean + SD (n=6). Statistical significance was determined using a one-way ANOVA with Šídák's multiple comparisons test; n.s. = non-significant ($p>0.05$), * indicating $p\leq0.05$ and ** indicating $p\leq0.01$.

Furthermore, we assessed lipid peroxidation using the C11-BODIPY (581/591) probe, which undergoes oxidation upon exposure to reactive oxygen species. The fluorescence emission peak of the dye shifts from approximately 595 nm to around 520 nm upon oxidation[105]. Interestingly, we observed a significant decrease in the PE channel fluorescence after hemin treatment, indicating increased lipid peroxidation. However, treatment with DEA/NO and riociguat or cinaciguat and ODQ respectively did not have a significant impact on lipid peroxidation **(Figure 23B)**.

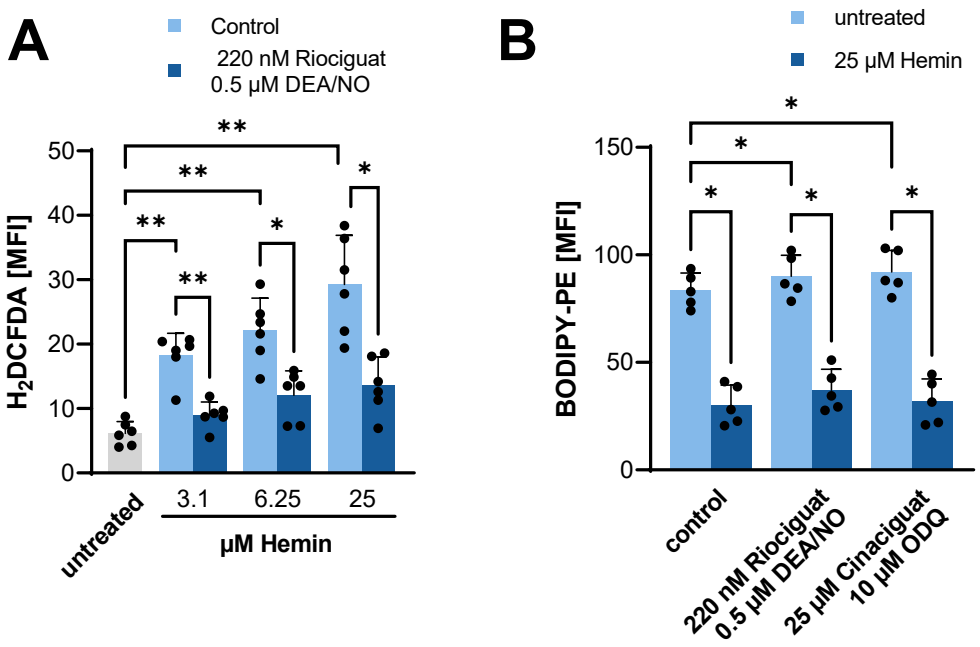

Figure 23: Regulation of ROS generation and lipid peroxidation by hemin and the cGMP Signaling. (A) Flow cytometry analysis of isolated platelets showing hemin-induced ROS generation measured by H2DCFDA fluorescence. The presence of DEA/NO and riociguat attenuates hemin induced ROS generation. (B) Evaluation of hemin-induced lipid peroxidation in isolated platetes using C11-BODIPY (581/591) fluorescence. The presence of DEA/NO and riociguat and cinaciguat and ODQ respectively have no significant effect on hemin induced lipid peroxidation. All data are presented as mean + SD (n=6). Statistical significance was determined using a one-way ANOVA with Šídák's multiple comparisons test with * indicating p≤0.05 and ** indicating p≤0.01.

These findings highlight the regulatory role of cGMP in platelet ferroptosis, as evidenced by the attenuation of hemin-induced changes in phosphatidyl serine exposure, ROS activity, and mitochondrial membrane potential. Nevertheless, it is important to note that lipid peroxidation appeared to be independent of cGMP modulation, suggesting the involvement of additional mechanisms in this process.

3.4 Hemin-induced changes of the platelet lipidome is dependent on cGMP

Ferroptosis is mediated by lipid peroxidation within cellular membranes, resulting in membrane damage, cellular dysfunction, and cell death[55]. To investigate the effects of hemin and cGMP modulation on platelet lipids, isolated platelets were treated with different concentrations of hemin (3.1 and 25 µM) in the presence or absence of DEA/NO and riociguat. The platelet lipidome was comprehensively analyzed using mass spectrometry.

The effects of hemin treatment on the platelet lipidome were profound, leading to significant alterations across the entire lipid profile. This is evident in the volcano plot **(Figure 24)**, which compares the lipidome of platelets treated with hemin at a concentration of 25 µM to the control.

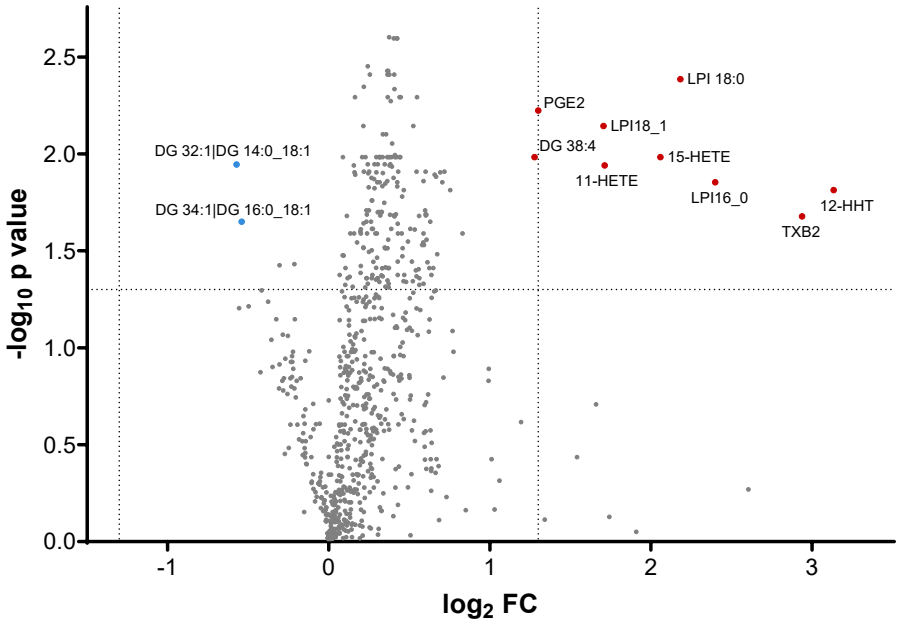

Figure 24: Impact of hemin on platelet lipidome. The volcano plot illustrates the profound alterations in the platelet lipid profile induced by hemin treatment at a concentration of 25 µM compared to the control. The X-axis (fold change, FC) represents the logarithm to the base 2 of the averaged ratios (hemin versus control) of peak intensities for each lipid. Values >1 indicate upregulation of the lipid by hemin, while values <1 indicate downregulation. The Y-axis represents the negative log10-transformed p-value of the ANOVA (hemin versus control). The significance threshold was set at 1.3 ($p<0.05$). Experiments performed in cooperation with Fu X., analysis made by Kremser M.

Importantly, the changes in the platelet lipidome induced by hemin were concentration-dependent, as illustrated in **Figure 25**. This figure displays all the lipid changes observed in response to five different treatments: control, hemin 3 µM, hemin 25 µM, hemin 3 µM with DEA/NO and riociguat, and hemin 25 µM with DEA/NO and riociguat. These findings highlight the comprehensive impact of hemin on platelet lipid composition and the modulating effects of DEA/NO and riociguat in the context of different hemin concentrations.

Next, we focused on investigating the impact of hemin and cGMP modulation on platelet ferroptosis by analyzing ferroptosis-related lipids. These lipids include PUFAs like arachidonic acid and docosahexaenoic acid (DHA) that are prone to oxidation and contribute to lipid peroxidation and MUFAs with their ability of to inhibit ferroptosis and suppress lipid ROS accumulation[106]. To visualize the effects, we created a heatmap displaying PUFAs and their metabolites treated with different concentrations of hemin (3.1 and 25 µM) in the presence or absence of DEA/NO and riociguat **(Figure 26)**. The metabolites were moreover analyzed in box plots classified by the involving pathway to facilitate further statistical analyses, such as those involving COX, non-enzymatic oxidation, 5-LOX, 12-LOX, and 15-LOX **(Figure 27A to E respectively)**.

Our findings showed that higher concentrations of hemin (25 µM) led to an upregulation of thromboxane B_2 (TXB_2), prostaglandin E_2 (PGE_2), 11-HETE, 15-HETE, and 12-HHT. However, notably, the presence of DEA/NO and riociguat significantly prevented the hemin-induced upregulation of these ferroptosis-associated lipids except for PGE_2.

Taken together, our findings provide compelling evidence for the critical regulatory role of cGMP in hemin-dependent platelet function and ferroptosis. By modulating cGMP levels, DEA/NO and riociguat effectively mitigate the hemin-induced changes in platelet lipid composition, particularly those associated with ferroptosis. These results highlight the therapeutic potential of targeting the sGC-cGMP pathway to modulate platelet function and mitigate the detrimental effects of hemin-induced ferroptosis in platelets.

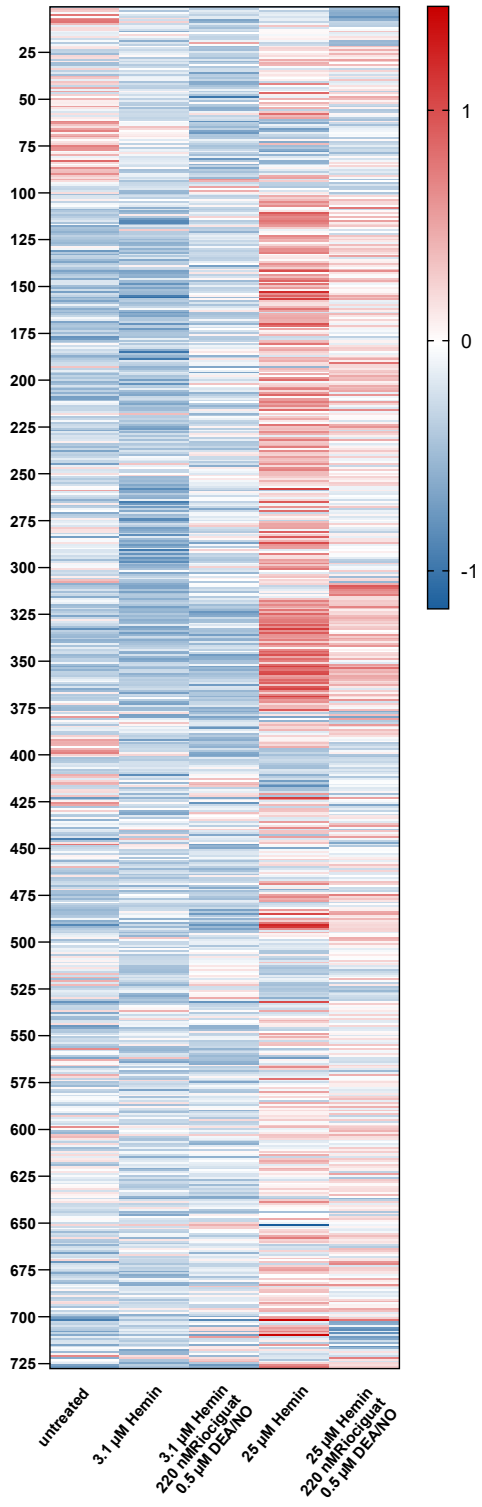

Figure 25: Heatmap representation of the platelet lipidome changes induced by hemin and cGMP modulation. The heatmap of 727 identified lipids illustrates the alterations in lipid composition observed in response to five conditions: Platelets were treated with different concentrations of hemin (3.1 and 25 µM) in the presence or absence of DEA/NO and riociguat. The color intensity indicates the relative abundance of each lipid, with higher intensities representing higher levels. The scale displayed represents the z-score, reflecting the relative deviation of each lipid abundance from the mean abundance across the samples. Experiments performed in cooperation with Fu X., analysis made by Kremser M.

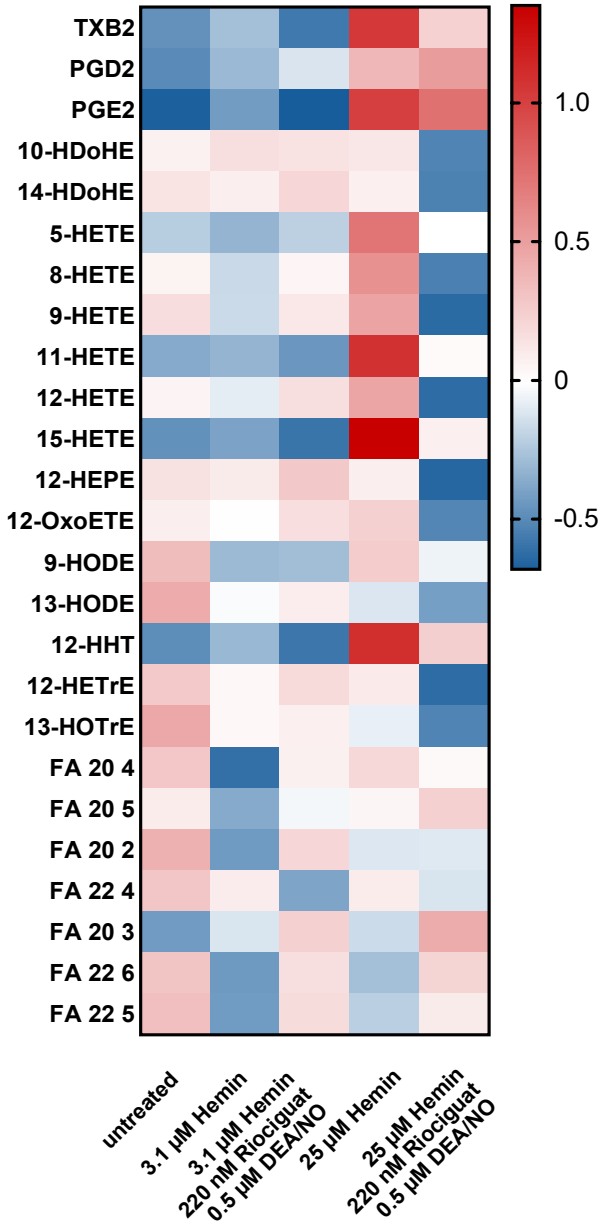

Figure 26: Heatmap representation of the impact of hemin and cGMP modulation on ferroptosis-related lipids in platelets. The heatmap illustrates the levels of various PUFAs and MUFAs and their metabolites treated with different concentrations of hemin (3.1 and 25 µM) in the presence or absence of DEA/NO and riociguat. The color intensity indicates the relative abundance of each lipid, with higher intensities representing higher levels. The scale displayed represents the z-score, reflecting the relative deviation of each lipid abundance from the mean abundance across the samples. FA 20:5, eicosapentaenoic acid (EPA); FA 20:3, dihomo-gamma-linolenic acid (DGLA); FA 22:4, adrenic acid; FA 20:3, nervonic acid; FA 22:6, docosahexaenoic acid (DHA); FA 22:5, docosapentaenoic acid (DPA). Experiments performed in cooperation with Fu X., analysis made by Kremser M.

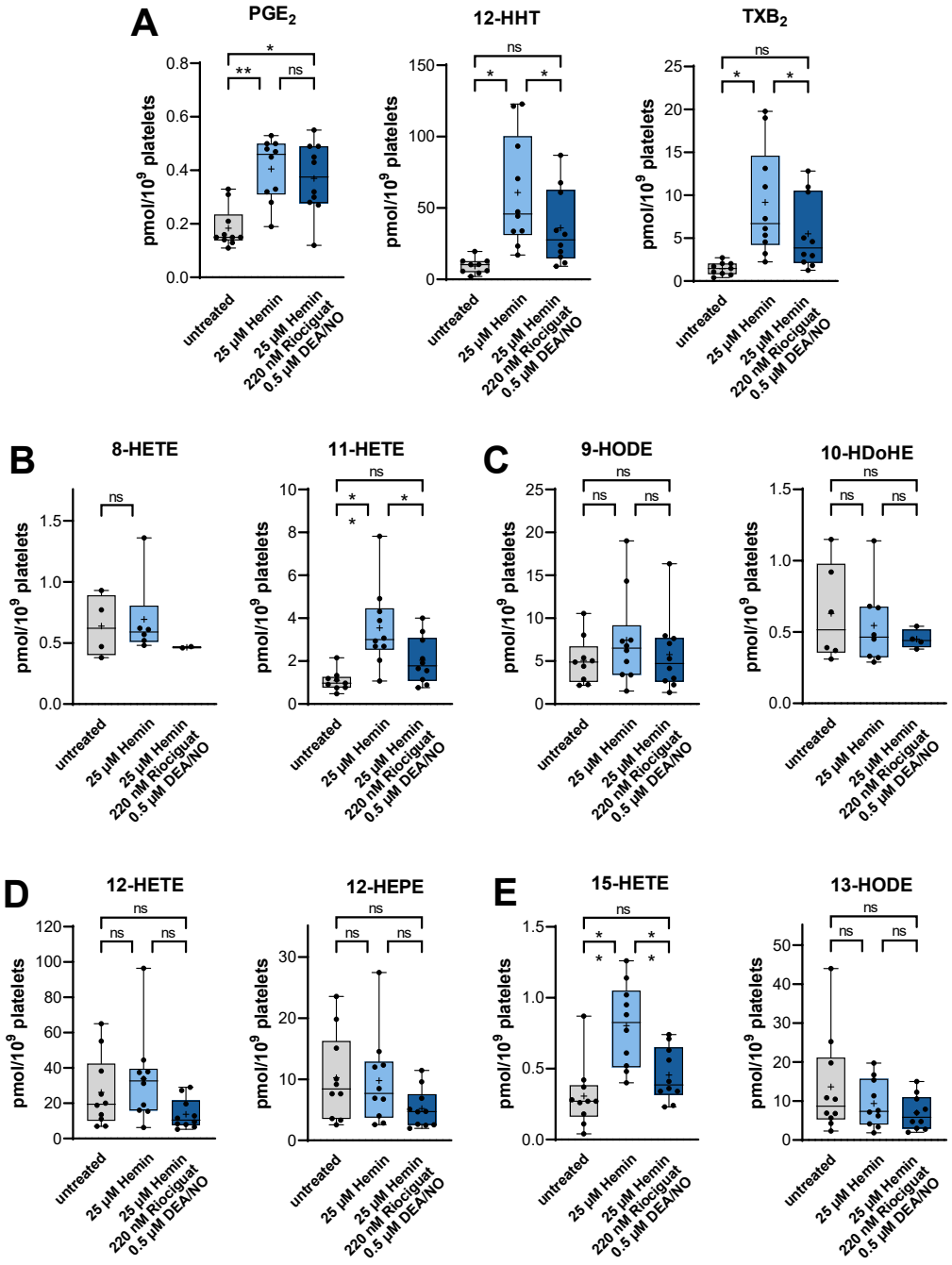

Figure 27: Box plots of ferroptosis-related lipid metabolites changes induced by hemin and cGMP modulation. Isolated platelets were treated with hemin (25 µM) in the presence or absence of DEA/NO and riociguat. The box plots categorize PUFA metabolites based on the enzyme responsible for their production: Cyclooxygenases (COX) (Figure 27A), non-enzymatic oxidation (Figure 27B), 5-lipoxygenase (5-LOX) (Figure 27C), 12-lipoxygenase (12-LOX) (Figure 27D), and 15-lipoxygenase (15-LOX) (Figure 27E). The y-axis represents the abundance of each lipid metabolite in pmol per 10^8 platelets. Statistical significance was determined using a one-way ANOVA with Šídák's multiple comparisons test (n=10); n.s. = non-significant ($p>0.05$), * indicating $p\leq0.05$ and ** indicating $p\leq0.01$. Experiments performed in cooperation with Fu X., analysis made by Kremser M.

4 Discussion

4.1 Pro-thrombotic properties of hemolytic plasma in autoimmune hemolysis

During hemolysis, Hb and its metabolite, free heme, are released from RBCs directly into circulation, resulting in hemolytic plasma and promoting oxidative stress and inflammation. Emerging evidence suggests that hemolytic plasma in autoimmune hemolysis possesses pro-thrombotic properties, contributing to the increased risk of thrombotic events observed in these patients[107].

Several studies have investigated the molecular mechanisms underlying the pro-thrombotic effects of hemolytic plasma. It has been demonstrated that hemoglobin and heme released from lysed RBCs can directly interact with platelets, endothelial cells, and coagulation factors, promoting platelet activation, endothelial dysfunction, and the activation of the coagulation cascade[23,108].

Given that intravascular hemolysis rapidly depletes NO due to NO consumption by hemoglobin[109] and inhibition of NO synthesis by arginases[102], our hypothesis proposed a beneficial effect of cGMP modulation on platelet activation associated with hemolysis.

To test this hypothesis, we resuspended platelets in plasma obtained from patients with autoimmune hemolysis and healthy controls and measured platelet aggregation. The results revealed a significant enhancement in platelet aggregation when platelets were resuspended in plasma derived from patients with autoimmune hemolysis, particularly when stimulated with ADP. This finding indicates a pro-thrombotic effect associated with hemolytic plasma. Interestingly, the effect of hemolytic plasma on platelet aggregation appeared to be specific to ADP stimulation, as no significant differences were observed when platelet aggregation was induced by CRP. This finding underscores the need for further investigation into the specific mechanisms underlying platelet activation in the context of autoimmune hemolysis.

To further investigate the potential involvement of cGMP modulation in platelet activation, platelets were pre-treated with DEA/NO and riociguat. Remarkably, a reduction in platelet aggregation was observed in samples obtained from patients, suggesting that modulation of cGMP levels within platelets may play a critical role in mitigating the heightened platelet activation observed in the presence of hemolytic plasma.

These findings align with current literature on the pro-thrombotic condition during hemolysis, which is partly attributed to NO depletion and support the notion that modulating cGMP could reduce the increased platelet activation observed. The results emphasize the need for further investigation into the underlying mechanisms driving platelet activation in the context of autoimmune hemolysis and highlight the potential of cGMP modulation as a therapeutic approach to counteract platelet activation. Advancing our understanding of the pathophysiology of autoimmune hemolysis and identifying novel therapeutic strategies to prevent thrombotic complications are crucial areas for future research.

4.2 Hemin-induced platelet activation and its dependence on cGMP

Since hemin is one of the major parts released by RBCs during hemolysis and previous studies have highlighted hemin as an endogenous agonist for CLEC-2 leading to platelet activation[19], we further focused our research on hemin induced platelet activation.

Consistent with previous studies, we observed that erythrocyte lysates and hemin alone stimulated P-selectin surface expression, indicating platelet degranulation. However, intriguingly, hemin alone did not significantly activate platelets in the PRP of healthy donors, suggesting the presence of factors in PRP, such as hemopexin, that might neutralize hemin's pro-thrombotic properties. This finding emphasizes the need for further investigation to understand the underlying mechanisms.

We explored the influence of cGMP modulation on hemin-induced platelet activation by using DEA/NO and riociguat, which enhance cGMP signaling. Lower concentrations of hemin showed a significant reduction in P-selectin expression in the presence of DEA/NO and riociguat, indicating the involvement of cGMP modulation. However, at higher concentrations of hemin, the decrease in P-selectin expression was independent of cGMP modulation, suggesting the activation of additional pathways. Additionally, we observed a significant reduction in hemin-induced PAC-1 surface expression, indicative of αIIbβ3 integrin activation, in the presence of DEA/NO and riociguat at every concentration of hemin used.

To further understand the impact of cGMP modulation, we investigated the effect of the sGC activator cinaciguat on hemin-induced platelet activation markers. Our results demonstrated that cinaciguat, in combination with the sGC inhibitor ODQ, significantly inhibited hemin-dependent P-selectin expression and GPIIb/IIIa activation. Furthermore, significant reductions in P-selectin expression and GPIIb/IIIa activation were observed when using indomethacin and cangrelor alone, indicating the involvement of other pathways, such as COX inhibition and $P2Y_{12}$ receptor blockade, in mitigating hemin-induced platelet activation.

Furthermore, we investigated the impact of hemin and CRP stimulation on ATP release, a measure of platelet activation. Significant increases in ATP release were observed, which were attenuated by DEA/NO and riociguat treatment. DEA/NO and riociguat also effectively inhibited both hemin-induced and ADP-induced platelet aggregation, with a more pronounced effect on ADP-induced aggregation. Similarly, cinaciguat, alone and in combination with ODQ, exhibited inhibitory effects on platelet aggregation induced by both hemin and ADP.

Inhibitor studies provided insights into the mechanisms underlying hemin-induced platelet aggregation. We found that neither indomethacin nor cangrelor prevented hemin-induced platelet aggregation, suggesting that other pathways might be involved. However, the inhibitor eptifibatide, which targets the fibrinogen receptor GPIIb/IIIa, significantly inhibited hemin-induced platelet aggregation, highlighting the crucial role of fibrinogen-GPIIb/IIIa interaction in this pathway.

The controversial results observed between flow cytometry measurements of isolated platelets demonstrating inhibitory effects of cangrelor and indomethacin and platelet aggregation measurements using light transmittance aggregometry not showing the same inhibitory effects raise several possible explanations. One potential reason for the discrepancy is the mechanisms assessed by FACS and light transmittance aggregometry differ. FACS analysis provides detailed information about specific platelet activation markers and intracellular signaling events, while light transmittance aggregometry measures the overall aggregation response. It is conceivable that cangrelor and indomethacin have specific effects on platelet activation pathways or signaling events that are more sensitively detected by FACS analysis but may not strongly influence the overall aggregation response measured by light transmittance aggregometry.

Another factor to consider is the timing of the measurements. Platelet activation and aggregation are dynamic processes that evolve over time. The inhibitory effects of cangrelor and indomethacin might become more evident at certain time points after hemin stimulation, which could be captured differently by FACS and light transmittance aggregometry.

The enhanced hemin-induced increase in intracellular and extracellular calcium, known to play a role in platelet activation, was significantly attenuated in the presence of riociguat, further supporting the involvement of cGMP modulation in mitigating hemin-induced platelet activation.

Western blot analysis revealed concentration-dependent reductions in VASP phosphorylation and increases in AKT phosphorylation upon hemin treatment. However, these effects were counteracted by cGMP modulation through DEA/NO and riociguat, suggesting their role in regulating intracellular signaling pathways.

Finally, Raman spectroscopy provided valuable insights into morphological changes and hemin binding on platelets. We observed that hemin treatment induced morphological changes and promoted hemin binding, which could be attenuated by cGMP modulation. Dose-response experiments showed a concentration-dependent increase in hemin-induced platelet aggregation.

In conclusion, our study so far provides valuable insights into hemin-induced platelet activation and the modulation of cGMP signaling. These findings contribute to a better understanding of the mechanisms underlying hemin-induced platelet activation and highlight potential targets for therapeutic intervention in conditions associated with hemolysis and platelet activation. Further research is warranted to elucidate the precise mechanisms involved and explore the therapeutic potential of cGMP modulation in this context.

4.3 Hemin-induced ferroptosis and its dependence on cGMP

Heme-mediated lipid peroxidation and ferroptosis in platelets have emerged as possible important factors in hemolytic disorders[23]. Previous research has primarily focused on ferroptosis in the context of RBC transfusions, hemorrhagic stroke, and kidney and liver damage associated with intravascular hemolysis[110]. Considering that RBCs contain a significant amount of iron, it is highly likely that hemolytic disorders contribute to platelet ferroptosis. However, further investigation is needed to fully understand this phenomenon.

In this study, we aimed to explore the involvement of cGMP in the regulation of platelet ferroptosis. We observed a concentration-dependent increase in phosphatidyl serine exposure and ROS activity, along with a decrease in mitochondrial membrane potential, indicating the induction of ferroptosis in platelets following hemin treatment. Notably, modulation of cGMP through DEA/NO and riociguat effectively attenuated these ferroptosis-associated platelet changes, underscoring the crucial role of cGMP signaling in the regulation of ferroptosis. However, the precise underlying mechanisms by which cGMP modulation influences ferroptosis in platelets require further investigation.

Furthermore, we conducted a comprehensive analysis of the platelet lipidome using mass spectrometry to gain insights into the effects of hemin and cGMP modulation on platelet lipids. Hemin treatment resulted in significant alterations across the entire lipid profile, indicating the profound impact of hemin on platelet lipid composition. These changes were found to be concentration-dependent, further highlighting the dose-dependent effects of hemin on platelet function and

lipid metabolism. Notably, biliverdin, a product of heme catabolism, was below the detection limit in our analysis.

Heatmap analysis of ferroptosis-related lipids revealed that higher concentrations of hemin upregulated several lipids associated with ferroptosis, including TXB_2, PGE_2, 11-HETE, 15-HETE, and 12-HHT. Importantly, cGMP modulation by DEA/NO and riociguat effectively prevented the hemin-induced upregulation of these ferroptosis-associated lipids, with the exception of PGE_2. These findings emphasize the regulatory role of cGMP in modulating the lipid composition of platelets, particularly in the context of ferroptosis.

It is worth noting that while flow cytometry measurements of lipid peroxidation, a crucial feature of ferroptosis, appeared to be independent of cGMP modulation, the comprehensive analysis of the platelet lipidome using mass spectrometry elucidated the alterations induced by hemin treatment and the modulatory effects of cGMP modulation, particularly on ferroptosis-associated lipids. This discrepancy may be attributed to the differential sensitivity of the measurement techniques, as flow cytometry and mass spectrometry assess different aspects of lipid peroxidation and lipidome alterations. The flow cytometry assay employed to measure lipid peroxidation may not capture subtle changes or specific lipid species affected by cGMP modulation, which are detected by mass spectrometry.

Moreover, significantly changes were only observed in metabolites of PUFAs rather than the PUFAs themselves. PGE_2, 12-HHT (12-hydroxyheptadecatrienoic acid), and TXB_2 are bioactive lipid mediators derived from arachidonic acid metabolism through the enzymatic action of COX. On the other hand, 11-HETE is generated through the non-enzymatic oxidation of arachidonic acid and 15-HETE is generated through the metabolism of arachidonic acid by the enzyme 15-LOX. In contrast, fatty acids (FAs) such as arachidonic acid (FA 20:4), a PUFA, and nervonic acid (FA 20:3), a MUFA, did not show significant changes in the context of this study. It is possible that the effects of hemin on the metabolism of PUFAs manifest later in the form of altered metabolites. However, additional research is necessary to deepen our understanding and obtain a comprehensive interpretation of these findings, thus enhancing the clarity of the observed effects.

Additionally, a study demonstrated the catalytic consumption of NO by 12/15-LOX, resulting in the inhibition of monocyte sGC activation[111]. This establishes 12/15-LOX as a potential catalytic sink for NO. Considering the reduced NO bioavailability in hemolysis, it is plausible that increased LOX-15 activity, leading to NO consumption, could contribute to decreased platelet NO reactivity and potentially promote ferroptosis. The study sheds light on the complex interplay between NO, cGMP, and LOX, indicating that LOX activity can modulate the NO-cGMP signaling pathway, which may impact downstream physiological processes regulated by cGMP. These findings highlight the significance of considering LOX as a potential regulator of NO-mediated cellular responses, including those involved in ferroptosis. Further investigation is warranted to explore the specific mechanisms by which LOX-15 activity and NO availability influence platelet reactivity and ferroptosis in the context of hemolysis. This knowledge may uncover potential therapeutic targets for managing hemolytic disorders and preventing platelet-mediated complications associated with ferroptosis.

Overall, our study provides valuable insights into hemin-induced ferroptosis in platelet activation, with cGMP modulation proving to be effective in attenuating associated platelet changes. The effects of cGMP modulation on ferroptosis-associated platelet parameters and the platelet lipidome underscore the therapeutic potential of targeting the sGC-cGMP pathway to mitigate the detrimental effects of hemin-induced ferroptosis in platelets. Further research is needed to fully elucidate the underlying mechanisms and explore the clinical implications of these findings.

Collectively, these findings highlight the intricate role of cGMP in mediating platelet ferroptosis and offer potential therapeutic interventions in hemin-mediated platelet dysfunction and thrombotic disorders. This study significantly contributes to our understanding of platelet activation and thrombotic disorders in the context of autoimmune hemolysis. It advances the existing literature by elucidating the role of cGMP signaling in regulating platelet activation and ferroptosis, providing insights into potential therapeutic targets for managing thrombotic complications. Furthermore, it is important to note that the treatment

options for hemolytic diseases are currently limited and often ineffective. This underscores the urgent need for novel therapeutic approaches.

Considering the role of ferroptosis in platelet dysfunction and thrombotic disorders is a relatively new area of research, further research can explore the clinical translation of these findings and evaluate the efficacy of targeting the sGC-cGMP pathway as a therapeutic approach in patients with autoimmune hemolysis and other thrombotic disorders.

4.4 Limitations and Methodological Considerations

Despite the valuable insights gained from this study, several limitations and methodological considerations should be acknowledged. First, this study primarily relied on *in vitro* experiments using isolated platelets and patient plasma samples. While these experimental setups allowed for controlled investigations of platelet activation and modulation of cGMP signaling, they may not fully reflect the complexity of platelet function *in vivo*. Future studies should aim to validate these findings using animal models or *ex vivo* experiments using whole blood samples to better mimic the physiological conditions.

Another limitation is the use of hemin as a model for studying platelet activation in the context of hemolytic disorders. Although hemin is a relevant byproduct of hemolysis, it may not fully capture the complexity of platelet activation in autoimmune hemolysis. Other components present in hemolytic plasma, such as antibodies and complement factors, could contribute to platelet activation and thrombotic complications. Future studies should consider including these factors in experimental setups to better mimic the pathophysiological conditions of autoimmune hemolysis.

Additionally, the use of specific pharmacological agents, such as DEA/NO and riociguat, to modulate cGMP levels in platelets introduces potential limitations. These agents may have off-target effects or interact with other signaling pathways, which could influence the observed outcomes. Therefore, future studies should consider employing genetic approaches, such as platelet-specific

knockout models, to directly manipulate cGMP signaling pathways and validate the specific role of sGC-cGMP signaling in platelet activation and ferroptosis. While some initial experiments have been conducted in this direction (data not shown), it is necessary to expand the scope and diversity of experiments to strengthen the overall findings.

Furthermore, this study focused on the role of cGMP signaling in platelet activation and ferroptosis, but other signaling pathways and mechanisms may also be involved in hemin-induced effects on platelets. One such important player in ferroptosis is glutathione peroxidase 4 (GPX4), an enzyme involved in lipid peroxidation and protection against oxidative stress. GPX4 plays a crucial role in suppressing ferroptosis by reducing lipid hydroperoxides and maintaining redox balance within cells. Future investigations should explore the potential involvement of GPX4 and its regulation in platelet ferroptosis in the context of hemin-induced effects. Understanding the interplay between cGMP signaling and GPX4-mediated mechanisms will provide a more comprehensive understanding of the complex processes underlying platelet dysfunction and ferroptosis.

In addition, previous research has highlighted the role of proprotein convertases (PCs) in mediating the endoproteolytic cleavage of PKGI, a key player in cGMP signaling pathways. Specifically, the PC furin has been shown to dose-dependently increase PKGI cleavage, indicating its essential role in modulating the effects of cGMP[112]. Interestingly, genome-wide association studies have also suggested a potential involvement of furin in cGMP signaling pathways, particularly in the context of cardiovascular diseases[71]. These findings emphasize the importance of furin in cGMP-mediated processes and recent research could show the contribution of furin on modulating hemin-induced ferroptosis[113]. Therefore, it is important to consider the interplay between different signaling pathways, such as the NO-cGMP pathway and the furin pathway, in platelet function and ferroptosis. Future studies should explore the crosstalk between these pathways and identify potential synergistic interactions.

To address these limitations and improve the methodology, future studies could consider incorporating more comprehensive experimental designs. This could involve the use of animal models, *ex vivo* studies using whole blood samples, and the inclusion of additional relevant factors present in hemolytic plasma. Moreover, employing advanced imaging techniques, such as intravital microscopy, could provide real-time visualization of platelet activation and thrombus formation *in vivo*.

In terms of specific outcomes, conducting a study with hemolytic patients would provide substantial value, although it is a long-term endeavor. Adding hemin to platelet-rich plasma (PRP) obtained from patients with hemolysis and measuring platelet aggregation would yield direct insights into the inhibitory effects of factors like hemopexin under healthy conditions. Additionally, performing whole blood aggregometry and perfusion experiments on immobilized collagen using hemolytic samples could provide valuable observations.

Another avenue to explore would be the utilization of animal models, such as a platelet-specific sGC depleted mice compared to control mice, followed by hemin administration to examine the occurrence of hemolysis and prothrombotic events. Assessing potential differences based on the functionality of the cGMP pathway would further enhance the understanding of the underlying mechanisms.

Expanding the scope of lipidomics investigations to include not only metabolites of PUFAs but also metabolites of MUFAs would be intriguing. It is possible that cGMP may increase MUFA metabolites, as MUFAs are known to inhibit ferroptosis. Examining the role of MUFA metabolites in the context of cGMP signaling could provide valuable insights into the regulation of ferroptosis.

In conclusion, while this study provides valuable insights into the pro-thrombotic properties of hemolytic plasma and the role of cGMP signaling in platelet activation and ferroptosis, it is important to acknowledge the limitations and methodological considerations. By addressing these limitations and incorporating more comprehensive experimental approaches, future studies can further advance our understanding of platelet dysfunction in autoimmune hemolysis and contribute to the development of novel therapeutic strategies.

4.5 Practical Implications

The practical implications of the findings from this study are significant for the management of thrombotic complications in autoimmune hemolysis. The observed pro-thrombotic properties of hemolytic plasma and the enhanced platelet activation associated with this condition combined with the currently limited and often ineffective treatment options for hemolytic diseases emphasize the need for targeted interventions to prevent thrombotic events in affected individuals. Modulating cGMP levels within platelets through pharmacological agents such as DEA/NO and riociguat could potentially serve as a therapeutic strategy to mitigate platelet dysfunction and reduce the risk of thrombosis. Furthermore, the identification of cGMP signaling as a key mediator of platelet activation and ferroptosis in the context of autoimmune hemolysis opens up new ways for therapeutic interventions. Developing novel therapies that specifically target the sGC-cGMP pathway could potentially alleviate platelet dysfunction and prevent thrombotic complications in patients with autoimmune hemolysis.

However, there are several challenges and limitations that need to be considered when implementing these findings in practice. One limitation is the complex and multifactorial nature of autoimmune hemolysis, which involves interactions between various components of the immune system, red blood cells, and platelets. The effectiveness of cGMP modulation as a therapeutic strategy may vary among individuals based on the specific underlying mechanisms driving their disease. Additionally, the use of pharmacological agents to modulate cGMP levels may have potential side effects and require careful monitoring. Further research is needed to determine optimal dosages, treatment durations, and potential long-term effects of cGMP-modulating compounds in the context of autoimmune hemolysis.

In terms of practical applications, the findings from this study have the potential to guide the development of targeted therapies that focus on the sGC-cGMP pathway in managing platelet dysfunction and thrombotic complications in autoimmune hemolysis. Clinical trials could be designed to evaluate the efficacy and safety of pharmacological agents targeting this pathway in patients with autoimmune hemolysis.

Moreover, the comprehensive analysis of the platelet lipidome and the identification of specific lipid alterations associated with ferroptosis provide insights into potential biomarkers for monitoring disease progression and treatment response. Future studies could explore the clinical utility of these lipid markers in assessing the severity of autoimmune hemolysis and predicting thrombotic risk.

In conclusion, the findings of this study have practical implications for the development of targeted therapies and the identification of biomarkers in autoimmune hemolysis. While challenges and limitations exist, the potential benefits of modulating the sGC-cGMP pathway to mitigate platelet dysfunction and prevent thrombotic complications warrant further research and clinical exploration.

The therapeutic potential of cGMP-modulating pharmacological agents extends beyond patients with autoimmune hemolysis. These compounds have already been successfully utilized in the treatment of various diseases, such as pulmonary hypertension and erectile dysfunction. Therefore, the class of hemolytic conditions could potentially be added to the list of diverse applications for modulating the sGC-cGMP pathway.

cGMP has been identified as a promising candidate for the treatment of SCD. The modulation of cGMP signaling holds the potential to alleviate the pathophysiological processes associated with SCD, including vaso-occlusive crises and endothelial dysfunction.

Interestingly, even COVID-19 patients have shown elevated heme plasma levels similar to those observed in hemolytic conditions. This suggests that cGMP-modulating pharmacological agents may have additional application possibilities in the management of COVID-19, potentially targeting the underlying hemolytic processes and associated complications. Further research is warranted to fully uncover the therapeutic potential and mechanisms of action of cGMP modulation in these contexts.

5 Conclusion

The research objectives of this study were to investigate the pro-thrombotic properties of hemolytic plasma in autoimmune hemolysis, to understand the role of cGMP signaling in platelet activation and ferroptosis, and to explore potential therapeutic strategies for managing thrombotic complications in this disorder. The findings of this study have provided significant insights and advancements in our understanding of platelet dysfunction and thrombotic disorders in the context of autoimmune hemolysis.

The study demonstrated that hemolytic plasma derived from patients with autoimmune hemolysis possesses pro-thrombotic properties, leading to increased platelet aggregation compared to control plasma. The identification of ADP as a potent stimulator of platelet aggregation in patient plasma highlights the relevance of this signaling pathway in autoimmune hemolysis-associated thrombotic complications. Furthermore, modulating cGMP levels within platelets through pre-treatment with DEA/NO and riociguat effectively mitigated the enhanced platelet activation associated with hemolytic plasma. These findings offer potential therapeutic strategies for managing thrombotic complications by targeting the sGC-cGMP pathway.

Additionally, the study revealed the role of cGMP signaling in regulating platelet ferroptosis. Hemin, a pro-oxidant molecule released during hemolysis, was found to induce platelet activation in a cGMP-dependent manner. The inhibitory effects of cGMP modulation on hemin-induced platelet activation and the modulation of ferroptosis-associated lipids highlight the importance of cGMP signaling in platelet function and offer avenues for further investigation.

The significance and implications of these findings extend beyond the context of autoimmune hemolysis. They contribute to the existing literature on platelet activation and thrombotic disorders by providing novel insights into the mechanisms underlying platelet dysfunction and identifying potential therapeutic targets. The modulation of the sGC-cGMP pathway emerges as a promising strategy for managing thrombotic complications, not only in autoimmune hemolysis but also in other thrombotic disorders.

In conclusion, this study significantly contributes to our understanding of platelet activation and thrombotic disorders in the context of autoimmune hemolysis. The findings highlight the pro-thrombotic properties of hemolytic plasma, the involvement of cGMP signaling in platelet activation and ferroptosis, and the potential therapeutic strategies for managing thrombotic complications. By elucidating the underlying mechanisms and offering new insights, this study opens up avenues for further research and clinical translation, ultimately aiming to improve the management and outcomes of patients with autoimmune hemolysis and other thrombotic disorders.

6 References

1. Dhaliwal, G., Cornett, P. A. & Tierney, L. M. Hemolytic anemia. *American family physician* **69,** 2599–2606; Review (2004).

2. Bender, M. A. *GeneReviews®. Sickle Cell Disease* (Seattle (WA), 1993).

3. Martin, A. & Thompson, A. A. Thalassemias. *Pediatric clinics of North America* **60,** 1383–1391; 10.1016/j.pcl.2013.08.008 (2013).

4. Phillips, M. A. *et al.* Malaria. *Nature reviews. Disease primers* **3,** 17050; 10.1038/nrdp.2017.50 (2017).

5. Karpman, D., Loos, S., Tati, R. & Arvidsson, I. Haemolytic uraemic syndrome. *Journal of internal medicine* **281,** 123–148; 10.1111/joim.12546 (2017).

6. Arndt, P. A. Drug-induced immune hemolytic anemia: the last 30 years of changes. *Immunohematology* **30,** 44–54; Review (2014).

7. Harewood, J., Ramsey, A. & Master, S. R. *StatPearls. Hemolytic Transfusion Reaction* (Treasure Island (FL), 2022).

8. Zhong, H. & Yazdanbakhsh, K. Hemolysis and immune regulation. *Current opinion in hematology* **25,** 177–182; 10.1097/MOH.0000000000000423 (2018).

9. Gehrs, B. C. & Friedberg, R. C. Autoimmune hemolytic anemia. *American journal of hematology* **69,** 258–271; 10.1002/ajh.10062 (2002).

10. Xiao, Z. & Murakhovskaya, I. Development of New Drugs for Autoimmune Hemolytic Anemia. *Pharmaceutics* **14**; 10.3390/pharmaceutics14051035 (2022).

11. Ataga, K. I. Hypercoagulability and thrombotic complications in hemolytic anemias. *Haematologica* **94,** 1481–1484; 10.3324/haematol.2009.013672 (2009).

12. Marengo-Rowe, A. J. Structure-function relations of human hemoglobins. *Proceedings (Baylor University. Medical Center)* **19,** 239–245; 10.1080/08998280.2006.11928171 (2006).

13. Hrkal, Z., Vodrázka, Z. & Kalousek, I. Transfer of heme from ferrihemoglobin and ferrihemoglobin isolated chains to hemopexin. *European journal of biochemistry* **43,** 73–78; 10.1111/j.1432-1033.1974.tb03386.x (1974).

14. Belcher, J. D. *et al.* Haptoglobin and hemopexin inhibit vaso-occlusion and inflammation in murine sickle cell disease: Role of heme oxygenase-1 induction. *PloS one* **13,** e0196455; 10.1371/journal.pone.0196455 (2018).

15. Nielsen, M. J., Møller, H. J. & Moestrup, S. K. Hemoglobin and heme scavenger receptors. *Antioxidants & redox signaling* **12,** 261–273; 10.1089/ars.2009.2792 (2010).

16. Schaer, D. J., Buehler, P. W., Alayash, A. I., Belcher, J. D. & Vercellotti, G. M. Hemolysis and free hemoglobin revisited: exploring hemoglobin and hemin scavengers as a novel class of therapeutic proteins. *Blood* **121,** 1276–1284; 10.1182/blood-2012-11-451229 (2013).

17. Santiago, R. P. *et al.* Serum Haptoglobin and Hemopexin Levels in Pediatric SS and SC Disease Patients: Biomarker of Hemolysis and Inflammation. *Blood* **128,** 3649; 10.1182/blood.V128.22.3649.3649 (2016).

18. MULLER-EBERHARD, U., JAVID, J., LIEM, H. H., HANSTEIN, A. & HANNA, M. Brief Report: Plasma Concentrations of Hemopexin, Haptoglobin and Heme in Patients with Various Hemolytic Diseases. *Blood* **32,** 811–815; 10.1182/blood.V32.5.811.811 (1968).

19. Bourne, J. H. *et al.* Heme induces human and mouse platelet activation through C-type-lectin-like receptor-2. *Haematologica* **106,** 626–629; 10.3324/haematol.2020.246488 (2021).

20. Wang, G. R., Zhu, Y., Halushka, P. V., Lincoln, T. M. & Mendelsohn, M. E. Mechanism of platelet inhibition by nitric oxide: in vivo phosphorylation of thromboxane receptor by cyclic GMP-dependent protein kinase.

Proceedings of the National Academy of Sciences of the United States of America **95,** 4888–4893; 10.1073/pnas.95.9.4888 (1998).

21. Reiter, C. D. *et al.* Cell-free hemoglobin limits nitric oxide bioavailability in sickle-cell disease. *Nature medicine* **8,** 1383–1389; 10.1038/nm1202-799 (2002).

22. Delvasto-Nuñez, L., Jongerius, I. & Zeerleder, S. It takes two to thrombosis: Hemolysis and complement. *Blood reviews* **50,** 100834; 10.1016/j.blre.2021.100834 (2021).

23. NaveenKumar, S. K. *et al.* The Role of Reactive Oxygen Species and Ferroptosis in Heme-Mediated Activation of Human Platelets. *ACS chemical biology* **13,** 1996–2002; 10.1021/acschembio.8b00458 (2018).

24. Schubothe, H. The cold hemagglutinin disease. *Seminars in hematology* **3,** 27–47 (1966).

25. Swiecicki, P. L., Hegerova, L. T. & Gertz, M. A. Cold agglutinin disease. *Blood* **122,** 1114–1121; 10.1182/blood-2013-02-474437 (2013).

26. Berentsen, S. *et al.* Primary chronic cold agglutinin disease: a population based clinical study of 86 patients. *Haematologica* **91,** 460–466 (2006).

27. Jaffe, C. J., Atkinson, J. P. & Frank, M. M. The role of complement in the clearance of cold agglutinin-sensitized erythrocytes in man. *The Journal of clinical investigation* **58,** 942–949; 10.1172/JCI108547 (1976).

28. Berentsen, S. *et al.* Rituximab for primary chronic cold agglutinin disease: a prospective study of 37 courses of therapy in 27 patients. *Blood* **103,** 2925–2928; 10.1182/blood-2003-10-3597 (2004).

29. Schöllkopf, C. *et al.* Rituximab in chronic cold agglutinin disease: a prospective study of 20 patients. *Leukemia & lymphoma* **47,** 253–260; 10.1080/10428190500286481 (2006).

30. Thon, J. N. & Italiano, J. E. Platelets: production, morphology and ultrastructure. *Handbook of experimental pharmacology,* 3–22; 10.1007/978-3-642-29423-5_1 (2012).

31. Grozovsky, R., Giannini, S., Falet, H. & Hoffmeister, K. M. Regulating billions of blood platelets: glycans and beyond. *Blood* **126,** 1877–1884; 10.1182/blood-2015-01-569129 (2015).

32. Tsoupras, A. B., Iatrou, C., Frangia, C. & Demopoulos, C. A. The implication of platelet activating factor in cancer growth and metastasis: potent beneficial role of PAF-inhibitors and antioxidants. *Infectious disorders drug targets* **9,** 390–399; 10.2174/187152609788922555 (2009).

33. Ruggeri, Z. M. & Mendolicchio, G. L. Adhesion mechanisms in platelet function. *Circulation research* **100,** 1673–1685; 10.1161/01.RES.0000267878.97021.ab (2007).

34. Munnix, I. C. A., Cosemans, J. M. E. M., Auger, J. M. & Heemskerk, J. W. M. Platelet response heterogeneity in thrombus formation. *Thrombosis and haemostasis* **102,** 1149–1156; 10.1160/TH09-05-0289 (2009).

35. Ali, R. A., Wuescher, L. M. & Worth, R. G. Platelets: essential components of the immune system. *Current trends in immunology* **16,** 65–78; have (2015).

36. Cognasse, F. *et al.* Evidence of Toll-like receptor molecules on human platelets. *Immunology and cell biology* **83,** 196–198; 10.1111/j.1440-1711.2005.01314.x (2005).

37. Cox, D., Kerrigan, S. W. & Watson, S. P. Platelets and the innate immune system: mechanisms of bacterial-induced platelet activation. *Journal of thrombosis and haemostasis : JTH* **9,** 1097–1107; 10.1111/j.1538-7836.2011.04264.x (2011).

38. Krishnegowda, M. & Rajashekaraiah, V. Platelet disorders: an overview. *Blood coagulation & fibrinolysis : an international journal in haemostasis and thrombosis* **26,** 479–491; 10.1097/01.mbc.0000469521.23628.2d (2015).

39. del Zoppo, G. J. The role of platelets in ischemic stroke. *Neurology* **51,** S9-14; 10.1212/wnl.51.3_suppl_3.s9 (1998).

40. Schanze, N., Bode, C. & Duerschmied, D. Platelet Contributions to Myocardial Ischemia/Reperfusion Injury. *Frontiers in immunology* **10,** 1260; 10.3389/fimmu.2019.01260 (2019).

41. Mitchell, J. A., Ali, F., Bailey, L., Moreno, L. & Harrington, L. S. Role of nitric oxide and prostacyclin as vasoactive hormones released by the endothelium. *Experimental physiology* **93,** 141–147; 10.1113/expphysiol.2007.038588 (2008).

42. Makhoul, S. *et al.* Effects of the NO/soluble guanylate cyclase/cGMP system on the functions of human platelets. *Nitric oxide : biology and chemistry* **76,** 71–80; 10.1016/j.niox.2018.03.008 (2018).

43. *Platelets, Haemostasis and Inflammation.* 1st ed. (Springer International Publishing, Cham, 2017).

44. Green, D. R. & Llambi, F. Cell Death Signaling. *Cold Spring Harbor perspectives in biology* **7**; 10.1101/cshperspect.a006080 (2015).

45. Galluzzi, L. *et al.* Molecular mechanisms of cell death: recommendations of the Nomenclature Committee on Cell Death 2018. *Cell death and differentiation* **25,** 486–541; 10.1038/s41418-017-0012-4 (2018).

46. Dixon, S. J. *et al.* Ferroptosis: an iron-dependent form of nonapoptotic cell death. *Cell* **149,** 1060–1072; 10.1016/j.cell.2012.03.042 (2012).

47. Li, J. *et al.* Ferroptosis: past, present and future. *Cell death & disease* **11,** 88; 10.1038/s41419-020-2298-2 (2020).

48. Su, L.-J. *et al.* Reactive Oxygen Species-Induced Lipid Peroxidation in Apoptosis, Autophagy, and Ferroptosis. *Oxidative medicine and cellular longevity* **2019,** 5080843; 10.1155/2019/5080843 (2019).

49. Tang, D. & Kroemer, G. Ferroptosis. *Current biology : CB* **30,** R1292-R1297; 10.1016/j.cub.2020.09.068 (2020).

50. Lundqvist, A. *et al.* The Arachidonate 15-Lipoxygenase Enzyme Product 15-HETE Is Present in Heart Tissue from Patients with Ischemic Heart Disease and Enhances Clot Formation. *PloS one* **11,** e0161629; 10.1371/journal.pone.0161629 (2016).

51. Ikei, K. N. *et al.* Investigations of human platelet-type 12-lipoxygenase: role of lipoxygenase products in platelet activation. *Journal of lipid research* **53,** 2546–2559; 10.1194/jlr.M026385 (2012).

52. Wong, P. Y. *et al.* 15-Lipoxygenase in human platelets. *Journal of Biological Chemistry* **260,** 9162–9165; 10.1016/S0021-9258(17)39346-8 (1985).

53. Singh, N. K. & Rao, G. N. Emerging role of 12/15-Lipoxygenase (ALOX15) in human pathologies. *Progress in lipid research* **73,** 28–45; 10.1016/j.plipres.2018.11.001 (2019).

54. Manke, M.-C. *et al.* ANXA7 Regulates Platelet Lipid Metabolism and Ca2+ Release in Arterial Thrombosis. *Circulation research* **129,** 494–507; 10.1161/CIRCRESAHA.121.319207 (2021).

55. Kuang, F., Liu, J., Tang, D. & Kang, R. Oxidative Damage and Antioxidant Defense in Ferroptosis. *Frontiers in cell and developmental biology* **8,** 586578; 10.3389/fcell.2020.586578 (2020).

56. Yang, W. S. *et al.* Regulation of ferroptotic cancer cell death by GPX4. *Cell* **156,** 317–331; 10.1016/j.cell.2013.12.010 (2014).

57. Papucci, L. *et al.* Coenzyme q10 prevents apoptosis by inhibiting mitochondrial depolarization independently of its free radical scavenging property. *Journal of Biological Chemistry* **278,** 28220–28228; 10.1074/jbc.M302297200 (2003).

58. Levine, A. B., Punihaole, D. & Levine, T. B. Characterization of the role of nitric oxide and its clinical applications. *Cardiology* **122,** 55–68; 10.1159/000338150 (2012).

59. NaveenKumar, S. K., Hemshekhar, M., Kemparaju, K. & Girish, K. S. Hemin-induced platelet activation and ferroptosis is mediated through

ROS-driven proteasomal activity and inflammasome activation: Protection by Melatonin. *Biochimica et biophysica acta. Molecular basis of disease* **1865,** 2303–2316; 10.1016/j.bbadis.2019.05.009 (2019).

60. Kajarabille, N. & Latunde-Dada, G. O. Programmed Cell-Death by Ferroptosis: Antioxidants as Mitigators. *International journal of molecular sciences* **20**; 10.3390/ijms20194968 (2019).

61. ASHMAN, D. F., LIPTON, R., MELICOW, M. M. & PRICE, T. D. Isolation of adenosine 3', 5'-monophosphate and guanosine 3', 5'-monophosphate from rat urine. *Biochemical and biophysical research communications* **11,** 330–334; 10.1016/0006-291x(63)90566-7 (1963).

62. Beavo, J. A. & Brunton, L. L. Cyclic nucleotide research -- still expanding after half a century. *Nature reviews. Molecular cell biology* **3,** 710–718; 10.1038/nrm911 (2002).

63. Hofmann, F. The cGMP system: components and function. *Biological chemistry* **401,** 447–469; 10.1515/hsz-2019-0386 (2020).

64. Kemp-Harper, B. & Feil, R. Meeting report: cGMP matters. *Science signaling* **1,** pe12; 10.1126/stke.19pe12 (2008).

65. Friebe, A., Sandner, P. & Schmidtko, A. cGMP: a unique 2nd messenger molecule - recent developments in cGMP research and development. *Naunyn-Schmiedeberg's archives of pharmacology* **393,** 287–302; 10.1007/s00210-019-01779-z (2020).

66. Sessa, W. C. The nitric oxide synthase family of proteins. *Journal of vascular research* **31,** 131–143; 10.1159/000159039 (1994).

67. Park, C. S. *et al.* Differential and constitutive expression of neuronal, inducible, and endothelial nitric oxide synthase mRNAs and proteins in pathologically normal human tissues. *Nitric oxide : biology and chemistry* **4,** 459–471; 10.1006/niox.2000.0300 (2000).

68. Förstermann, U. *et al.* Nitric oxide synthase isozymes. Characterization, purification, molecular cloning, and functions. *Hypertension (Dallas, Tex. : 1979)* **23,** 1121–1131; 10.1161/01.hyp.23.6.1121 (1994).

69. Smolenski, A. Novel roles of cAMP/cGMP-dependent signaling in platelets. *Journal of thrombosis and haemostasis : JTH* **10,** 167–176; 10.1111/j.1538-7836.2011.04576.x (2012).

70. Feil, R. & Kemp-Harper, B. cGMP signalling: from bench to bedside. Conference on cGMP generators, effectors and therapeutic implications. *EMBO reports* **7,** 149–153; 10.1038/sj.embor.7400627 (2006).

71. Petraina, A. *et al.* Cyclic GMP modulating drugs in cardiovascular diseases: mechanism-based network pharmacology. *Cardiovascular research* **118,** 2085–2102; 10.1093/cvr/cvab240 (2022).

72. Sandner, P. *et al.* Soluble Guanylate Cyclase Stimulators and Activators. *Handbook of experimental pharmacology* **264,** 355–394; 10.1007/164_2018_197 (2021).

73. Gaggin, H. K. & Januzzi, J. L. Biomarkers and diagnostics in heart failure. *Biochimica et biophysica acta* **1832,** 2442–2450; 10.1016/j.bbadis.2012.12.014 (2013).

74. Kuwahara, K. The natriuretic peptide system in heart failure: Diagnostic and therapeutic implications. *Pharmacology & therapeutics* **227,** 107863; 10.1016/j.pharmthera.2021.107863 (2021).

75. Burnett, A. L. *et al.* Erectile Dysfunction: AUA Guideline. *The Journal of urology* **200,** 633–641; 10.1016/j.juro.2018.05.004 (2018).

76. Gambaryan, S. The Role of NO/sGC/cGMP/PKG Signaling Pathway in Regulation of Platelet Function. *Cells* **11**; 10.3390/cells11223704 (2022).

77. Li, Z. *et al.* A stimulatory role for cGMP-dependent protein kinase in platelet activation. *Cell* **112,** 77–86; 10.1016/s0092-8674(02)01254-0 (2003).

78. Zhang, G. *et al.* Biphasic roles for soluble guanylyl cyclase (sGC) in platelet activation. *Blood* **118,** 3670–3679; 10.1182/blood-2011-03-341107 (2011).

79. Wen, L., Feil, S. & Feil, R. cGMP Signaling in Platelets. In *Platelets, Haemostasis and Inflammation,* edited by A. Zirlik, C. Bode & M. Gawaz. 1st ed. (Springer, Cham, 2018), Vol. 5, pp. 231–252.

80. Walter, U. & Gambaryan, S. cGMP and cGMP-dependent protein kinase in platelets and blood cells. *Handbook of experimental pharmacology,* 533–548; 10.1007/978-3-540-68964-5_23 (2009).

81. Estevez, B. & Du, X. New Concepts and Mechanisms of Platelet Activation Signaling. *Physiology (Bethesda, Md.)* **32,** 162–177; 10.1152/physiol.00020.2016 (2017).

82. Haslam, R. J., Dickinson, N. T. & Jang, E. K. Cyclic nucleotides and phosphodiesterases in platelets. *Thrombosis and haemostasis* **82,** 412–423 (1999).

83. Zaccolo, M. & Movsesian, M. A. cAMP and cGMP signaling cross-talk: role of phosphodiesterases and implications for cardiac pathophysiology. *Circulation research* **100,** 1569–1578; 10.1161/CIRCRESAHA.106.144501 (2007).

84. Mullershausen, F. *et al.* Direct activation of PDE5 by cGMP: long-term effects within NO/cGMP signaling. *The Journal of cell biology* **160,** 719–727; 10.1083/jcb.200211041 (2003).

85. Sager, G. Cyclic GMP transporters. *Neurochemistry international* **45,** 865–873; 10.1016/j.neuint.2004.03.017 (2004).

86. Jedlitschky, G. *et al.* The nucleotide transporter MRP4 (ABCC4) is highly expressed in human platelets and present in dense granules, indicating a role in mediator storage. *Blood* **104,** 3603–3610; 10.1182/blood-2003-12-4330 (2004).

87. Krawutschke, C., Koesling, D. & Russwurm, M. Cyclic GMP in Vascular Relaxation: Export Is of Similar Importance as Degradation. *Arteriosclerosis, thrombosis, and vascular biology* **35,** 2011–2019; 10.1161/ATVBAHA.115.306133 (2015).

88. Antl, M. *et al.* IRAG mediates NO/cGMP-dependent inhibition of platelet aggregation and thrombus formation. *Blood* **109,** 552–559; 10.1182/blood-2005-10-026294 (2007).

89. Massberg, S. *et al.* Enhanced in vivo platelet adhesion in vasodilator-stimulated phosphoprotein (VASP)-deficient mice. *Blood* **103,** 136–142; 10.1182/blood-2002-11-3417 (2004).

90. Schinner, E., Salb, K. & Schlossmann, J. Signaling via IRAG is essential for NO/cGMP-dependent inhibition of platelet activation. *Platelets* **22,** 217–227; 10.3109/09537104.2010.544151 (2011).

91. Horstrup, K. *et al.* Phosphorylation of focal adhesion vasodilator-stimulated phosphoprotein at Ser157 in intact human platelets correlates with fibrinogen receptor inhibition. *European journal of biochemistry* **225,** 21–27; 10.1111/j.1432-1033.1994.00021.x (1994).

92. Wentworth, J. K. T., Pula, G. & Poole, A. W. Vasodilator-stimulated phosphoprotein (VASP) is phosphorylated on Ser157 by protein kinase C-dependent and -independent mechanisms in thrombin-stimulated human platelets. *The Biochemical journal* **393,** 555–564; 10.1042/BJ20050796 (2006).

93. Wen, L. *et al.* A shear-dependent NO-cGMP-cGKI cascade in platelets acts as an auto-regulatory brake of thrombosis. *Nature communications* **9,** 4301; 10.1038/s41467-018-06638-8 (2018).

94. Kato, G. J. Defective nitric oxide metabolism in sickle cell disease. *Pediatric blood & cancer* **62,** 373–374; 10.1002/pbc.25297 (2015).

95. Kato, G. J., Gladwin, M. T. & Steinberg, M. H. Deconstructing sickle cell disease: reappraisal of the role of hemolysis in the development of clinical subphenotypes. *Blood reviews* **21,** 37–47; 10.1016/j.blre.2006.07.001 (2007).

96. Morris, C. R. *et al.* Dysregulated arginine metabolism, hemolysis-associated pulmonary hypertension, and mortality in sickle cell disease. *JAMA* **294,** 81–90; 10.1001/jama.294.1.81 (2005).

97. Föller, M. *et al.* Anemia and splenomegaly in cGKI-deficient mice. *Proceedings of the National Academy of Sciences of the United States of America* **105,** 6771–6776; 10.1073/pnas.0708940105 (2008).

98. Tchernychev, B. *et al.* Olinciguat, a stimulator of soluble guanylyl cyclase, attenuates inflammation, vaso-occlusion and nephropathy in mouse models of sickle cell disease. *British journal of pharmacology* **178,** 3463–3475; 10.1111/bph.15492 (2021).

99. Mack, A. K. *et al.* Sodium nitrite promotes regional blood flow in patients with sickle cell disease: a phase I/II study. *British journal of haematology* **142,** 971–978; 10.1111/j.1365-2141.2008.07259.x (2008).

100. Conran, N. & Torres, L. cGMP modulation therapeutics for sickle cell disease. *Experimental biology and medicine (Maywood, N.J.)* **244,** 132–146; 10.1177/1535370219827276 (2019).

101. Grynkiewicz, G., Poenie, M. & Tsien, R. Y. A new generation of Ca2+ indicators with greatly improved fluorescence properties. *Journal of Biological Chemistry* **260,** 3440–3450 (1985).

102. Helms, C. C. *et al.* Mechanisms of hemolysis-associated platelet activation. *Journal of thrombosis and haemostasis : JTH* **11,** 2148–2154; 10.1111/jth.12422 (2013).

103. La Pérez de Lastra, J. M., Moreno, A., Pérez, J. & Llanes, D. Characterization of the porcine homologue to human platelet glycoprotein IIb-IIIa (CD41/CD61) by a monoclonal antibody. *Tissue antigens* **49,** 588–594; 10.1111/j.1399-0039.1997.tb02806.x (1997).

104. Dean, W. L. Role of platelet plasma membrane Ca-ATPase in health and disease. *World journal of biological chemistry* **1,** 265–270; 10.4331/wjbc.v1.i9.265 (2010).

105. Drummen, G. P. C., van Liebergen, L. C. M., Op den Kamp, J. A. F. & Post, J. A. C11-BODIPY(581/591), an oxidation-sensitive fluorescent lipid peroxidation probe: (micro)spectroscopic characterization and validation

of methodology. *Free radical biology & medicine* **33,** 473–490; 10.1016/s0891-5849(02)00848-1 (2002).

106. Magtanong, L. *et al.* Exogenous Monounsaturated Fatty Acids Promote a Ferroptosis-Resistant Cell State. *Cell chemical biology* **26,** 420-432.e9; 10.1016/j.chembiol.2018.11.016 (2019).

107. Capecchi, M., Ciavarella, A., Artoni, A., Abbattista, M. & Martinelli, I. Thrombotic Complications in Patients with Immune-Mediated Hemolysis. *Journal of clinical medicine* **10**; 10.3390/jcm10081764 (2021).

108. Belcher, J. D. *et al.* Heme triggers TLR4 signaling leading to endothelial cell activation and vaso-occlusion in murine sickle cell disease. *Blood* **123,** 377–390; 10.1182/blood-2013-04-495887 (2014).

109. Jeffers, A., Gladwin, M. T. & Kim-Shapiro, D. B. Computation of plasma hemoglobin nitric oxide scavenging in hemolytic anemias. *Free radical biology & medicine* **41,** 1557–1565; 10.1016/j.freeradbiomed.2006.08.017 (2006).

110. Youssef, L. A. & Spitalnik, S. L. Ferroptosis in Hemolytic Disorders. In *Ferroptosis in Health and Disease,* edited by D. Tang (Springer International Publishing, Cham, 2019), pp. 257–272.

111. Coffey, M. J. *et al.* Catalytic consumption of nitric oxide by 12/15-lipoxygenase: inhibition of monocyte soluble guanylate cyclase activation. *Proceedings of the National Academy of Sciences of the United States of America* **98,** 8006–8011; 10.1073/pnas.141136098 (2001).

112. Kato, S., Zhang, R. & Roberts, J. D. Proprotein convertases play an important role in regulating PKGI endoproteolytic cleavage and nuclear transport. *American journal of physiology. Lung cellular and molecular physiology* **305,** L130-40; 10.1152/ajplung.00391.2012 (2013).

113. Fink, A. *et al.* The Subtilisin-Like Protease Furin Regulates Hemin-Dependent Ectodomain Shedding of Glycoprotein VI. *Thrombosis and haemostasis*; 10.1055/s-0043-1768057 (2023).

7 Erklärung zum Eigenanteil

Die Arbeit wurde innerhalb des Graduiertenkollegs 2381 cGMP: „Vom Krankenbett an die Laborbank“ unter Betreuung von Prof. Dr. Meinrad Gawaz, Prof. Dr. Robert Feil und M.D. Ph.D. Dmitriy Atochin durchgeführt.

Das Studienkonzept wurde von Prof. Dr. Meinrad Gawaz (Universitätsklinikum Tübingen, Abteilung Kardiologie und Kreislauferkrankungen) entwickelt.

Die Versuche wurden von mir eigenständig durchgeführt. Die Methode der Raman Spektroskopie wurde von Manuel Sigle (Universitätsklinikum Tübingen, Abteilung Kardiologie und Kreislauf-erkrankungen AG Prof. Gawaz) am Raman Mikroskop der AG Schenke-Layland durchgeführt. Die Methode der Calcium Messung wurde mit Unterstützung von Dr. Patrick Münzer (Universitätsklinikum Tübingen, Abteilung Kardiologie und Kreislauferkrankungen AG Prof. Borst) durchgeführt. Die Methode der ATP-Messung wurde mit Unterstützung von Melina Fischer (Universitätsklinikum Tübingen, Abteilung Kardiologie und Kreislauferkrankungen AG Prof. Borst) durchgeführt. Die Methode der Western Blots wurde mit Unterstützung von Dr. Anne-Katrin Rohlfing (Universitätsklinikum Tübingen, Abteilung Kardiologie und Kreislauferkrankungen AG Prof. Gawaz) durchgeführt. Die Methode der Lipidomics wurde mit Unterstützung von Xiaoqing Fu (Universität Tübingen, Abteilung Pharmazie/Biochemie, Pharmazeutische Chemie, AG Prof. Lämmerhofer) durchgeführt.

Die statistische Auswertung erfolgte eigenständig durch mich, die Grafiken wurden mit Unterstützung von Dr. Anne-Katrin Rohlfing erstellt.

Ich versichere an Eides statt, dass ich das Manuskript selbständig verfasst habe und keine weiteren als die von mir angegebenen Quellen verwendet habe.

Tübingen, den	03.07.2023	Marcel Kremser
	Datum	Unterschrift

8 Publications

Petersen-Uribe, Á., **Kremser, M.**, Rohlfing, A. K., Castor, T., Kolb, K., Dicenta, V., Emschermann, F., Li, B., Borst, O., Rath, D., Müller, K. A. L., & Gawaz, M. P. (**2021**). Platelet-Derived PCSK9 Is Associated with LDL Metabolism and Modulates Atherothrombotic Mechanisms in Coronary Artery Disease. **International journal of molecular sciences**, 22(20), 11179. https://doi.org/10.3390/ijms222011179

Nestele, J. A., Rohlfing, A. K., Dicenta, V., Bild, A., Eißler, D., Emschermann, F., **Kremser, M.**, Krutzke, K., Schäffer, T. E., Borst, O., Levi, M., Korin, N., & Gawaz, M. P. (**2021**). Characterization of GPVI- or GPVI-CD39-Coated Nanoparticles and Their Impact on In Vitro Thrombus Formation. **International journal of molecular sciences**, 23(1), 11. https://doi.org/10.3390/ijms23010011

Rohlfing, A. K., Kolb, K., Sigle, M., Ziegler, M., Bild, A., Münzer, P., Sudmann, J., Dicenta, V., Harm, T., Manke, M. C., Geue, S., **Kremser, M.**, Chatterjee, M., Liang, C., von Eysmondt, H., Dandekar, T., Heinzmann, D., Günter, M., von Ungern-Sternberg, S., Büttcher, M., … Gawaz, M. (2022). ACKR3 regulates platelet activation and ischemia-reperfusion tissue injury. **Nature communications**, 13(1), 1823. https://doi.org/10.1038/s41467-022-29341-1

Fink, A., Rohlfing, A. K., Dicenta, V., Schaale, D., **Kremser, M.**, Laspa, Z., Sigle, M., Fu, X., Pelzer, A., Fischer, M., Münzer, P., Castor, T., Müller, K. A. L., Borst, O., Lämmerhofer, M., & Gawaz, M. P. (**2023**). The Subtilisin-Like Protease Furin Regulates Hemin-Dependent Ectodomain Shedding of Glycoprotein VI. **Thrombosis and haemostasis**, 10.1055/s-0043-1768057. Advance online publication. https://doi.org/10.1055/s-0043-1768057


Fin.